NBS TECHNICAL NOTE 896

U.S. DEPARTMENT OF COMMERCE / National Bureau of Standards

NBS Reactor: Summary of Activities July 1974 to June 1975

NATIONAL BUREAU OF STANDARDS

The National Bureau of Standards[1] was established by an act of Congress March 3, 1901. The Bureau's overall goal is to strengthen and advance the Nation's science and technology and facilitate their effective application for public benefit. To this end, the Bureau conducts research and provides: (1) a basis for the Nation's physical measurement system, (2) scientific and technological services for industry and government, (3) a technical basis for equity in trade, and (4) technical services to promote public safety. The Bureau consists of the Institute for Basic Standards, the Institute for Materials Research, the Institute for Applied Technology, the Institute for Computer Sciences and Technology, and the Office for Information Programs.

THE INSTITUTE FOR BASIC STANDARDS provides the central basis within the United States of a complete and consistent system of physical measurement; coordinates that system with measurement systems of other nations; and furnishes essential services leading to accurate and uniform physical measurements throughout the Nation's scientific community, industry, and commerce. The Institute consists of the Office of Measurement Services, the Office of Radiation Measurement and the following Center and divisions:

Applied Mathematics — Electricity — Mechanics — Heat — Optical Physics — Center for Radiation Research: Nuclear Sciences; Applied Radiation — Laboratory Astrophysics[2] — Cryogenics[2] — Electromagnetics[2] — Time and Frequency[2].

THE INSTITUTE FOR MATERIALS RESEARCH conducts materials research leading to improved methods of measurement, standards, and data on the properties of well-characterized materials needed by industry, commerce, educational institutions, and Government; provides advisory and research services to other Government agencies; and develops, produces, and distributes standard reference materials. The Institute consists of the Office of Standard Reference Materials, the Office of Air and Water Measurement, and the following divisions:

Analytical Chemistry — Polymers — Metallurgy — Inorganic Materials — Reactor Radiation — Physical Chemistry.

THE INSTITUTE FOR APPLIED TECHNOLOGY provides technical services to promote the use of available technology and to facilitate technological innovation in industry and Government; cooperates with public and private organizations leading to the development of technological standards (including mandatory safety standards), codes and methods of test; and provides technical advice and services to Government agencies upon request. The Institute consists of the following divisions and Centers:

Standards Application and Analysis — Electronic Technology — Center for Consumer Product Technology: Product Systems Analysis; Product Engineering — Center for Building Technology: Structures, Materials, and Life Safety; Building Environment; Technical Evaluation and Application — Center for Fire Research: Fire Science; Fire Safety Engineering.

THE INSTITUTE FOR COMPUTER SCIENCES AND TECHNOLOGY conducts research and provides technical services designed to aid Government agencies in improving cost effectiveness in the conduct of their programs through the selection, acquisition, and effective utilization of automatic data processing equipment: and serves as the principal focus within the executive branch for the development of Federal standards for automatic data processing equipment, techniques, and computer languages. The Institute consists of the following divisions:

Computer Services — Systems and Software — Computer Systems Engineering — Information Technology.

THE OFFICE FOR INFORMATION PROGRAMS promotes optimum dissemination and accessibility of scientific information generated within NBS and other agencies of the Federal Government; promotes the development of the National Standard Reference Data System and a system of information analysis centers dealing with the broader aspects of the National Measurement System; provides appropriate services to ensure that the NBS staff has optimum accessibility to the scientific information of the world. The Office consists of the following organizational units:

Office of Standard Reference Data — Office of Information Activities — Office of Technical Publications — Library — Office of International Relations — Office of International Standards.

---

[1] Headquarters and Laboratories at Gaithersburg, Maryland, unless otherwise noted; mailing address Washington, D.C. 20234.

[2] Located at Boulder, Colorado 80302.

NBS Reactor: Summary of Activities July 1974 to June 1975

Robert S. Carter

Reactor Radiation Division
Institute for Materials Research
National Bureau of Standards
Washington, D.C. 20234

U.S. DEPARTMENT OF COMMERCE, Rogers C. B. Morton, *Secretary*

James A. Baker, III, *Under Secretary*

Dr. Betsy Ancker-Johnson, *Assistant Secretary for Science and Technology*

NATIONAL BUREAU OF STANDARDS, Ernest Ambler, *Acting Director*

Issued January 1976

National Bureau of Standards Technical Note 896

Nat. Bur. Stand. (U.S.), Tech. Note 896, 150 pages (Jan. 1976)

CODEN: NBTNAE

U.S. GOVERNMENT PRINTING OFFICE
WASHINGTON: 1976

For sale by the Superintendent of Documents, U.S. Government Printing Office, Washington, D.C. 20402
(Order by SD Catalog No. C13.46:896). Price $2.15 (Add 25 percent additional for other than U.S. mailing).

FOREWORD

The National Bureau of Standards Reactor was built not only to serve the needs of the NBS but also those of the greater Washington Scientific Community and other government agencies. The Reactor Radiation Division was established to operate the reactor and to foster its scientific and technological use. Toward this end, the Division has a small nucleus of scientists experienced in the use of reactors for a wide range of scientific and technical problems. In addition to pursuing their own research and developing sophisticated experimental facilities, they actively seek out and encourage collaboration with other scientists, engaged in challenging programs, whose work can benefit from use of the reactor, but who as yet do not have the reactor experience necessary to take full advantage of the facilities available. The Division also provides irradiation services to a wide variety of users as well as engineering and other technical services.

The reactor operates at 10 MW and is designed to provide a broad spectrum of facilities ranging from intense neutron beams to extensive irradiation facilities, making it one of the most versatile high flux research reactors in the country. Thus it is able to serve a large number of scientists and engineers in a broad range of activities both within and outside the NBS.

This report attempts to summarize all the work done which is dependent on the reactor including a large number of programs outside the Division. The first section summarizes those programs based primarily on Reactor Radiation Division (RRD) initiatives whereas the second and third sections summarize collaborative programs between RRD scientists and other NBS or non-NBS scientists respectively. The fourth section summarizes NBS work originating entirely outside the RRD which requires no collaboration with RRD scientists. The section entitled, "Service Programs" covers those programs originating outside NBS but for which RRD provides irradiation services. The remaining sections are self-explanatory.

ABSTRACT

This report summarizes all those programs which depend on the NBS reactor. It covers the period from July 1974 through June 1975. The programs range from the use of neutron beams to study of the structure and dynamics of materials through nuclear physics and neutron standards to sample irradiations for activation analysis, isotope production and radiation effects studies.

Key words: Activation analysis; crystal structure; diffraction; isotopes; molecular dynamics; neutron; nuclear reactor; radiation.

TABLE OF CONTENTS

TABLE OF CONTENTS

TABLE OF CONTENTS

A. Reactor Radiation Division Programs

NEUTRON SCATTERING STUDIES OF HYDROGEN IN METALS

Our program to study the binding and diffusion of hydrogen in bcc and fcc metals in collaboration with scientists from Oak Ridge and Argonne National Laboratories has continued. New results have been obtained for the lattice dynamics of NbD_x and VD_x and for the diffusion of hydrogen in ThH_x. In addition, further analysis of the results for the lattice dynamics of $PdD_{0.63}$ have led to increased understanding of many of the phenomena observed in this alloy system. The results obtained from this work will be used to extend the program to other metal hydrides and to help derive new models for the behavior of this important class of non-stoichiometric interstitial alloys.

1. The Lattice Dynamics of $PdD_{0.63}$ - J. M. Rowe and J. J. Rush

In a continuation of our collaboration with H. G. Smith and Mark Mostoller at ORNL and H. E. Flotow at ANL, we have completed our measurements and analysis of the lattice dynamics of $PdD_{0.63}$. We have used a Born-von Kaŕmán model for this system to produce the density of states $g(\omega)$ shown in figure 1. In this figure, the dashed line represents the predicted spectrum for $PdH_{0.63}$ assuming no force constant changes. These frequency distributions and related integrals (e.g. the mean frequency weighted by atom type) have been used by various groups to explain other data. For example Papaconstantapolous and Klein (NRL) have used the properly weighted mean square frequency in conjunction with their electronic band structure calculations to derive the parameters determining the superconducting transition temperature. The comparisons with experimental data have already led to a new understanding of superconductivity in this system. Also, M. H. Mueller and J. Faber (ANL) have used the mean square displacements derived from our data to show the existence of static displacements in their single crystal

samples of PdD_x and PdH_x.

Finally, in what is perhaps the most exciting and stimulating development, A. Rahman (ANL) has used the parameters derived from our data to initiate a series of calculations on high concentration defect systems. These calculations are both a test of the validity of our own fitting and analysis routines and an advance in the more general problem of the effect of vacancies on crystal dynamics. The results show that our admittedly arbitrary procedure for handling the lack of stoichiometry in our sample gives surprisingly good results for derived properties (a point of great importance to the applications discussed above). Also the calculations show that much of the discrepancy between our results and earlier polycrystal spectra can be understood in terms of the non-stoichiometry. In order to fully exploit this new development, further experiments will be undertaken to test the detailed predictions of the function of the one-phonon cross-section as a function of momentum transfer. This represents the first experimental and theoretical study of the effects of vacancies on the lattice dynamics of solids.

Finally, we are still attempting to produce higher concentration samples of PdD_x. We hope to achieve values of χ larger than 0.9 (which will provide a T_c>4 K) so that we can determine the behavior of a high T_c sample. We are also extending this program to studies of $Pd_y M_{1-y} D_x$ where M=Ag, Cu. Such alloys have Tc's as high as 18 K and are of great current interest. Progress in this area is dependent upon availability of adequate single crystal samples.

2. The Acoustic Modes of the Phonon Dispersion Relation of NbD_x -
J. M. Rowe, J. J. Rush and N. Vagelatos

We have completed our measurements of the acoustic modes of the phonon dispersion relation in Nb, $Nbd_{.15}$, and $NbD_{.45}$ at 473K. The results of these measurements have been analyzed in terms of Born-von Kármán models in order to derive approximate frequency distributions to aid in comparisons of the overall features. The measured dispersion

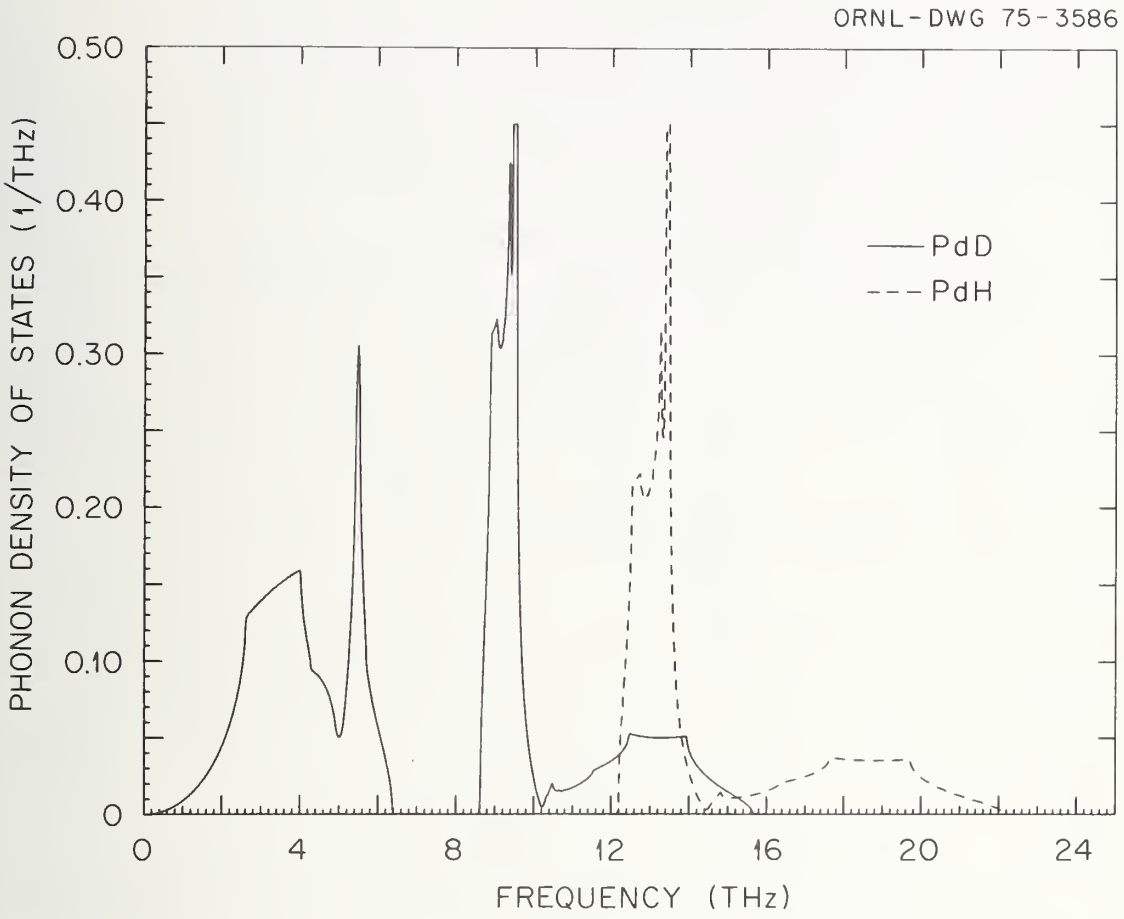

Figure 1. Phonon density states in PdD and PdH, calculated from the twelve parameter Born-von Karman fit to the neutron scattering data for $PdD_{0.63}$.

relations are shown in figure 2, and the derived frequency distributions are shown in figure 3.

Several interesting features of this system of alloys are apparent from the results shown in these figures.

1. The marked positive dispersion in the transverse acoustic modes which is characteristic of pure Nb decreases as deuterium is added.

2. The dip in the [100] longitudinal acoustic branch near $\zeta=0.7$ persists even in the $NbD_{.45}$ results.

3. The "kink" in the [110] L branch near $\zeta=0.35$ is present in

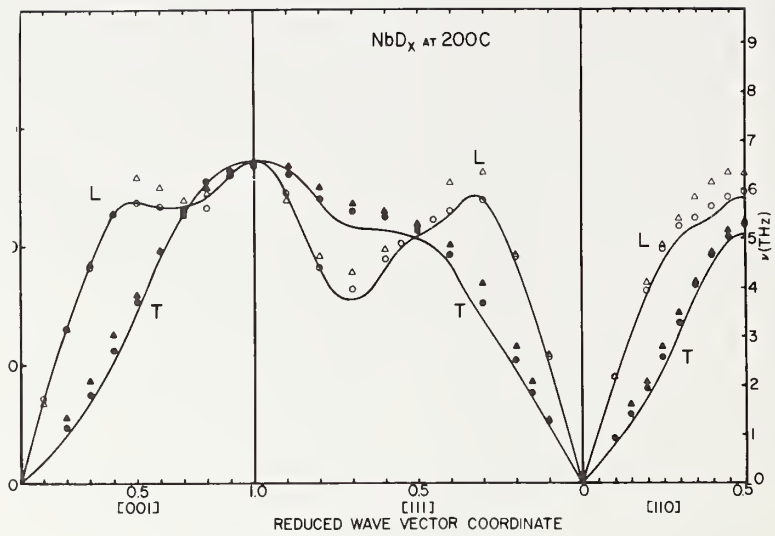

Figure 2. The phonon dispersion curves of Nb(——), $NbD_{.15}$ (full and open circles) and $NbD_{.45}$ (full and open triangles) at 473K. Error bars are omitted for clarity.

Nb and $NbD_{0.15}$, but not in $NbD_{0.45}$

4. The shape of the [111] branches of $NbD_{0.45}$ are quite different from those of Nb or $NbD_{.15}$, especially near ζ=0.7, an area of particular interest in connection with electronic instabilities.

5. The overall frequencies increase as deuterium is added, even though the lattice parameter increases by over 2% in $NbD_{.45}$. This behavior is opposite to that observed for PdD_x.

Many of the above features are undoubtedly connected to the complex electronic structure of Nb and its alloys. This problem is extremely complicated, but recent developments give some hope that our understanding will improve soon. However, in the absence of such theoretical understanding, we can still make some progress by comparing the present results to those of other authors for Nb-Mo alloys and to our own results for $PdD_{0.63}$. From these comparisons, we can infer that the great majority of the above features are due to rigid-band electronic effects because of the similarity of the present results to the Nb-Mo alloy data.

However, as expected, there are differences which must be ascribed to local strain and non-rigid bond effects. It is hoped that the present detailed results will lead to further theoretical progress in understanding these interstitial alloys.

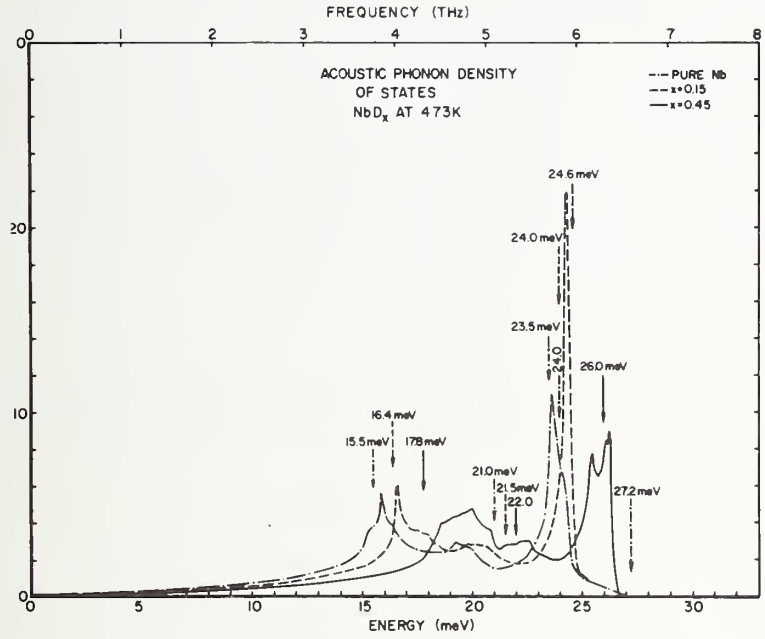

Figure 3. Phonon density of states for Nb(-·-) $NbD_{0.15}$ (---) and $NbD_{0.45}$ (——). The arrows denote critical points or other points of high phonon density suggested from data of figure 2.

3. The Diffusion of Hydrogen in Polycrystalline Thorium - J. M. Rowe, and J. J. Rush

In collaboration with Kurt Sköld, C.A. Pelizzari and H. E. Flotow at Argonne National Laboratory, we have obtained preliminary results on the quasielastic scattering of neutrons from $ThH_{0.05}$ and $ThH_{0.20}$ at 800°C. The data from these experiments are severely distorted by scattering from the quartz sample containers, but preliminary analysis suggests that the hydrogen in this fcc metal occupies tetrahedral sites, in contrast with the octahedral site occupation in fcc Pd. This exciting

result will be pursued in a single crystal sample of Th in a molybdenum sample container in collaboration with J. G. Traylor of Ames Laboratory.

4. Lattice Dynamics of Vanadium Deuteride - J. J. Rush, J. M. Rowe and N. Vagelatos

Some preliminary phonon measurements have been made in a study of lattice dynamics of vanadium deuteride ($VD_{0.7}$) single crystal using the BT-9 three-axis spectrometer. Acoustic phonons up to 15 meV have been observed, but great difficulty has been experienced at higher energies due to very high incoherent background and the shape of the dispersion curves. Experiments and analysis are continuing.

CRYSTAL DYNAMICS, PHASE TRANSITIONS AND ORIENTATIONAL DISORDER IN IONIC CRYSTALS

More work has been completed in our continuing studies of the dynamics of interatomic forces, rotational disorder and phase transitions in prototype orientationally disordered crystals. The precise nature of the orientational disorder and interatomic forces in the various crystal phases of broad classes of analogous solid materials is not generally well understood, nor is the microscopic basis of the changes in physical, thermodynamic and mechanical properties associated with the related order-disorder transitions.

Our research during the past year has concentrated on careful studies of the lattice dynamics of ND_4I and alkali cyanide single crystals by coherent neutron scattering, although some optical (KCN) and quasielastic scattering (ND_4I) measurements were also done on these systems. Preliminary reports on previous measurements have been made in last years' progress report (NBS Tech. Note 860).

1. Alkali Cyanides - J. M. Rowe, J. J. Rush, N. Vagelatos, N. J. Chesser

During the past year we have completed a study of the crystal dynamics of KCN and NaCN in their disordered (NaCl) cubic phase by

coherent inelastic scattering and infrared reflection techniques. We have also obtained new information on the nature of the cubic-orthohombic phase transition in these crystals and its relationship to the lattice dynamics by a careful, high resolution measurements of the acoustic phonons (including soft shear modes in the [100] and [110] directions in these crystals as a function of temperature).

In general the observed acoustic phonon intensities were superimposed on a varying "background" (non-one phonon scattering) which tended to increase as measurements were extended to higher energy phonons. The phonon intensities were also unusually weak, particularly at higher energies and q values. In fact we have thus far been unable to clearly

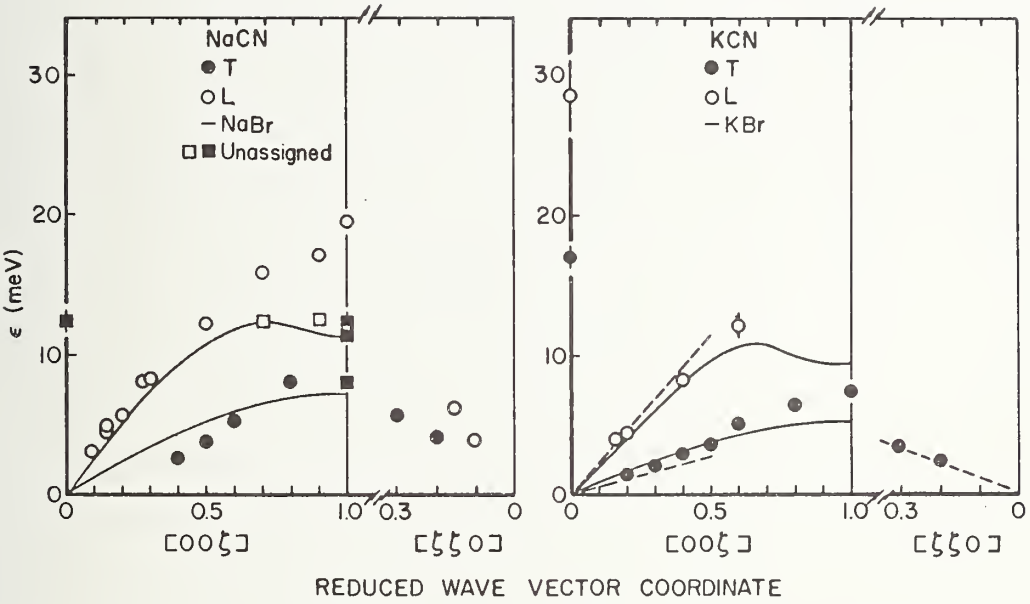

Figure 1. Acoustic phonon branches measured for NaCN and KCN at room temperature. The TA and LA dispersion curves for NaBr and KBr (solid lines) are also shown for comparison, as are the long wavelength slopes (dashed lines) of the acoustic branch determined from the measured elastic constate.

assign any optical vibration frequencies from our neutron measurements.

Phonon frequencies measured and assigned for KCN and NaCN in the [001] direction are shown in figure 1. It is difficult to give a clear explanation of the large background and lack of observation of phonon peaks at higher energies. It would seem that a combination of factors such as multiphonon scattering and other scattering processes involving the hindered rotations of the disordered cyanide ions, must provide the large background observed in our phonon scans. We also suspect that phonon lifetimes in these crystals are decreased significantly through interaction of the translational modes with the large amplitude rotational motions of the cyanide ions. This likely provides at least part of the reason that phonons do not appear to exist (according to our neutron measurements) as well characterized excitations in the cyanide crystals at higher frequencies and finite wave vectors.

Comparison of the cyanide dispersion curves with comparable measurements for KBr and NaBr (figure 1) show some significant differences. For example the LA[100] branch of NaCN shows no evidence of the dip in frequency exhibited close to the zone boundary by the KBr and NaBr dispersion curves. In fact, the shape of the measured branches for the cyanides is similar to that predicted by a rigid ion force model, while the alkali halides generally require a more completed "shell" model which takes into account ionic polarizability. A more interesting feature is the positive dispersion shown at low ζ in the [001] TA branches in both KCN and NaCN. This is associated with what appears to be anomalously low mode frequencies close to the zone center, as indicated by the fact that both NaCN and KCN are lower in frequency than the corresponding bromides. This observation is consistent with recent elastic constant (ultrasonic) data on KCN which show that C_{44} decreases rapidly as the temperature approaches the phase transition (167.5K)

In view of these results we have initiated a series of high-resolution phonon measurements in both KCN and NaCN down to the cubic-orthohombic phase transition. Some preliminary results of these

measurements are shown in figure 2, where we have plotted the observed phonon energies for the [100] TA branch for KCN at 293 and 175K. These phonon results (and similar measurements for the [110] TA branches) provide clear evidence that the phase transition is associated with a soft shear mode. The shape of the phonon peaks observed at ζ=0.1 are shown in figure 3, and again illustrate a clear soft mode behavior, with the phonon peaks approaching zero frequency and very large relative widths as the temperature is lowered. There are several notable features of our preliminary results: (1) The onset of "soft" behavior occurs over a wide temperature range and terminates in a first order phase transition. (2) The dispersion curves are "soft" more than half way across the zone. (3) The (in)ability to observe higher energy phonons is not changed by lowering the temperature. A particularly interesting and challenging question is the nature of the correlation of the orientational disorder of the cyanide ions with the observed soft mode behavior. We are extending our measurements on this system to a careful study of phonon line shapes and elastic scattering behavior, as well as to phonon measurements at higher temperatures. Further neutron diffraction investigations of the cubic and orthohombic phases are also planned.

2. Ammonium Iodide (ND_4I) - N. Vagelatos, J. M. Rowe and J. J. Rush

The analysis of the phonon-dispersion curve measurements for ND_4I in its NaCl phase described in our last report have been completed. This work provides the first detailed information on the lattice dynamics and crystal force fields in the high-temperature phase of an ammonium halide. In addition, since the orientationally-disordered high temperature-phases of ND_4I and the alkali cyanides are isomorphous, a comparison of the ND_4I and KCN (and NaCN) results should be useful in assessing the effect of rotational disorder on the crystal dynamics and character of the phonons in such crystals.

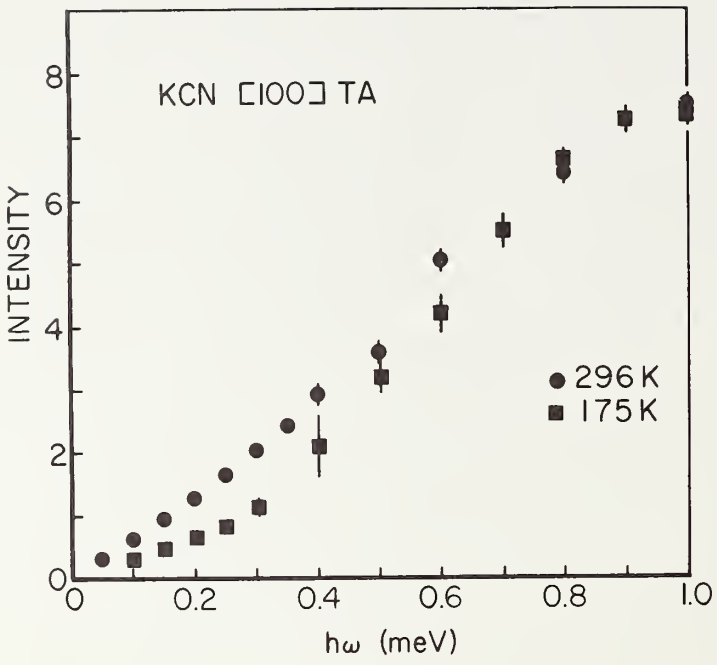

Figure 2. Transverse acoustic phonon branches of KCN in the [001] direction at 296 and 175 K.

The measured dispersion curves for ND_4I are shown in figure 4, along with the (16-parameter) fits obtained by analyzing the data in terms of "simple" and "breathing" shell models with general repulsive short-range forces out to second neighbors. In these models both ions are considered to be spherical and polarizable. The "breathing" shell model, which takes into account the isotropic deformation of the spherical shells, gives the best overall fit to the data. In addition the model predictions for the bulk crystal properties (shown in table 1) are generally in good agreement with observations, with the "breathing" model again providing better overall agreement. The character of our results closely resemble those of the alkali halides. It should also be noted that a separate time-of-flight neutron spectrum measurement suggests the absence of well-characterized torsional mode phonons, so that no attempt was made to investigate the rotational modes by the triple-axis method.

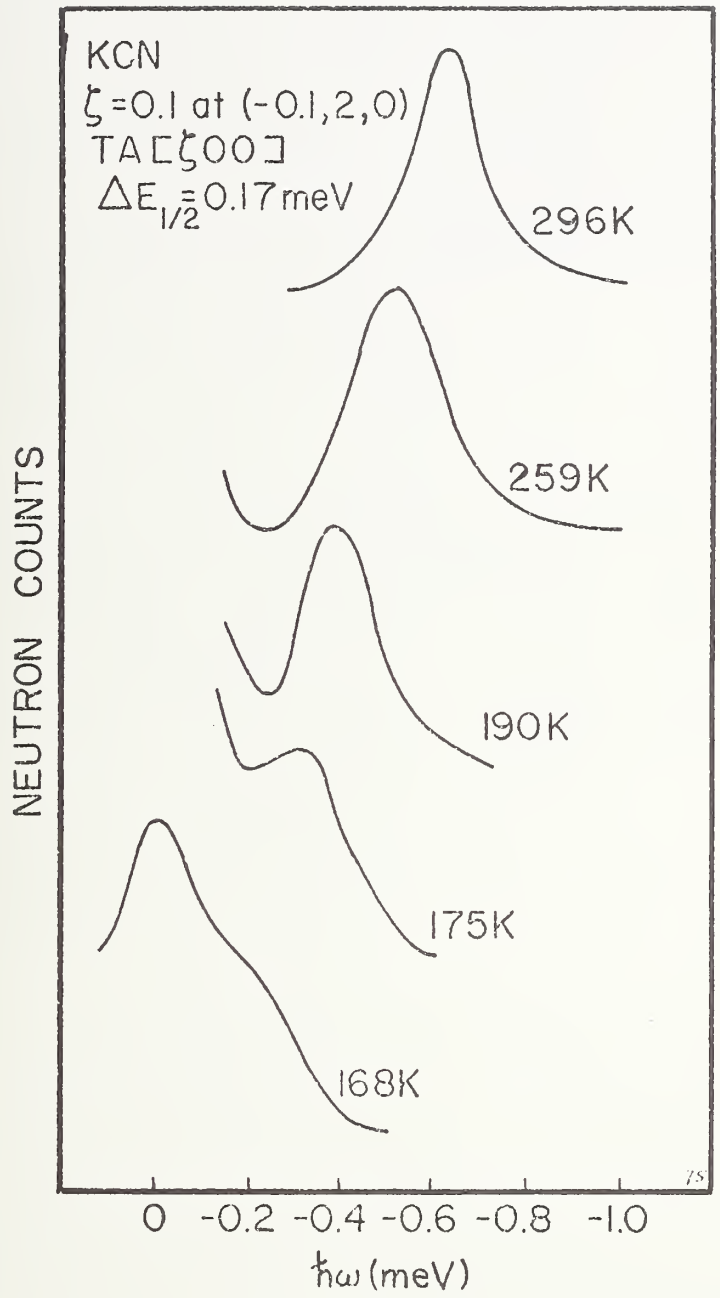

Figure 3. Smoothed representation of the measured [00ζ] TA temperature (Transition temperature = 167.5 K)

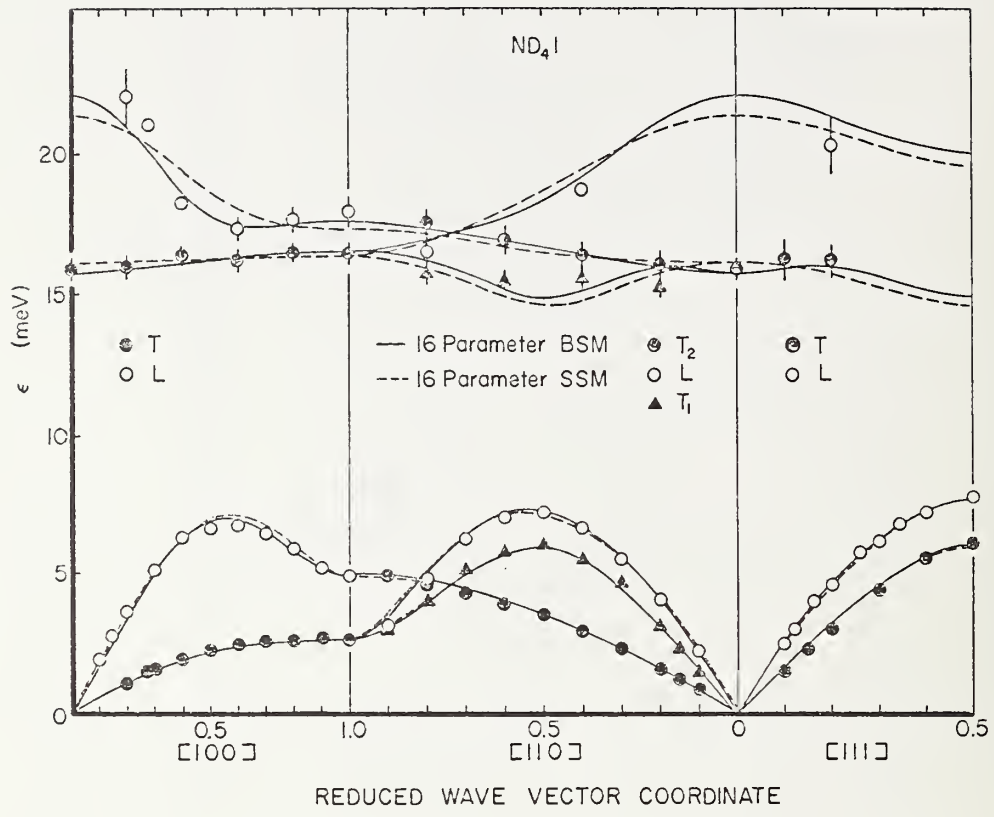

Figure 4. Measured phonon dispersion curves for ND_4I at 296 K) and the 16-parameter simple and "breathing" shell model fits.

The breathing shell model fit was used to derive the translational phonon frequency distribution, $g(\nu)$, for ND_4I, which is shown in figure 5. The structure of the calculated $g(\nu)$ displays critical-point and cut-off frequencies in close agreement with the details of the measured dispersion curves in figure 4, moreover the mean-square vibrational amplitudes are in excellent agreement with those derived from earlier neutron diffraction work and thus would seem to rule out the conclusion (from the diffraction results) that the rather large thermal amplitude ($\tilde{\sim}0.05\text{Å}^2$) indicate static displacements away from their face-centered positions.

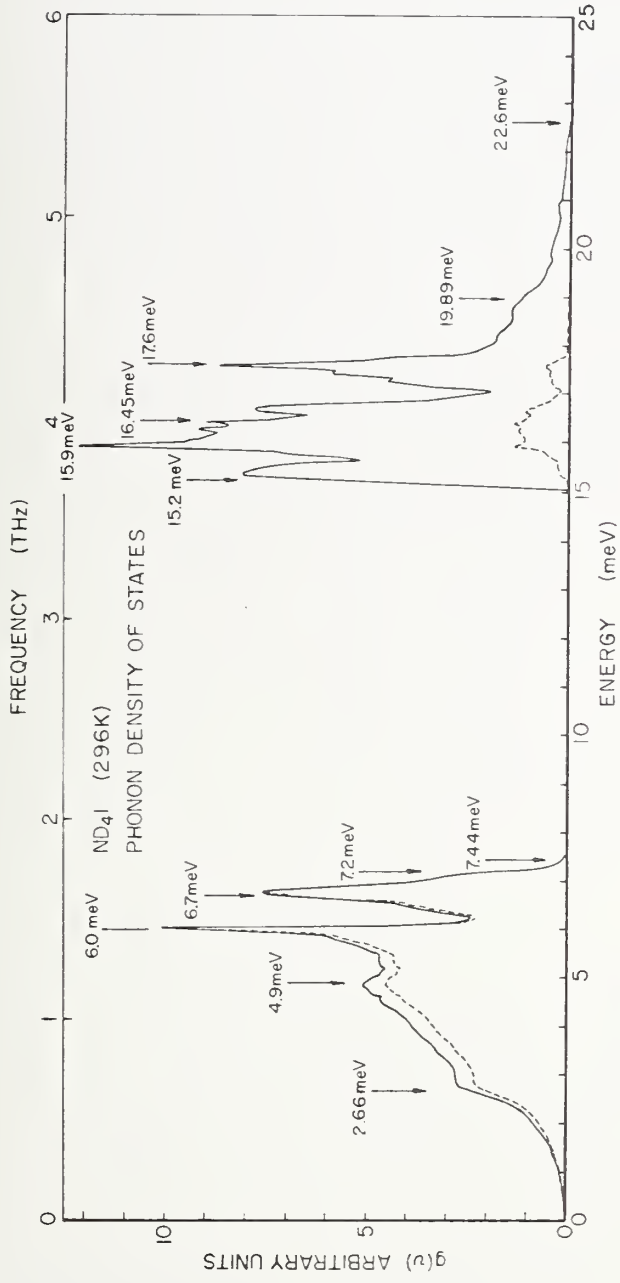

Figure 5. Translational phonon density of states for ND_4I, using the "breathing" shell model parameter values. (--) total density of states; (---) partial density of states for the I^- ions.

Finally it is interesting to compare these lattice dynamics results with those described above for the analogous(fcc) phases of the alkali cyanides. The fact that phonon dispersion curves (including the optic modes) were successfully measured for ND_4I strongly suggests that the high molecular reorientational rates do not greatly affect translational phonon lifetimes. The fact that the rotational disorder in the cyanides apparently does seriously perturb the existence or lifetimes of higher energy phonons suggests several possible explanations: (1) the

Table 1. Bulk properties of NB_4I calculated from SSM and BSM model parameters compared to observed values for NH_4I.

Property	SSM(ND_4I)	BSM(ND_4I)	OBSERVED(NH_4I)
C_{11} (10^{11} d/cm^2)	2.82±0.08	2.55±0.03	2.448
C_{12} "	0.85±0.08	0.74±0.03	0.428
C_{44} "	0.32±0.02	0.26±0.01	0.240
ε_o		9.78±11.60	9.8
ε_∞	4.42±1.27	1.94±0.24	2.90
β (10^{-12}cm^2/d)	6.62±0.27	7.41±0.13	∿6.6

hindered rotational modes in the alkali cyanides interact with the translational motions of neighboring ions, since the rotational modes are expected to have energies (∿10 meV) in the range of the translational modes, (2) the reorientations of the linear CN^- ions affect the lifetimes of the translational vibrations more strongly than the tetrahedral (pseudospherical) ND_4^+ ions.

We intend to pursue our measurements on ND_4I further to (1) a quasielastic scattering study of the ND_4^+ reorientation behavior and (2) further lattice dynamics studies close to the fcc↔bcc transition.

SYMMETRY ANALYSES OF NEUTRON SCATTERING IN CRYSTALS - APPLICATION OF TIME REVERSAL SYMMETRY

R. C. Casella, J. M. Rowe, and S. F. Trevino

Work has continued on the algorithm stated earlier by Casella[1] for computing the number of independent real parameters in the phonon dynamical matrix. Firstly, a clearer conceptual distinction has been drawn between the number of real parameters in the phonon dynamical matrix at fixed wave vector $\vec{k}$ and the number of real parameters in some assumed model potential (designed to reproduce the spectrum at all $\vec{k}$). Secondly, the algorithm has been applied to several illustrative cases: Zinc Blende with $\vec{k}$ along Λ and Δ in the Brillouin zone, diamond with $\vec{k}$ along Λ, graphite with $\vec{k}$ at A, and wurtzite with $\vec{k}$ along R. The results were compared with the computer generated dynamical matrices of Warren and Worlton[2] where conceptional difficulties of several types are found, particularly the need to count independent real parameters rather than matrix elements. All ambiguities in the Warren-Worlton procedure are cleared up via application of the algorithm in ref. 1. A summary of our results may be found in table 1. Of particular interest is the case of wurtzite for $\vec{k}$ along the line R. Whereas the procedure in ref. 2 leads to 77 to 80 real parameters, we see from table 1 that the properly reduced dynamical matrix can contain no more than 34 real parameters. This case (II-c, in the nomenclature of ref. 1) refers to one where a representation sticks to itself due to time reversal symmetry.

---

1. R. C. Casella, *Phys. Rev.* B11, 4795 (1975).

2. J. L. Warren and T. G. Worlton, Argonne National Laboratory Report ANL-8053 (1973). [Available from Natl. Tech. Info. Service, U.S. Dept. of Commerce, Springfield, VA]

Table 1. Computation of the maximum number $\mathcal{N}$, of real parameters for several cases

Crystal	$\vec{k}$ [a]	nomenclature[b]	$G_o^{\vec{k}}$ [c]	decomposition of $\Delta^{\vec{k}}$ [b,d]	case(s) contained [e]	$\mathcal{N}$ [f]
Zinc Blende	$(\mu,\mu,\mu)(\pi/a)$	line Λ	C_{3v}	$2\Lambda_1+2\Lambda_3$	I	8
Diamond	$(\mu,\mu,\mu)(\pi/a)$	line Λ	C_{3v}	$2\Lambda_1+2\Lambda_3$	II-a	6
Graphite[g]	$(0,0,1)(\pi/c)$	point A	C_{6v}	$(2A_1+2A_5)+(2A_3+2A_4)$	II-b	8
Wurtzite	$(0,\mu',1)(\pi/c)$	line R	C_s	$8R_1+4R_2$	II-c	34
Zinc Blende	$(\mu,0,0)(2\pi/a)$	line Δ	C_{2v}	$2\Delta_1+(2\Delta_3+2\Delta_4)$	{II-a, II-b}	7

[a] Cartesion coordinates. $0<\mu<1$. $\mu'=(2/\sqrt{3})(c/a)\mu$. For cubic systems a denotes the simple cube edge. For hexagonals c and a are the customary parameters.

[b] The nomenclature (which is generally standard), is selected identical with that in Ref. 2.

[c] $G_o^{\vec{k}}$ is the point group of the little group $G^{\vec{k}}$.

[d] When case II-b occurs, irreducible representations which stick together are enclosed in parentheses.

[e] Cases I and II are defined in the text. Subcases II-a, II-b, and II-c are distinguished by application of the Wigner-Herring test. [See Eq.(10) of Ref. 1.]

[f] $\mathcal{N}$ is computed via Eq.(2) and Eq.(3) of the text.

[g] Puckered.

THEORETICAL ANALYSIS OF PHONON DECAY WIDTHS IN KCN, $N_aC N$

R. C. Casella

Previously, an analysis of the Debye-Waller factor for heteronuclear diatomic "free rotators" in a vibrating lattice has been carried out. These affect the amplitude of phonon and rotator induced peaks in inelastic neutron scattering via an effective renormalization of the Fermi nuclear scattering amplitudes. However, the decay widths require separate analysis. Since, recently, N. Chesser has obtained data on the frequency and temperature dependence of these widths in KCN, including particularly, those of the soft TA mode, I have begun a theoretical analysis of the line-width problem for these systems, aided by insights provided by the experimentalists, N. Chesser, J. Rush, and J. M. Rowe, associated with various aspects of the problem. An attempt is underway to separate the effects of mode softening from those of strong interaction with (localized) hindered-rotator modes, the existence of which is evidenced in independent experiments.

THE USE OF POSITION SENSITIVE DETECTORS IN SINGLE CRYSTAL DIFFRACTOMETERS

E. Prince and A. Santoro

In recent years quantum counters have been developed for x-rays and neutrons which produce output pulses whose amplitude is a function of the linear position along the center wire at which the quantum was absorbed. Such position-sensitive detectors (PSDs) make possible a large increase in the efficiency of data collection in single crystal diffractometers, particularly for crystals with complex structures and correspondingly large unit cells. In view of the interest of the Reactor Division in the analysis of crystal structures involving large molecules, we have carried out a study of the possible designs of single crystal diffract-

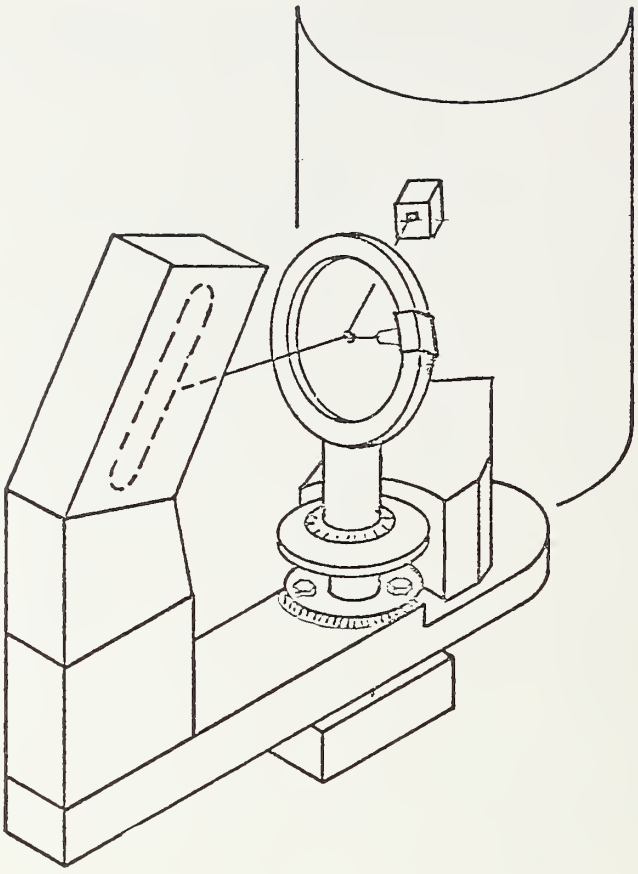

Figure : Schematic representation of the flat-cone geometry. The crystal in figure is rotated about the c-axis and the angle μ is adjusted so that the ℓ-th level of the reciprocal lattice is in flat-cone position (the plane of the level is perpendicular to the plane of figure). The circle is the trace of the intersection of the reflection sphere with the plane of figure.

ometers utilizing linear PSDs(*), and of the related problems of data collection and processing.

In order to utilize the properties of the linear PSD it is necessary to arrange for many diffracted beams to pass through the sensitive volume of the detector. While there are a number of possible ways to achieve that objective, for example the detector could be made to simulate the motion of a row line in a precession camera, the most straightforward

*Although two dimensional PSDs have been constructed, they are still in an early stage of development, and have not been considered in our study.

system is to arrange for all of the diffracted beams corresponding to points in a layer of the reciprocal lattice to be on a common plane. This is accomplished by using the flat-cone Weissenberg geometry. The crystal is mounted so that it may be rotated around a zone axis normal to a set of dense planes of the reciprocal lattice, and oriented with respect to the primary beam so that the lattice points of any desired layer will intersect the reflection sphere on a great circle. If the detector lies in the plane of the great circle it will intercept all diffracted beams from that layer (figure 1).

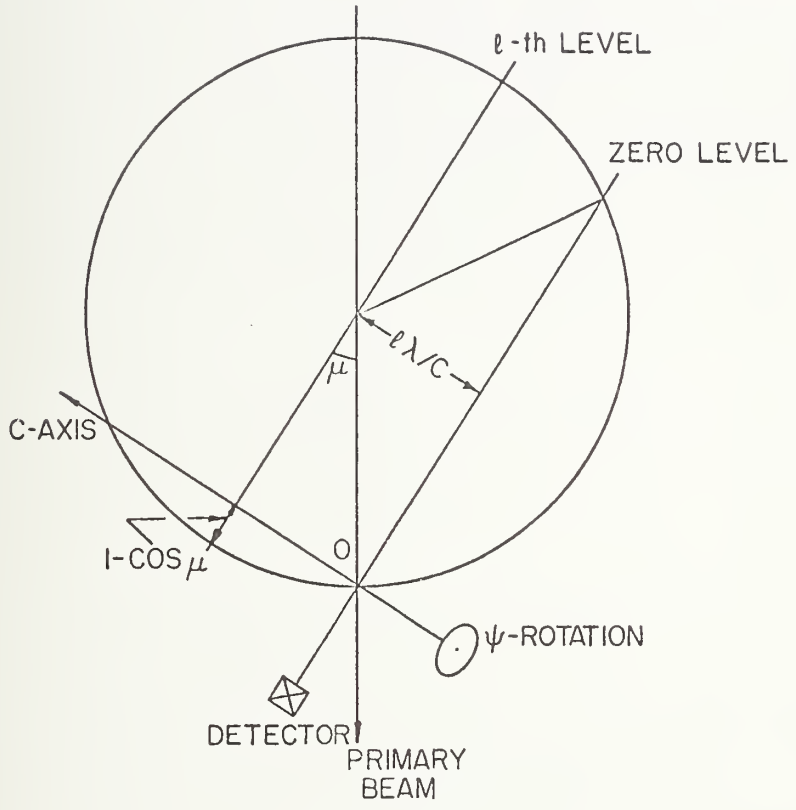

Figure 2. Sketch of a four circle diffractometer adapted to the flat cone Weissenberg geometry. The conventional ϕ, χ and ω circles of the diffractometer permit to rotate the crystal about more than one zone axis with a single setting of the crystal.

A disadvantage of the flat-cone geometry is that, for upper levels, there is a region of reciprocal space which is not accessible to the diffractometer. If the rotation around the zone axis is performed by a single circle, a remounting of the crystal will be necessary to measure reflections in this region. However, if we perform the rotation of the crystal by using the three independent angles of a four circle diffractometer more than one zone axis may be used with a single setting of the crystal. Figure 2 shows how a PSD may be mounted on a four circle diffractometer to take advantage of the flat-cone geometry.

If, due to crystal symmetry, the chosen zone axis is also a reciprocal lattice row, the flat-cone method, like the equi-inclination and normal-beam methods, has the undesirable property of intrinsic simultaneous diffraction. For complex organic crystals such as proteins this is unlikely to be a problem, but for certain inorganic crystals great care will be needed to avoid systematic errors in intensity measurements.

The use of PSDs is associated with two important features in the intensity measurement procedure which are not present in conventional counter methods. First, the peak and background intensities of several reflections may be measured simultaneously, and, second, the counter's horizontal width needed for the measurements of integrated intensities is not fixed by slits, but can be determined by computer for each reflection(*).

In a typical data collection procedure (the diffractometer is assumed to be under real time control by a computer) the crystal is rotated in small steps around the rotation axis. In each step position quanta are counted for a specified length of time, and accumulated counts are stored in a buffer according to the position in the detector at which they were detected. At the end of the counting interval the buffer is examined and for all detected counts a determination is made whether they come from a region near a reciprocal lattice point or from a background region. Counts corresponding to a peak or to a

*The vertical width is fixed by the lateral extent of the sensitive volume of the linear detector and cannot be adjusted.

background are stored, while the others need not be retained. The same procedure is repeated for each step position. A complete reciprocal lattice layer is examined by a complete revolution around the rotation axis.

The diffractometer settings and the conditions required for the measurement of integrated intensities have been evaluated by adapting known procedures to our particulary geometry (Burger, 1942; Busing & Levy, 1967; Burbank, 1964; Alexander & Smith, 1962; 1964a; 1964b).

---

1. L. E. Alexander and G. S. Smith, *Acta Cryst.* 15, 983 (1962).
2. L. E. Alexander and G. S. Smith, *Acta Cryst.* 17, 447 (1964a).
3. L. E. Alexander and G. S. Smith, *Acta Cryst.* 17, 1195 (1064b).
4. M. J. Buerger, *X-ray Crystallography* (1942) Wiley, New York.
5. R. D. Burbank, *Acta Cryst.* 17, 434 (1964).
6. W. R. Busing and H. A. Levy, *Acta Cryst.* 22, 457 (1967).

THERMAL NEUTRON FLUX MEASUREMENTS

V. W. Myers and M. Ganoczy

Analysis of the data for the measurement of the absolute thermal neutron intensity of a beam by means of a manganese sulfate bath is continuing. The beam was used for activating boron loaded cobalt glass beads which are essentially black to thermal neutrons. A thermal flux can then be determined by activating a bead in the unknown flux and comparing the counting rate to that of a bead activated in the known thermal beam.

Activation and decay times for Co-60 enter, of course, into the Co-comparison. The long half-life Co-60 ($\sim$5 years) is advantageous in that an activated bead can be used for several years.

NEUTRON RADIOGRAPHY

H. Berger, M. Ganoczy, and V. Myers

and

W. Parker
(Reed College, Portland, OR)

A survey of the neutron radiography community was conducted to determine the needs for standards in this expanding method of nondestructive evaluation. Representatives of more than 50 organizations including universities, government laboratories, and commercial suppliers were contacted in the survey. The results show that there is strong interest in, and support for the development of standards for neutron radiography and gauging.

The standards needs as determined by this survey are given below in priority order:

1. Define divergence characteristics of neutron radiographic beams in order to determine sharpness qualities of radiographs of thick objects.
2. Characterize neutron beams used for through-transmission and scatter gauging so that test data can be more thoroughly understood and interpreted.
3. Better define neutron spectral measurements over present ASTM image quality indicator (IQI) capability, and also better define gamma content of beams (including an improved measure of gamma energy) in order to better interpret test results.
4. Develop beam characterization methods better suited to low neutron intensity, relatively high gamma content non-reactor neutron sources (such as radioactive and accelerator sources).
5. Develop image quality indicator (IQI) methods for nonfilm detectors such as real-time, track-etch, gas-cell, etc., to take into account differences in viewing methods, neutron spectral and gamma sensitivity, and motion response.

6. Develop concepts for standards for neutron inspection methods employing neutrons in the cold, resonance, epithermal, and fast energy ranges.

The NBS program in neutron radiography is being adjusted to reflect the needs and interests shown by this survey. A report on the study was issued and sent to survey participants in May and June, 1975. Additional information obtained from comments on the report will be factored into the program plans.

Inputs for an ASTM Recommended Practice For Thermal Neutron Radiography have been collected and are now being placed in a single document to be submitted to ASTM Committee 37.05, Neutron Radiography. The document will discuss procedures for good quality thermal neutron radiography.

An additional collaborative effort with ASTM resulted in an NBS-ASTM Symposium on Practical Applications of Neutron Radiography and Gauging, held at NBS Feb. 10-11, 1975. The 150 attendees heard 28 papers during the two-day meeting. Papers were presented on subjects ranging from biological applications to those involving explosives, ordnance, adhesives, rubber, electronic components, wood, nuclear fuel and museum objects. The proceedings of the meeting will be published by ASTM as Special Technical Publication 586.

A new neutron radiography beam facility at the reactor has been designed and construction of components has begun. The new beam will provide higher neutron intensity (thereby permitting improved collimation potential), and a broad neutron spectrum. The anticipated neutron intensity for the new vertical beam facility will be greater than $10^8 n/cm^2 s$ at medium collimation and will provide approximately the same intensity as the thermal column beam ($2 \times 10^6 n/cm^2 s$) but with a collimator L/D ratio more than ten times greater (1000 vs. 90). This collimation will permit the production of high resolution thermal neutron radiographs.

The spectrum broadening of the new beam will also provide a major advantage. Beam filtering can be used to provide either a beam

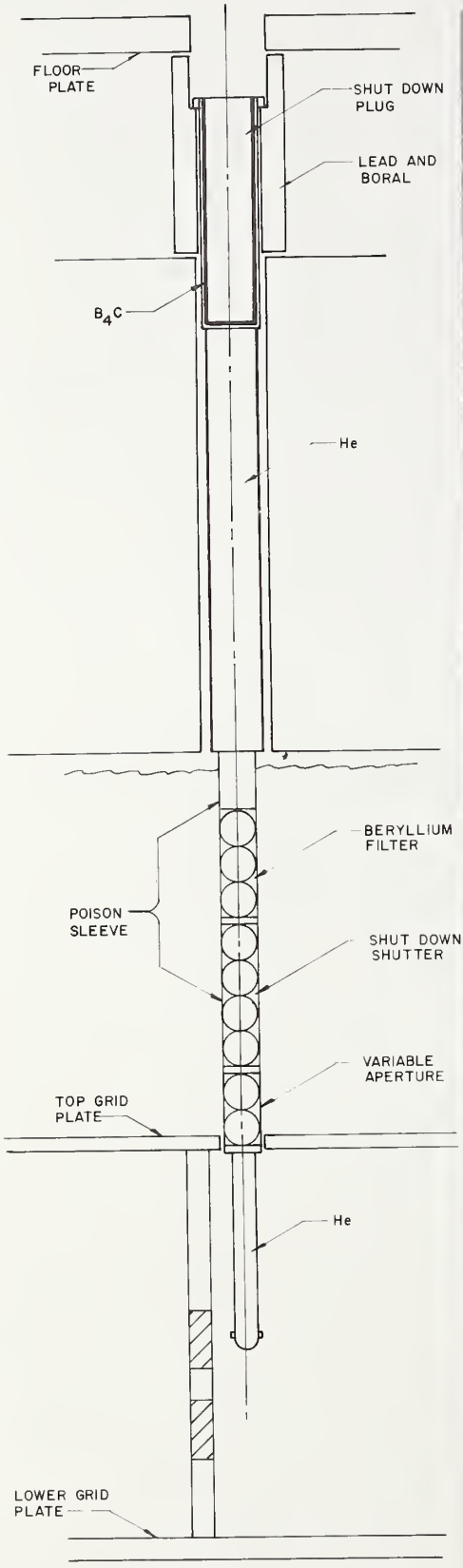

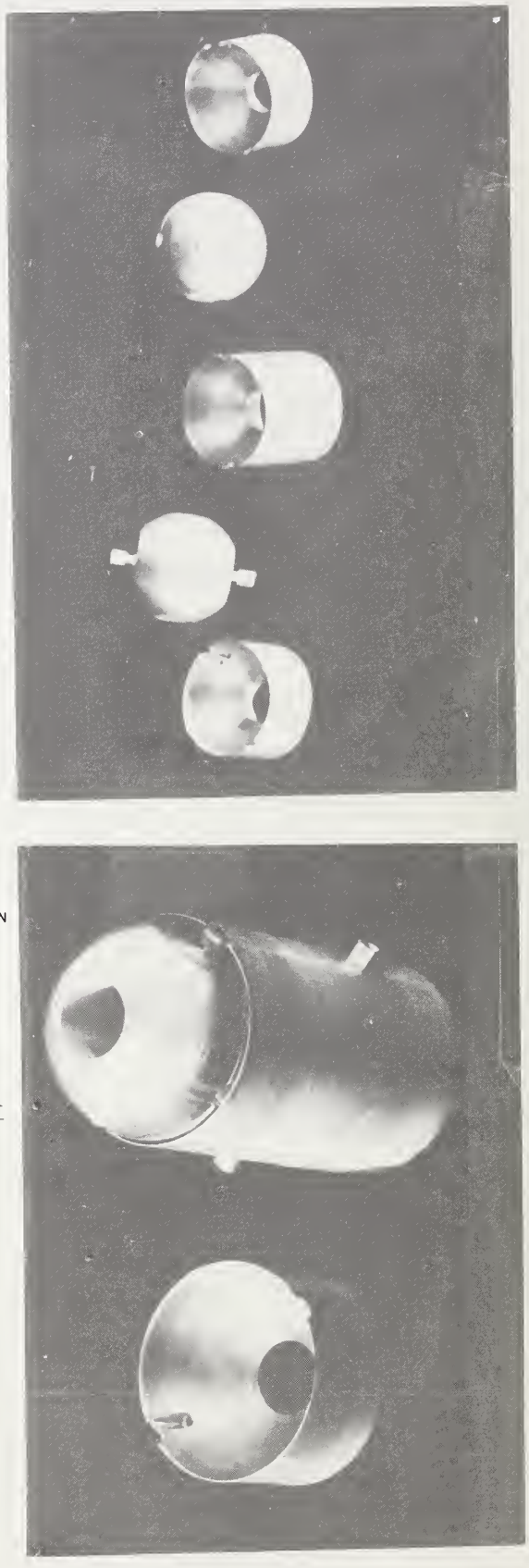

Figure 1. A diagram of the proposed new vertical neutron radiographic beam facility is shown in figure 1(a). The expanded view (figure 1(b)) shows the spherical aperture-filter assemblies which can be moved by remote control.

Figure 2. Prints of thermal neutron radiographs of a gadolinium nitrate filled fatigue crack in aluminum are shown. The object was placed normal to the radiographic beam axis (0°) and rotated 2° between exposures. The crack front can be visualized in the rotated views and the front shape can be reconstructed from the angled images.

that is primarily cold or a beam of epicadmium neutrons (anticipated cadmium ratio with gold is less than 5 versus 600 for the present thermal column beam). The high intensity will offer an advantage because even after filtering, exposure times will not be unduly long. An experiment was performed to obtain these design data.

Another possible use of the greatly increased intensity of the beam from the new facility is the use of a large metallic single crystal to form a crude neutron diffractometer, thereby making possible neutron radiography with approximately monoenergetic neutrons and with reasonable exposure times.

An unusual feature of the new beam will be the capability to change collimation ratio (input aperature size) and also to filter the beam remotely while the reactor is in operation. This will be accomplished by rotating assemblies containing apertures or filter materials. A diagram of the vertical beam design is shown in figure 1.

Application studies during the past year have involved a variety of samples. Work reported last year on the characterization of fatigue cracks has continued, in collaboration with D. G. Eitzen, NBS Mechanics Division. Progress includes a more uniform contrast material to fill the crack (gadolinium nitrate dissolved in either oil or water) and better control over the angular orientation of the crack. This is illustrated in the series of neutron radiographs shown in figure 2. Further work is planned with Gd-157 enriched contrast agent material to see what angulation can be used to visualize the crack front.

Application studies to show the potential of thermal neutron radiography have continued with several government and industrial organizations. An interesting application study has involved samples of carbon cloth impregnated with phenolic resin, a material of interest for rocket applications. The neutron radiographs of a series of samples containing different amounts of resin demonstrated that thermal neutron radiography was capable of differentiating voids from resin concentration differences.

New developments in thermal neutron image detection include the use of a new single-emulsion film and progress in real-time neutron radiography. Electronic integration systems have been used with the real-time system to show that useful low-intensity, thermal neutron images can be obtained by television integration methods. Tests were made at intensities as low as $10^3 n/cm^2.s$, an intensity sufficiently low that normal 1/30 second frame time images were barely detectable; useful images could be brought out by image integration times in the order of minutes.

Neutron image tests have also been made with a film originally made for electron imaging (Eastman Kodak Type FE 4721). Tests are still in progress but it has been shown that the speed for neutron imaging with gadolinium metal screens is about equal to Type M X-Ray Film. The new electron-sensitive film offers the advantages of a single emulsion - namely improved spatial resolution and relative neutron-gamma response.

Some preliminary studies have been made to investigate methods for three-dimensional thermal neutron radiography.[1] The method involves the superposition of radiographs taken from different angular orientations.[1,2] This permits one to focus a given image plane while other, undesired image planes are blurred. By moving the films with respect to one another, the observer can choose the desired image plane. In previous three-dimensional x-ray and gamma[3] radiography, the radiation source was moved linearly to obtain the different angular radiographic views. In these thermal neutron tests, the object-detector combination is rotated to obtain the different angular views. It has been shown that these two motions yield identical results if the object-detector rotation motion is combined with some linear axial movement between source and object-detector. The axial movement (along the line connecting the source and object-detector) compensates for changes in geometric magnification. The neutron work has also clarified the necessity to hold source-object distances reasonably small in order to effectively separate images from different object planes. Further work

is planned to determine spatial resolution capabilities at different depths in the radiographic object.

---

1. E. R. Miller, E. M. McCurry and B. Hruska, Radiology, 98, 249-255 (1971).

2. A. G. Richards in Biomedical Sciences Instrumentation, Instrument Society of America, Pittsburgh, Pa., Vol. 6, pp. 194-199 (1969).

3. N. P. Lapinski and H. Berger, Trans. Am. Nuclear Soc., 17, pp. 178-179 (1973).

[1]Work done in collaboration with N. P. Lapinski and K. J. Reimann, Argonne National Laboratory.

GAUGE THEORIES

R. C. Casella

As noted in the previous report, the Salam-Weinberg utilization of Yang-Mills gauge fields to unify the weak and electromagnetic interactions has successfully predicted the existence of weak neutral currents. Central to such theories is the question of "mass generation" via Higgs scalars (or otherwise, e.g., dynamically) and its relation to gauge symmetry and its breaking (analogue of Landau's theory of second order phase transitions in chemical physics). In quantum electrodynamics (QED) it is usually held[1] that the masslessness of the photon is a direct consequence of the gauge invariance of electromagnetism. Since this question is of importance to the more general theories as well, we have re-examined it in the context of the canonical Dyson-Salam-Ward renormalization program (perturbation theory). While it is obvious that the inclusion of mass terms in the unperturbed Lagrangian destroys gauge invariance, the usual argument[1] for the absence of mass generation via interaction is found wanting. Granted that the Ward-Takahashi identities, which follow

from current conservation,[2] lead to the transversality condition $k_\mu \Pi^{\mu\nu}(k)=0$ for the vacuum polarization tensor $\Pi^{\mu\nu}$ (at four-momentum k), it is nevertheless our view that one can conclude therefrom only

$$\Pi^{\mu\nu}(k)=(g^{\mu\nu} - k^\mu k^\nu/k^2)\Pi(k^2), \tag{1}$$

rather than the usual assumption[1],

$$\Pi^{\mu\nu}(k)=(g^{\mu\nu}k^2-k^\mu k^\nu)\Pi_1(k^2). \tag{2}$$

($g^{\mu\nu}$ is the metric tensor.) Eq.(1) follows naturally as a solution to the Dyson equation for the radiatively corrected photon propagator $D'_{\mu\nu}(k)$ since (1) has the same form as the unperturbed propagator $D_{\mu\nu}(k)$ when $D_{\mu\nu}$ is written in the Landau form. Since $\Pi(k^2)$ is presumably analytic in k^2 about the (unperturbed) mass-shell point, $k^2=0$, we may write

$$\Pi(k^2)=\Pi(0) + k^2\Pi_1(k^2), \tag{3}$$

where $\Pi_1(k^2)$ is also analytic in k^2. Moreover, the Dyson equation reduces to

$$D'^{-1}(k^2)=D^{-1}(k^2)-\Pi(k^2), \tag{4}$$

where $D^{-1}(k^2)=k^2$, whence it follows from (3) that <u>provided</u> $\Pi(0)=0$, $D'(k^2)$ has a pole at $k^2=0$; i.e., the mass of the photon remains zero under the effects of interaction. That is, if $\Pi(0)=0$, Eq.(1) and Eq.(2) are the same and the usual argument holds. However, when $\Pi(0)\neq 0$ Eq.(4) yields a pole in $D'(k^2)$ at $k^2=m^2\simeq\Pi(0)$; i.e., a dynamically generated photon mass appears.[3,4] The usual assumption[1] that the W-T identities imply (2) rather than (1) cannot help but lead to zero photon mass since, from the point of view of (1), $\Pi(0)$ has been arbitrarily set equal to zero in writing (2). In QED, where the photon mass is known experimentally to be compatible with zero (stringent limits exist), the distinction drawn here is a fine one, but this need not be the case for the more general gauge

theories. Mechanisms for mass generation without Higgs scalars are currently being investigated.

---

1. See, e.g., J. Bjorken and S. Drell, Relativistic Quantum Fields (McGraw-Hill, New York, 1965) or S. Schweber, Introd. to Relativistic Quantum Field Theory (Row-Peterson, Evanston, IL, 1961).
2. Current conservation and gauge invariance are intimately related.
3. Albeit infinite or cut-off dependent and removable via renormalization.
4. The expression for m^2 is approximate in the perturbative sense (assuming a cut-off). Precisely m^2 is a solution of the equation, $m^2-\Pi(0)-m^2\Pi_1(m^2)=0$

TOTAL PROFILE ANALYSIS IN NEUTRON POWDER DIFFRACTOMETRY

A. Santoro and E. Prince

and

A. D. Mighell
(Inorganic Materials Division)

and

C. S. Choi
(Picatinny Arsenal, Dover, NJ)

The powder method has been employed in crystal structure analysis in all those cases in which suitable single crystals cannot be grown. The method has gained in importance especially in neutron diffraction, due to the difficulty of obtaining specimens of sufficiently large dimensions for single crystal work. The usual technique of integrating under the Bragg peaks to obtain the intensities of each reflection can only be applied to well resolved diffraction lines, i.e. to very simple structures. For structures of moderate complexity and low symmetry there is considerable overlap of the independent peaks in the power diagram and the application of conventional methods of analysis results in a serious loss of information. In these cases it is of particular importance to develop techniques for extracting from the complex profile of a powder pattern the maximum amount of information. The method recently proposed by Rictveld does not attempt to measure the intensities of individual Bragg reflections, nor those of separate groups of overlapping peaks, as it has been done so far. The method, instead, makes use of the total profile of the powder pattern, including the regions where there is no measurable diffracted intensity, to decide if any given structural model is consistent with the observed data and to refine the parameters of the model by least squares analysis. These computations can be carried out only if the theoretical shape of the

diffraction lines is known. Peak shapes of single diffraction lines are Gaussian for most neutron diffractometers, while in the case of x-rays a satisfactory function for describing single peaks has not

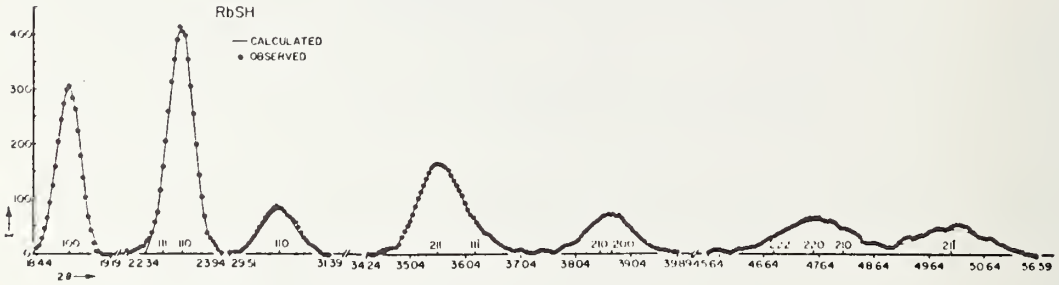

Figure 1. Observed and calculated neutron powder pattern for structure of the room temperature phase of RbSH. The final refined parameters for the structure are:

$a = b = c = 4.526(12)$ Å
$\partial = \beta = \gamma = 69.39(1)$ Space group $R\bar{3}m$
Atomic coordinates

Rb: $\frac{1}{2}\ \frac{1}{2}\ \frac{1}{2}$

S: 0 0 0

H: $\frac{1}{2}$ x x x

H: $\frac{1}{2}$ $\bar{x}$ $\bar{x}$ $\bar{x}$, x = 0.1252

Isotropic temperature factors
$B_{Rb} = 3.21$
$B_S = 1.25\ B_{Rb}$
$B_H = 8.39$

yet been found. The Rietveld procedure, therefore, can be applied only to neutron powder patterns.

Total profile analysis, if properly used, can be competitive with conventional single crystal procedures, at least for structures of moderate complexity. This means that it is often possible to refine a structure equally well with a powder pattern recorded in one day or with a set of single crystal intensity data collected over a period of days or weeks. In view of this important advantage, combined with the ease with which samples can be mounted and handled on the powder method, we have applied the Rietveld method to a number of problems now under investigation in the Reactor Division. The results of the refinement of the room temperature structure of RbSH are shown in figure 1 as an example. Efforts are now under way in this division to devise crystallographic methods for the generation of structural models in phase transformation studies. The completion of these investigations will considerably expand the measurement capabilities of the neutron spectrometers now in operation at the NBSR.

CONFORMATION OF POLYMERS IN DILUTE SOLUTION

C. Han
(Polymer Division)

and

B. Mozer

Conformation of polymers in dilute solutions are being studied in small angle scattering experiments. Both deuterated polystyrene-poly (methyl methacrylate), (dPS-PMMA) diblock copolymer, and deuterated polystyrene (dPS) homopolymer which is the precursor in the anionic polymerization have been chosen for this study. Deuterated toluene is used as the solvent in both cases. The coherent scattering cross-sections of deuterated styrene to that of methyl methacrylate has a

ratio about 1 to 100. Therefore, the PMMA block should have a very strong contribution to the scattering function $S(\kappa)$ in the diblock copolymer case.

In the preliminary study, we have been able to obtain the radius of gyration of the 90,000 molecular weight dPS, $\langle S^2 \rangle^{1/2} = 120\text{Å}$. The scattering function indicates that dPS exhibits a Gaussian chain distribution in toulene with an expansion coefficient $\nu \simeq 1.1$ which was obtained in the asymptotic limit of large κ

$$\lim_{x \to \infty} S(\kappa) = Ax^{-1/\nu} \qquad \text{where } x = \kappa^2 \langle S^2 \rangle$$

Some results for dPS-PMMA have been obtained. A pronounced difference in the scattering function was observed compared to that of the homopolymer. This difference may be caused by the interaction of polystyrene and poly(methyl metacrylate) segments which do not exist in the homopolymer case. More experiments on this system are still underway.

The scattering function of deuterated toluene which is the solvent as well as the major background source in the scattering experiments above, have been measured up to $\kappa \simeq 9.0\text{Å}^{-1}$. This scattering will be compared with x-ray results and theoretical models.

HYDROGEN BONDED DIMERS IN $SnHPO_4$

L. W. Schroeder
(Polymers Division)

and

E. Prince

Since the last progress report we have learned that Professor K. Ericks of Boston University has collected new x-ray data and further refined the crystal structure of $SnHPO_4$. The new refinement confirms the previous length of 2.52Å for the hydrogen bonds linking the HPO_4^{-2}

ions into dimers. The length of 2.52Å together with some features in the infrared and Raman spectra of this materials suggest proton tunneling. As soon as we obtain more accurate atomic coordinates from Professor Ericks we will proceed with the structure refinements using the neutron data.

CRYSTAL STRUCTURE OF 1,3,5-TRIACETO-2,4,6-HEXAHYDRO-S-TRIAZIZINE (TRAT)

C. S. Choi and P. Marinkas
(Picatinny Arsenal, Dover, NJ)

and

A. Santoro

The compound 1,3,5-triaceto-2,4,6-hexahydro-s-triazine, hereafter referred to as TRAT, is one of the byproducts in the reaction of hexamethylenetetramine with acetic anhydride. Chemically, TRAT is related to cyclotrimethylene-trinitramine, commonly called RDX and a well known explosive.

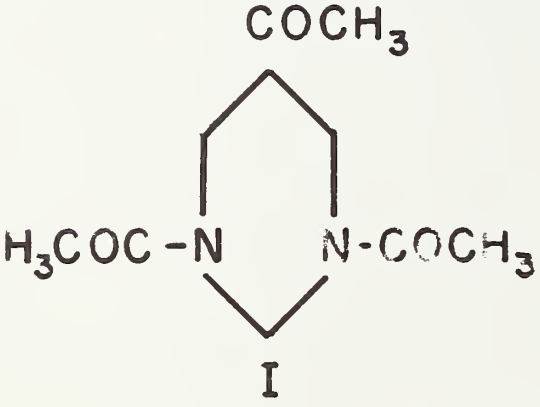

I

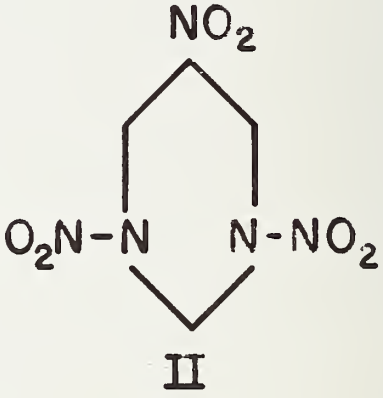

II

Single crystals of TRAT were obtained by slow cooling of a chloroform solution. Crystal symmetry and approximate all parameters were obtained from precession photographs. The cell parameters were then refined by least squares analysis from 16 reflections whose 2θ angles were determined with a diffractometer. A summary of the crystal data is given in table 1.

A total of 2484 independent reflections were measured with a 3-circle x-ray diffractometer (λ = 0.7107 Å). The structure was solved by direct and Fourier methods using programs of the X-RAY SYSTEM.

Table 1. Crystal data for 1,3,5-triaceto-2,4,6-trihydro-s-triazine (TRAT)

Space group	$P2_1/c$
a =	7.772(2) Å
b =	15.521(4) Å
c =	10.101(2) Å
β =	116.34
D_x =	1.30 g cm^{-3}
D_m =	1.31 g cm^{-3}
F(000) =	456

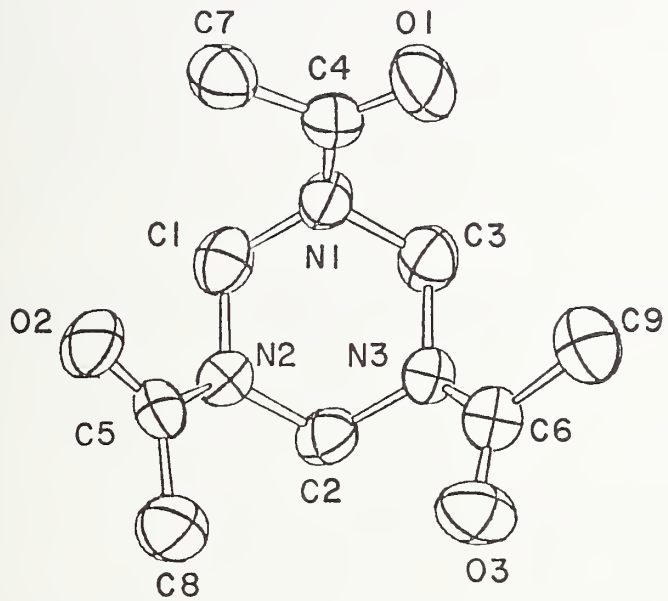

Figure 1. Perspective view of the molecule of TRAT with thermal ellipsoids.

Full matrix least squares refinements with anisotropic temperature factors for the heavy atoms and isotropic temperature factors for the hydrogen atoms resulted in R values of R = 0.051 and R_w = 0.035. Figures 1, 2, 3 show, respectively, a perspective view of the molecule with thermal ellipsoids, the unique bond distances and angles and the packing of the molecules in the crystals.

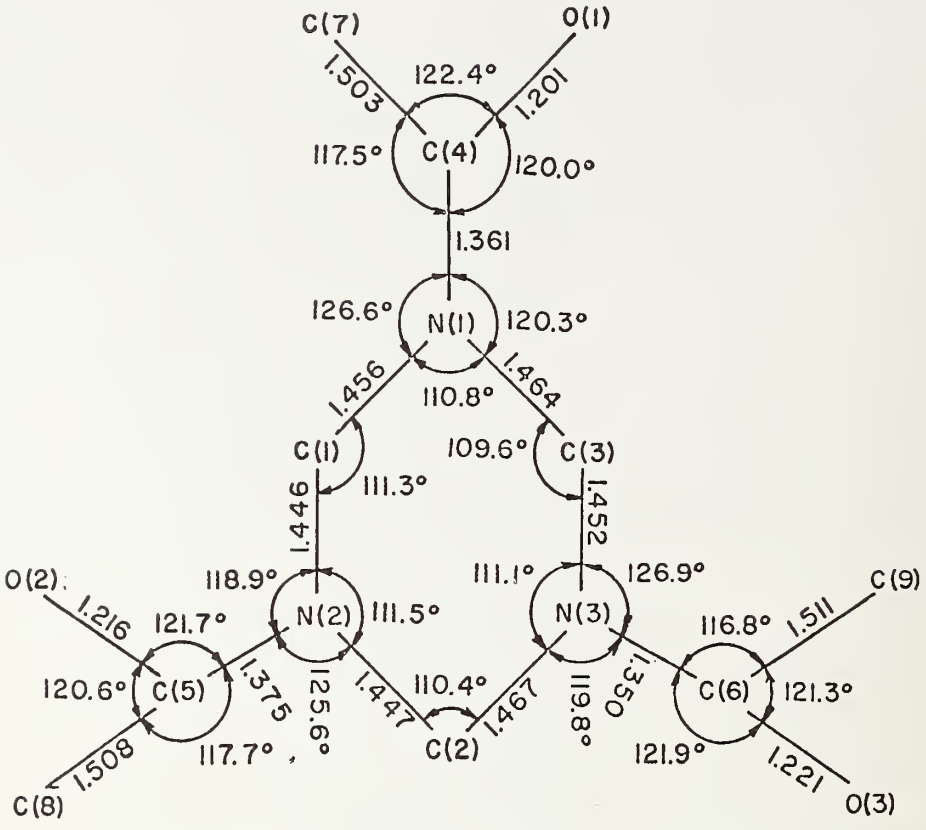

Figure 2. Schematic illustration of the TRAT molecule with the unique bond distances and angles. The standard deviations on distances and angles are 0.004 A and 0.4°, respectively.

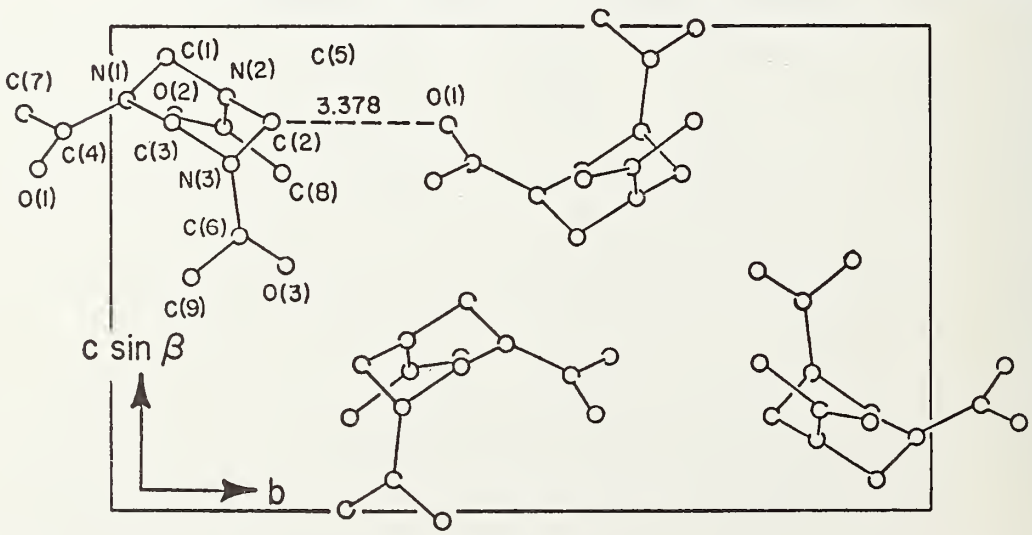

Figure 3. Packing of the molecules in the crystal structure of TRAT. The figure represents an orthogonal projection on the plane perpendicular to a.

The general features of RDX and TRAT are very similar. However, the molecular shape of the RDX molecule is much more distorted than that of TRAT (in RDX the planes of the three nitro groups are inclined to the plane through the carbon ring atoms of angles ranging from 18° to 62°, while in TRAT the planes of the acetamide groups are inclined to the plane of the carbon atoms with an average dihedral angle of 48°±2°).

Each ring carbon atom has short intramolecular contacts with the oxygen and carbon atoms of the adjacent acetyl groups (C...O = 2.73 Å and C...C = 2.93 Å). The shortest intermolecular distances are 3.21 and 3.38 Å for C...O contacts. There is no evidence of hydrogen bonding in the structure.

THE CRYSTAL STRUCTURE OF MONOVALENT METAL AZIDES

C. S. Choi
(Picatinny Arsenal, Dover, NJ)
and
E. Prince

The crystal structure of KN_3 (77K), RbN_3 (293K) and RbN_3 (77K) were investigated as a part of the continuing study on the structures of monovalent metal azides. Using 1.226 Å wavelength neutrons, the reflections in one half of a hemisphere of reciprocal space were measured out to a maximum 2θ of 105° for each crystal.

KN_3 (77K):

A crystal with cylindrical shape, 4 mm in diameter and 5 mm long, was used for this study. The unit cell dimensions were a = 6.085(5) Å and c = 6.997(5) Å in the space group I4/mcm. The structure was refined by the rigid body method, to the final R-indices of wR = 0.040 and R = 0.029 for 80 observed reflections.

Table 1. N-N bond lengths before and after correction for the azide libration. The shortest inter-ionic distances are based on parameters, corrected for the libration. The numbers given in parenthesis are the N-N bonds corrected for the librations obtained by Raman scattering.

Crystal	N-N bond length (Å)			Cation-Anion (Å)
	Raw	Corrected		
β-NaN_3	1.162(1)	1.180	(1.177)	2.504
KN_3(293)	1.174(1)	1.184	(1.183)	2.961
KN_3(77)	1.183(1)	1.187	(1.187)	2.936
RbN_3(293)	1.173(1)	1.187	(1.185)	3.099
RbN_3(77)	1.182(1)	1.187	(1.186)	3.068
TlN_3(293)	1.159(4)	1.181		3.037
TlN_3(260)	1.164(1)	1.184		3.033

RbN_3 at 293K and 77K:

A small flat crystal, 0.5 x 2 x 4 mm, was used for this study. RbN_3 also crystallizes in the tetragonal space group I4/mcm, with unit cell dimensions a = 6.304(5) Å, c = 7.53(1) Å at 293K and a = 6.261(5) Å, c = 7.44(1) Å at 77K. The structures were refined by the method of constrained rigid body refinement. The final R-indices were wR = 0.045, R = 0.020 for 97 observed reflections of the room temperature structure, and wR = 0.058, R = 0.045 for the 92 observed reflections of the 77K structure.

Summary on monovalent metal azides:

The N_3^- anions in the monovalent metal azide crystals are all centrosymmetric and linear, and are bonded internally by a strong resonance bond with double bond character. The thermal vibrations of such azide atoms may be described quite accurately by the rigid body

model since the amplitudes of the internal stretching modes in the azide group are negligible compared to those of the rigid body motion. The azide anions were refined with the constrained rigid body

Table 2. The librations of the azide anions obtained by the neutron diffraction method compared with those obtained by Raman scattering. Cruickshank's formula was used for the conversion:

$$\theta^2=(h/8\pi^2 I\nu) \coth (h\nu/kT)$$

Crystal	Neutron Diffraction			Raman Scattering		
	L(°)	$\nu(cm^{-1})$	$\bar{\nu}(cm^{-1})$	L(°)	$\nu(cm^{-1})$	$\bar{\nu}(cm^{-1})$
NaN_3	7.01	(110)	(110)	(6.42)	120	120
KN_3(293)	6.00	(128		(5.28)	147	
	4.56	(172)	(150)	(5.14)	151	149
KN_3(77)	3.51	(135)		(3.17)	157	
	2.75	(197)	(166)	(3.07)	165	161
TlN_3(293)	9.48	(81)		(15.86)	48	
	5.64	(137)	(109)	(4.55)	172	110
TlN_3(260)	9.42	(77)		(14.65)	49	
	4.75	(155)	(116)	(4.24)	175	112
RbN_3(293)	7.34	(105)		(6.03)	128	
	5.03	(155)	(130)	(5.53)	140	134
RbN_3(77)	3.84	(119)		(3.44)	139	
	3.21	(154)	(137)	(3.16)	158	149

refinement method to give skewness to the end nitrogens without increasing the number of variables in the refinement.

The interatomic distances in each crystal are summarized in table 1. The observed N-N distances are quite different from crystal to crystal and in the same crystal at different temperatures. However, when the bond lengths are corrected for the effect of the libration, they all converge to a narrow range of values; 1.186 Å,

within two times the observed standard deviations except for the β-NaN_3, as shown in table 1.

The librations derived from this diffraction study were compared with the corresponding librations measured by Raman scattering, as given in table 2. The agreements between the two libration amplitudes are quite satisfactory for all crystals except for TlN_3. The amplitude of libration in the TlN_3 crystals are too large to be harmonic, even at 260K. The observed N-N bond lengths were corrected also for the libration derived from Raman frequencies, as shown in table 1. The two corrected bond lengths are essentially the same with maximum difference of 0.003 Å. This suggests that the azide groups are essentially undergoing harmonic librations in these ionic crystals.

QUASIELASTIC NEUTRON SCATTERING STUDY OF AMMONIUM-ION REORIENTATIONS IN AMMONIUM PERCHLORATE

H. J. Prask and S. F. Trevino
(Picatinny Arsenal, Dover, N. J.)

and

J. J. Rush

The rotational motions of ammonium ions in polycrystalline NH_4ClO_4 have been investigated in the 55-150K temperature range by means of quasielastic neutron scattering for a momentum transfer range of 1-4 $Å^{-1}$. The gross behavior of the full-width at half-maximum (FWHM) of the quasielastic peaks (figure 1) are consistent with jump reorientations of either 180° about C_2 axes or 120° jumps about C_3 axes of the NH_4^+ ion. The data are not consistent with quasi-free rotation, rotational diffusion or 90° jump reorientations about C_2 axes of the NH_4^+ ion in the temperature range examined.

Under the assumption that 120° jump reorientations about C_3 axes (breaking three hydrogen bonds) are energetically more favorable

than 180° reorientations about C_2 axes (breaking four hydrogen bonds), the measured line shapes were analyzed to obtain hydrogen residence times[1,2] as a function of temperature. It was found that for T≲100K the line shapes are in agreement with either (instantaneous) jump reorientations about a single C_3 axis or random reorientations about all four C_3 axes. For T≳100K, reorientations about a single C_3 axis are ruled out. Residence times derived for C_3 reorientations about random axes range from 9.5 at 78K to 1.8 ps at 150K. If Arrhenius behavior is assumed for the temperature dependence of the residence time an activation energy of 2.26±0.25 kJ/mol (0.54±0.06 kcal/mole) and a frequency factor of $3.7 \times 10^{12} s^{-1}$ are obtained.

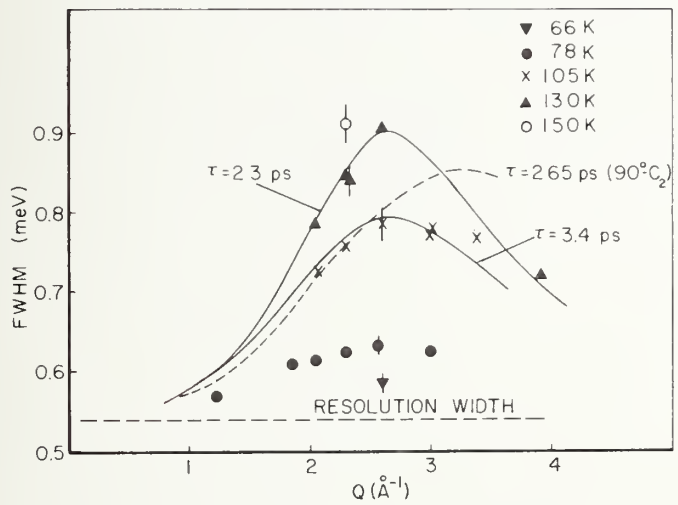

Figure 1. The full-widths at half-maximum (FWHM) of the measured quasielastic neutron scattering spectra vs wave vector transfer for several temperatures. The solid lines are the predictions of the C_3-axis reorientation model for the experimentally determined mean residence times. The dashed line is the prediction of the 90°-C_2 reorientation model with τ adjusted to give the experimentally observed FWHM at Q = 2.3Å-1 for NH_4ClO_4 at 105 K. Estimated uncertainties are shown.

To better characterize ammonium-ion dynamics in ammonium perchlorate, higher resolution measurements of polycrystalline NH_4ClO_4 and single-crystal ND_4ClO_4 are in progress.

1. K. Skold, J. Chem. Phys. 49, 2443 (1968).

2. H. J. Prask, S. F. Trevino and J. J. Rush, J. Chem. Phys. 62, 4156 (1975).

POLARIZED RAMAN STUDY OF AMMONIUM PERCHLORATE

H. J. Prask
(Picatinny Arsenal, Dover, N. J.)

and

G. J. Rosasco
(Inorganic Materials Division)

The dynamical behavior of molecular groups in ammonium perchlorate (AP) have been the subject of considerable interest for some time. Recent work in this laboratory with neutrons[1,2] has considerably advanced the understanding of the NH_4^+ dynamics at low temperature. In conjunction with this work we have examined the temperature dependence of all Raman-active vibrations from 12 to 297K in considerable detail, and a few modes to 500K.

The anomalous low-temperature behavior of certain B_{1g} and B_{3g} lattice modes has been described previously.[3] Recent work has been devoted to analysis and correlation of lattice and internal mode behavior of AP and d-AP. Figure 1 illustrates changes observed in the NH_4^+ internal modes in going from 32 to 297K. Similar changes do not occur in the ClO_4^- internal modes.

General conclusions that can be drawn from the vibrational mode analysis are as follows:

(1) The ammonium ions are bound in a very anharmonic and anisotropic potential which leads to pronounced multiphonon scattering

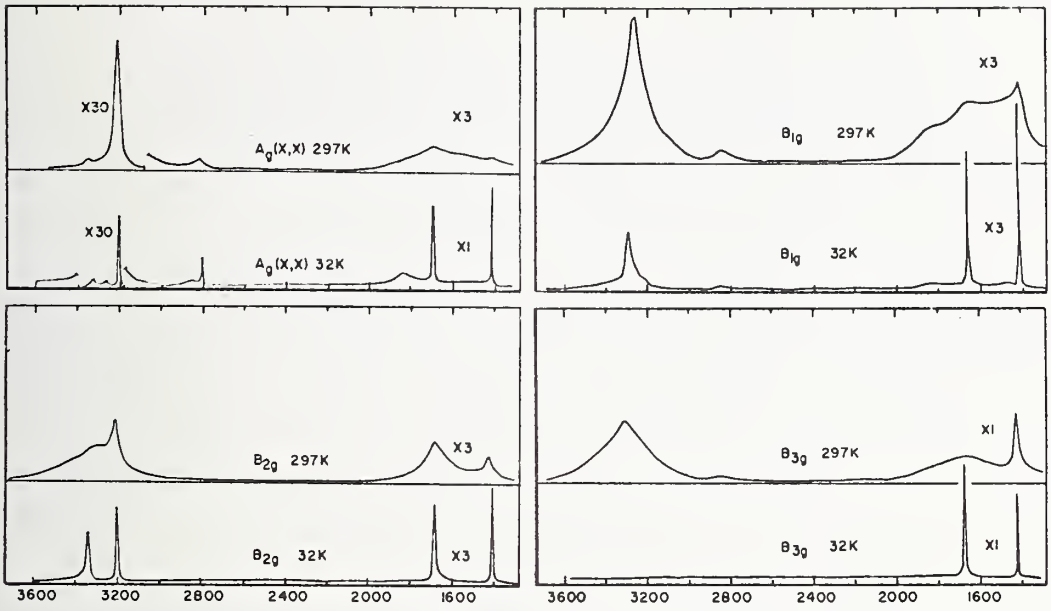

Figure 1. Polarized Raman spectra of the NH_4^+ internal mode region for single crystal NH_4ClO_4 at 32 and 297K.

at high temperature and the anomalous broadening of a few lattice modes at low temperature;[3]

(2) The structure inferred from the neutron diffraction[1] is consistent with Raman measurements and "selection rules" for D_{2h}^{16} symmetry in the 12 to 297K temperature range;

(3) Although no phase transition can be detected, both external and NH_4^+ internal mode behavior indicates a gradual but significant change in ammonium-ion dynamics in going from 12 to ∿150K which is associated with NH_4^+ reorientations.

(4) Gradual softening of an A_g lattice mode is observed from 12K to 500K which is associated with the orthorhombic to cubic phase transition at 513K.

1. C. S. Choi, H. J. Prask and E. Prince, J. Chem. Phys. 61, 3523 (1974).

2. H. J. Prask, S. F. Trevino and J. J. Rush, J. Chem. Phys. 62, 4156 (1975).

3. G. J. Rosasco and H. J. Prask, Sol. St. Comm. 16, 135 (1975); NBS Tech. Note 860 (1975), p. 69.

LOW TEMPERATURE PHASE STABILITY OF AMMONIUM NITRATE - POTASSIUM NITRATE SOLID SOLUTIONS

H. J. Prask, C. S. Choi, M. K. Farr and S. F. Trevino
(Picatinny Arsenal, Dover, N. J.)

Ammonium nitrate (AN) is, potentially, a very important ingredient in munitions because of its "energetic" properties, availability and relatively low cost. Its use, however, has been impeded in part by the fact that a structural phase transition (IV$\rightleftarrows$III) occurs at 32°C accompanied by a large change in density. Temperature cycling through this phase transition leads to irreversible expansion and cracking of cast fills. Addition of fractional amounts of potassium nitrate (KN) to AN has been found to change the phase diagram such that for 10%KN/90%AN (by weight), phase III is stable from ∿0 to ∿45°C, eliminating the cycling problem at warmer temperatures. The low temperature phase stability is of equal practical importance and this has been the subject of the present investigation.

Neutron diffraction has been used to determine the phase transition behavior of 90%AN/10%KN as a function of time at a storage temperature of -20°C. The results are summarized below:

(1) A phase transition (III→V) occurs very gradually in AN/KN "prills", cold-stored as received from the manufacturer;

(2) Indications of the occurrence of the transition begin after ∿5 days and it is not completed even after 35 days;

(3) The relative concentrations after 35 days of cold storage are ∿30% Phase III and 70% Phase V;

(4) Vacuum drying of the sample retards the phase transition even further so that the first changes are observed only after ∿25 days of cold-storage.

The practical conclusions to be drawn from this study are that dried AN/KN might exhibit acceptable low-temperature storage stability; however, "as received" samples do not. It appears that solid solutions containing larger fractions of KN should also be investigated.

MODE GRUNEISEN PARAMETERS OF KBr DETERMINED BY INELASTIC NEUTRON SCATTERING

M. K. Farr and S. F. Trevino
(Picatinny Arsenal, Dover, N. J.)

The room temperature acoustic phonon dispersion relations of KBr at 1 bar and at 6.3 kbar have been measured using conventional inelastic neutron scattering techniques. The mode Gruneisen parameters, $\gamma(\vec{q},j)$, for the measured modes have been calculated from the relation

$$\gamma(\vec{q},j) = - \frac{d \ln \omega(\vec{q},j)}{d \ln V} \Bigg|_T$$

The relative volume changes was determined by measuring the change in the lattice constant using Bragg scattering. Several calculations of mode Gruneisen parameters have been made using various lattice dynamics models.[1,2,3,4] The breathing shell model (BSM)[4] and anharmonic deformation dipole model (ADD)[3] calculations agree well with our acoustic mode measurements. Figure 1 shows the measured $\gamma(\vec{q},j)$'s together with curves calculated using the BSM.

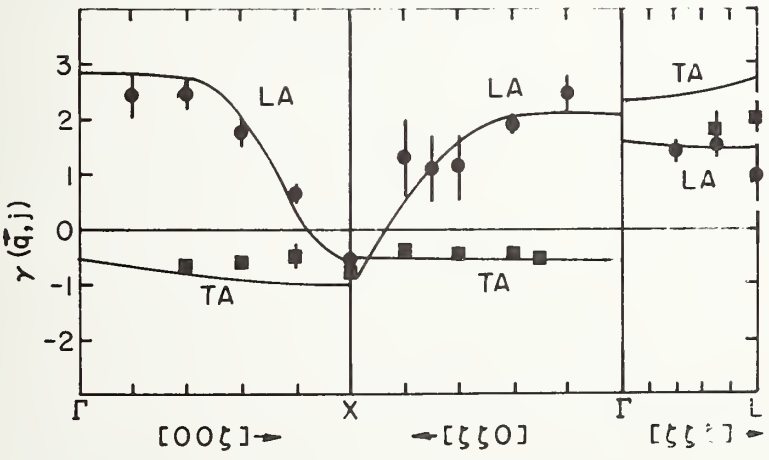

Figure 1. Mode Gruneisen parameters for acoustic modes in KBr. Solid Lines are BSM calculations of Mitra et al.[4] and points are present measurements.

The $\gamma(\vec{q},j)$'s for the optical modes of KBr are presently being measured. Our preliminary results indicate that there may be significant discrepancies between our measured $\gamma(\vec{q},j)$'s and the model predictions for these optical modes.

1. E. R. Cowley and R. A. Cowley, Proc. Roy. Soc. A292, 209 (1966).
2. R. Ruppin and R. W. Roberts, Phys. Rev. B, 3, 1406 (1971).
3. R. J. Hardy and A. M. Karo, Phys. Rev. B, 7, 4696 (1973).
4. S. S. Mitra and J. F. Vetelino, Private Communication.

HYDROGEN EMBRITTLEMENT IN TITANIUM

H. Alperin and J. Rhyne
(Naval Surface Weapons Center, White Oak, MD)

and

J. Rush

and

H. Flotow
(Argonne National Laboratory, Argonne, IL)

The phenomenon of hydrogen embrittlement of metals is well known and various theories have been proposed to explain the results of macroscopic metallurgical experiments. What is lacking, however, is the connection with the underlying microscopic behavior of the hydrogen in the host metal lattice. Several important aspects of the embrittlement process in titanium and its alloys are the role of stress, the solubility of hydrogen in the various phases and the diffusion of hydrogen from site to site.

Neutron scattering techniques offer the possibility of answering such questions as: Where in the host lattice do the hydrogen atoms reside in the different crystallographic phases of the Ti-H system? Does the site occupancy change with temperature? What are the activation energies and jump times for the diffusion of hydrogen? How are these characteristics affected by stress? Does the equilibrium phase diagram

of the Ti-H system accurately represent the actual non-equilibrium situation as it exists in the metal?

Neutron diffraction measurements were performed to determine the site occupancy of deuterium atoms in the α and β phases which play an important role in the hydrogen embrittlement process. A special vacuum furnace capable of temperatures to 900°C was built and used to measure the site occupancy of deuterium in the α-phase of Ti $D_{.075}$ at 375°C. The results show that the deuterium atoms are located approximately 68% on octahedral sites between the titanium atoms in their hexagonal close packed lattice. The remainder of the deuterium atoms reside on tetrahedral sites. Ti $D_{0.67}$ in the β-phase at 400°C was also measured.

A discrepancy was observed between the equilibrium amount of γ-phase expected in the $TiD_{.075}$ sample at room temperature and that actually observed. This is attributed to a quenching of the α-phase when cooling from high temperatures. This may be important for the embrittlement process. The difficulty of achieving equilibrium was also shown in the persistence of the lower temperature phases as the $TiD_{0.67}$ sample was raised to higher temperatures.

CRITICAL AND LOW TEMPERATURE NEUTRON SCATTERING FROM AMORPHOUS MAGNETS

H. A. Alperin, J. J. Rhyne and S. J. Pickart
(White Oak Laboratory, Naval Surface Weapons Center, White Oak, MD)

The investigation of the basic nature of the ferromagnetic transition in an entirely new kind of magnetic material, namely amorphous magnets has been extended to the compounds $HoFe_2$ and $GdFe_2$. This has been done in order to determine the generality of the critical scattering results previously obtained on $TbFe_2$. In addition, the role of anisotropy in the rare earth ion has been determined.

The results on $HoFe_2$ show that the scattered intensity has a Lorentzian shape as one approaches the Curie temperature ($T_c \sim 195K$) from higher temperatures. This yields a correlation length for the magnetic moment fluctuations which rise to a maximum value of only ~40A at T_c (in contrast to an infinite correlation range at T_c for a crystalline ferromagnet) and thus is similar to $TbFe_2$.[1] $GdFe_2$ also shows only a weak anomaly at T_c. We therefore conclude that for the rare earth amorphous ferromagnets in general, the critical anomaly is weak and the spin correlation length is finite at T_c.

The giant, anomalous, small angle scattering observed to increase with decreasing temperature below T_c in $TbFe_2$ is also seen now in $HoFe_2$. The present results however show that this effect is missing in $GdFe_2$. This effect which we interpret as due to the development of magnetic "grains" of size ~ 100 Å or less now appears to depend for its existence on an anisotropic magnetic rare earth ion since it is present for neither YFe_2 nor for $GdFe_2$ (isotropic s-state ion).

1. S. J. Pickart, J. J. Rhyne and H. A. Alperin, Phys. Rev. Letters 33, 424, (1974).

SPIN WAVES IN AMORPHOUS $TbFe_2$

J. J. Rhyne
(White Oak Laboratory, Naval Surface Weapons Center, White Oak, MD)

and

H. A. Mook
(Oak Ridge National Laboratory, ERDA, Oak Ridge, TN)

Using the Oak Ridge polarized beam time-of-flight spectrometer discrete spin wave excitations were observed in amorphous $TbFe_2$ at room temperature. Previous time-of-flight total scattering experiments had revealed only a broad inelastic magnetic distribution at large wave vector, Q, characteristic of the magnon density of states, plus

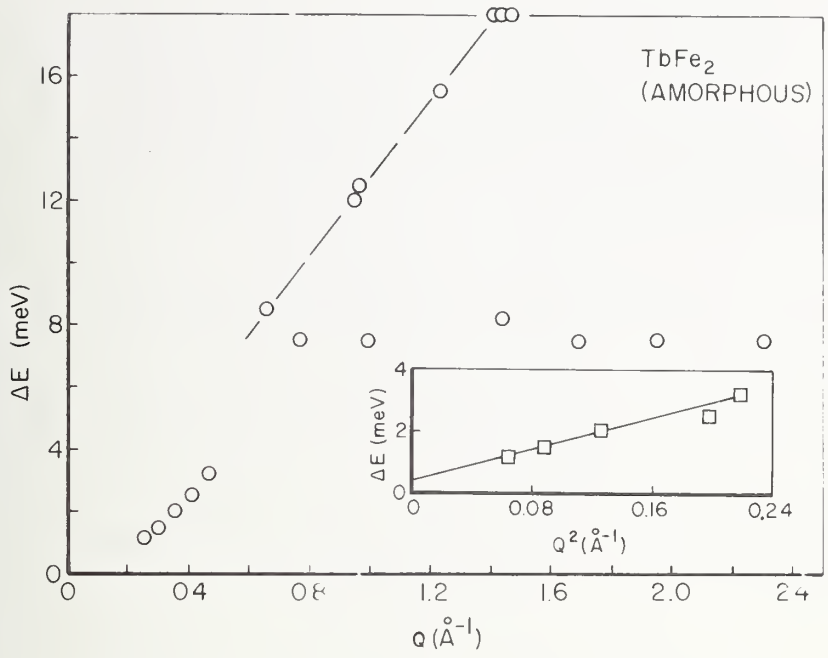

Figure 1. Magnetic inelastic scattering in amorphous $TbFe_2$. The data were taken on the Oak Ridge polarized beam time-of-flight spectrometer. The low Q dispersive branch is quadratic in Q (see inset) and represents an acoustic magnon with a weak stiffness constant D = 15 meV-Å^2 and evidence of a small anisotropy energy gap.

a strong elastic component at low Q representing the anomalous inhomogeneous magnetic structures[1] (micro-domains averaging approximately 100 Å) present in these materials. It was in fact the presence of this large elastic scattering which obscurred the observation of the expected long wavelength discrete spin waves and necessitated the use of the polarized beam spectrometer. Only neutron spin-flip (magnetic inelastic) scattering contributes to the scattering cross-section for this technique. The resulting suppression of the elastic peak made visible a dispersive acoustic magnon branch at low Q which is shown in figure 1. This branch (quadrant in Q) corresponds to a very small spin wave stiffness constant D = 15 meV-Å^2 apparently due to the structural disorder of the material and also shows evidence of a small (.25 meV) anisotropy energy gap. An additional higher energy branch was also observed as shown in the figure as well as a non-dispersive component

at approximately 9 meV energy transfer at large Q. It is planned to study the temperature dependence of the low Q magnetic excitations in this and other amorphous alloys using very fine energy resolution on a triple axis spectrometer.

ANOMALOUS CURIE TEMPERATURES OF RFe_2 AMORPHOUS MATERIALS

J. J. Rhyne
(White Oak Laboratory, Naval Surface Weapons Center, White Oak, MD)

As part of a continuing study[1] of the magnetization of the amorphous rare earth-iron (RFe_2) alloys, the alloys $DyFe_2$, $HoFe_2$, $ErFe_2$, and $TmFe_2$ have been examined as a function of temperature

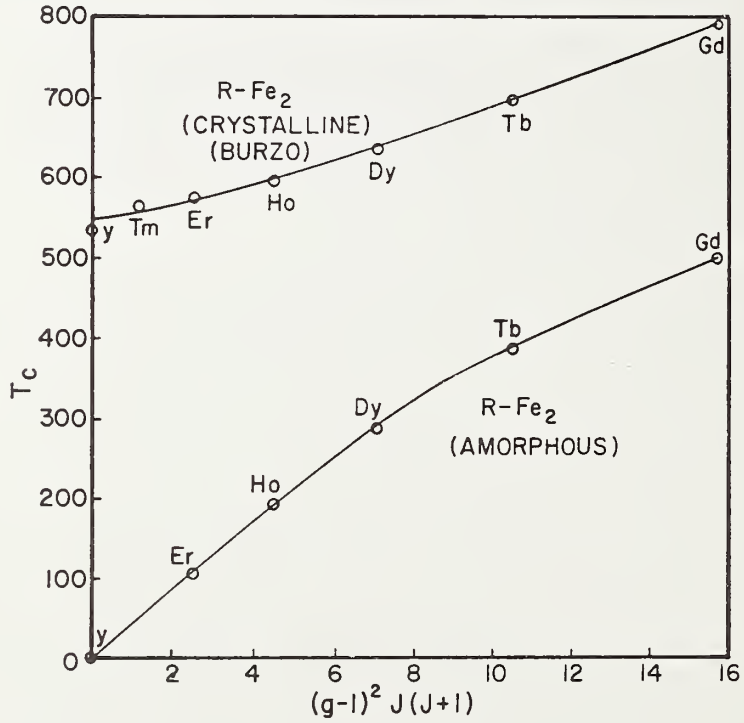

Figure 1. Curie temperatures of crystalline and amorphous RFe_2 metals as a function of the DeGennes factor (see text). Fundamental differences between the crystalline and disordered materials are noted in particular the vanishing of the amorphous T_c as the rare earth spins are removed.

both above and below the Curie temperature. Dy, Ho, and Er alloys are strongly ferromagnetic and exhibit the large "coercive" field effects at low temperatures characteristic also of $TbFe_2$. $HoFe_2$ exhibits significant time dependences in the magnetic properties at low temperature. The Curie temperatures of the amorphous alloys are suppressed below the corresponding crystalline compounds due to the effect of the topological disorder on the exchange interactions. This suppression in fact takes a very anomalous form as illustrated in figure 1, which gives T_c as a function of the DeGennes factor for the series of RFe_2 materials in both crystalline and amorphous form. The DeGennes factor is the projection of the effective rare earth (only) spin and is the quantity to which the R-R and R-Fe exchange should scale. The crystalline compounds show a 550 K background T_c from the Fe-Fe interaction (i.e. YFe_2) plus a montonic increase in T_c with DeGennes factor as the rare earth exchange interactions become stronger. In marked contrast, the amorphous materials show T_c vanishing smoothly as the DeGennes factor goes to zero, implying the absence of the constant background Fe-Fe exchange interaction in the highly disordered amorphous alloys. The curie temperatures rises rapidly with increasing rare earth spin and for $GdFe_2$ and $TbFe_2$ is sufficiently high to suggest a feed-back or catalytic effect on the iron-iron exchange interaction in the presence of strongly exchange-coupled rare earth spins. Such a mechanism is peculiar to these amorphous materials and is being investigated in detail.

1. J. J. Rhyne, J. H. Schelleng, and N. C. Koon, Phys. Rev. B10, 4672 (1974).

NEUTRON DIFFRACTION STUDIES ON TRANSITION-METAL SUBSTITUTED Fe_3Si

S. Pickart
(University of Rhode Island, Kingston, RI and
Naval Surface Weapons Center, White Oak, MD)

and

T. Litrenta
(Fordhan University, New York, NY)

and

T. Burch and J. Budnick
(University of Connecticut, Storrs, CT)

Neutron diffraction studies were performed on $Fe_{3-x}T_xSi$, with T = Co, V and Mn and $x \leq .06$ in order to check the site preferences inferred from earlier NMR spectra.[1] The neutron studies were taken on powdered and annealed samples with an external field of 8000 oe. applied along the scattering vector to eliminate magnetic scattering, and the site populations derived from the structure factor ratio of the first two superlattice lines. Large departures of this ratio from unity indicate that V and Mn prefer the Fe site with 8 Fe near neighbors, and Co that with 4 Fe and 4 Si n.n., thus confirming the NMR results. The ratio for pure Fe_3Si suggests a slight disorder consisting of a preferential occupancy by Si of the first type of site.

1. T. Burch, T. Litrenta and J. Budnick, Phys. Rev. Lett. 33, 421, (1974).

NEUTRON DIFFRACTION STUDIES OF BIOLOGICAL MATERIALS

J. C. Norvell and E. Prince

and

D. R. Davies
(National Institutes of Health)

A program to investigate the structure of biological materials, utilizing the techniques of neutron diffraction was initiated at NBS at the end of the fiscal year, in collaboration with the National Institutes

of Health. Recent neutron crystallographic studies of proteins[1,2] and low angle neutron studies of structures such as ribosomes, muscles, and membranes[2] have achieved some success at Brookhaven, Harwell and Grenoble. In the former experiments, the positions of the hydrogen atoms and bound water molecules are determined. Hydrogen atoms, which make up 1/2 of the atoms in a protein, are vital to the folding and enzymatic function of a protein, yet their positions cannot be determined from X-ray experiments. In the low angle work, large scale structural information is obtained. The program at NBS will begin with crystallographic work on a protein: ribonuclease A, rubredoxin, and lysozyme being the most likely candidates. Crystallization experiments are presently in progress, with the assistance of Dr. David R. Davies, Laboratory of Molecular Biology, NIAMDD, NIH. One of the main difficulties in protein neutron scattering experiments is the relatively low neutron flux, resulting in slow data acquisition rates. This should be greatly improved by the planned development of a neutron protein crystallographic station with a position sensitive detector.

---

1. Norvell, J. C., Nunes, A. C., and Schoenborn, B. P., *Science*, in press.
2. Brookhaven Symp. Biol. 27, in press.

MOSSBAUER STUDIES ON DYSPROSIUM-SCANDIUM AND AMORPHOUS $DyFe_2$

R. Abbundi and R. Segnan
(American University, Washington, DC)

and

D. Sweger
(Analytical Chemistry Division)

and

J. Rhyne

The NBS research reactor was used in this work to produce periodically a Dy-161 Mossbauer effect source by irradiation of

Gd_2F_3. The following is a summary of the results from this project on Dy-Sc alloys and on amorphous $DyFe_2$.

a. Dysprosium-Scandium Alloys

Mossbauer measurements were made in a series of Dy-Sc alloys ranging from 2% dysprosium to 75% dysprosium.[1] In figure 1 is shown the Mossbauer spectra for the 10% dysprosium concentration. All the measurements were taken at 4K. The 10% data clearly exhibit a hyperfine splitting in the Mossbauer lines. In the 5% sample the hyperfine pattern is not as clearly defined but it gives evidence of split lines. From these data we conclude that a magnetic hyperfine interaction exists for dysprosium concentrations above 5%.

Preliminary bulk magnetization measurements indicate that the Dy-Sc system is not ferromagnetically ordered below about 25% of dysprosium.[2] Tentatively we can possibly explain the presence of the hyperfine splitting of the Mossbauer spectra, as due to a local magnetic ordering of the Dy moments in the immediate surroundings of

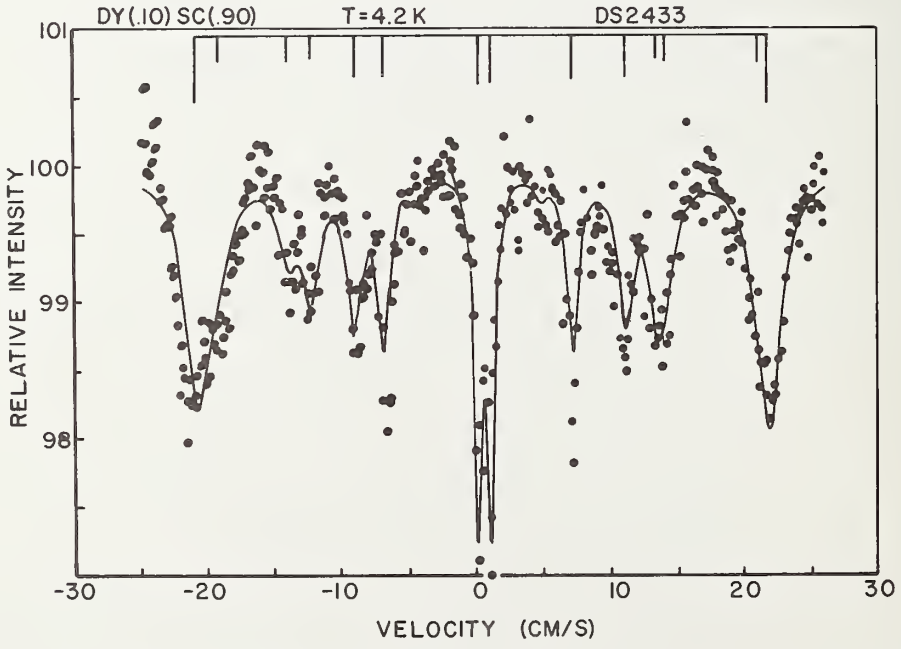

Figure 1. Mossbauer spectrum of DySc alloy - 10 at 90 dysprosium T = 4.2K.

dysprosium atoms used as Mossbauer probes. Alternatively, a more exciting explanation is that relaxation phenomena are responsible for the local ordering. Thus, the nuclear moment of a given dysprosium atom experiences slow spin-spin and spin-lattice relaxation times and therefore sees a slowly fluctuating hyperfine magnetic field. This result is quite important because slow relaxation phenomena are not normally expected in essentially metallic alloys.

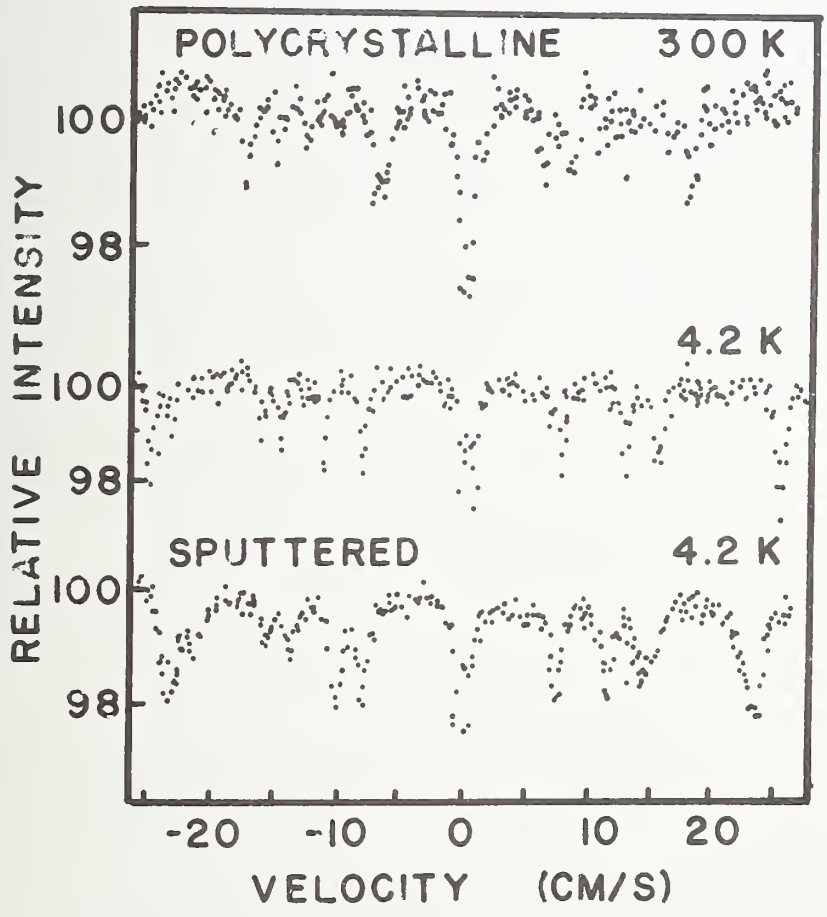

Figure 2. Dy-161 Mossbauer spectra in polycrystalline and amorphous $DyFe_2$.

b. Amorphous $DyFe_2$

Amorphous, magnetic, RE-TM metal alloys have now been prepared at several laboratories and x-ray[3] and neutron scattering[4] studies in sputtered $TbFe_2$ and $GdFe_2$ reveal a short-range atomic order significantly different from that in their crystalline (Laves phase) counterparts. Magnetization studies[5] of amorphous $TbFe_2$ have been described in terms of a model in which the Dy spins are more strongly coupled to their random-direction anisotropy axes than to the neighboring Fe spins. This also accounts for the reduced magnetic moment per formula unit compared with the corresponding crystalline alloy (RE and TM antialigned). Previous Mossbauer studies[6] have concentrated on the well-defined electric field gradient (EFG) observed in the paramagnetic state of amorphous $REFe_2$ alloys which can be explained in terms of a dense random packed sphere model. This model[6] yields an EFG at TM sites and a magnetic anisotropy at RE sites both of which are nearly constant in magnitude but random in direction.

There have been no previous Mossbauer studies of either H_{eff} or QS for RE atoms in the amorphous $REFe_2$ alloys. In figure 2 are shown our Dy-161 spectra in polycrystalline $DyFe_2$ at T = 4.2 K and 300 K and amorphous $DyFe_2$ at 4.2 K. The magnetic hyperfine splitting in the amorphous sample is completely collapsed at room temperature. At 4.2 K the average H_{eff}=6.3 MOe, is about half-way between the value for Dy metal and crystalline $DyFe_2$.[7] The QS ($e^2qQ/2$) is 6.3 cm/s. The outer lines of the amorphous spectrum are considerably broadened while the central lines are not. This requires a distribution of width ΔH_{eff} (Dy-161) $\cong$ 100 kOe at 4.2 K.

The Dy-161 hyperfine fields were found to collapse very rapidly with T/T_c and the spectral lines broadened by orders of magnitude indicating a distribution of local exchanges.

We note that, whereas 12 Fe nearest neighbors surround Re atoms in crystalline $ReFe_2$ this number is reduced, on the average, to about 6.7 in the amorphous state.[3] From our T = 4.2 K measurements we find a reduction in H_{eff} (Dy-161) of 0.5 MOe and a reduction in $e^2qQ/2$ of

about 2 cm/s in going from the crystalline to the amorphous state. If we attribute the decreases in H_{eff} to a change in the number of nearest neighbors, we find that H_{eff} is reduced by 75 kOe for each Fe neighbor removed. On the other hand, if the decrease is due to a reduction in (J_Z), then our results would imply a possible 6 percent decrease in the Dy moment.

1. L. L. Isaacs, D. J. Lam and F. Y. Fradin, J. Appl. Phys. 42, 1458 (1971).

2. J. J. Rhyne and R. Abbundi, private communication.

3. G. S. Cargill, AIP Conf. Proc. Series XVIII, 631 (1973).

4. J. J. Rhyne, S. J. Pickart and H. A. Alperin, Phys. Rev. Letters 29, 1562 (1972).

5. J. J. Rhyne, J. H. Schelleng and N. C. Koon, Phys. Rev. B, 10, 4672 (1974).

6. D. Sarkar, R. Segnan, E. K. Cornell, E. Callen, R. Harris, M. Plischke and M. J. Zuckerman, Phys. Rev. Letters 32, 542 (1974) (and references contained therein).

7. G. J. Bowden, D. St. P. Bunbury, A. P. Guimares and R. E. Snyder, J. Phys. C. (Proc. Phys. Soc.) 1, 1376 (1968).

SMALL ANGLE SCATTERING

C. S. Schneider
(U.S. Naval Academy, Annapolis, MD)

The prism refraction results for Ge, Cu, and O (using a quartz prism) have been reported for publication as b_{Ge}=8.1929(17) fm, b_{Cu}=7.689(6) fm and b_O=5.832(2) fm. The germanium amplitude agrees well with Shull's pendellösung result; the copper value is higher precision in agreement and the oxygen value is higher precision standing 5σ away from previous results.[2]

The small angle scattering diffractometer has been installed at BT-3 This raised beam instrument has one axis tipping on the first crystal and two axis tipping plus translation on the second crystal yielding a flux of roughly 3×10^5 n/cm^{2}s of Be filtered 4.0Å neutrons using a pair of 3° mosaic pyrolytic graphite crystals to extract the beam. The intensity passed through the following horizontal pair of silicon crystals (50 second mosaic) is 6×10^4 n/min which should be slightly improved when higher quality graphite crystals are used. A pair of germanium crystals have been prepared for a three-bounce (111) Bonse-Hart reflection and should yield about 10^4 n/min over the Darwin width with a sixth power angular tail decrease. This diffractometer can then resolve spherical defects well above one micron in size.

The procedure for data inversion of this nearly infinite slit height system by Mellin transform[3] has been computerized and studies have been completed on the "ringing" of defect density results due to upper and lower truncation of the data range and finite step size. A first application of the system will not involve inversion of intensity profiles but rather variation of intensity scattered at a fixed angle due to a Christiansen filter containing U-235 O_2 powder. This is a variation on the excellent technique developed in Germany[4] during this decade.

---

1. C. G. Shull and W. M. Shaw, *Zeit. fur Naturforschung*, 28, 657-661 (1973).

2. R. E. Donaldson, L. Passell, W. Bartolini and D. Groves, *Phys. Rev.* 138B, 1116-1119 (1965).

3. J. Riseman, *Acta Cryst.* 5, 193-196 (1951).

4. L. Koester and K. Knopf, *Zeit. fur Naturforschung*, 27a, 901 (1972).

A DIFFRACTION STUDY OF AMORPHOUS MATERIALS

G. A. Ferguson, J. H. Konnert and J. Karle
(Naval Research Laboratory, Washington, DC)

The neutron and x-ray diffraction technique has been employed to study vitreous samples of SiO_2, GeO_2, $KAlSi_3O_8$ and $NaAlSi_3O_8$. The information obtainable from analysis of these diffraction data is the distribution of interatomic distances expressed in the form of a radial distribution function. Details of the newly developed data reduction procedures which have yielded heretofore unseen detail in the radial distribution function for vitreous samples have been published elsewhere (1,2,3,4). The results obtained for silica (SiO_2) and germani (GeO_2), given in figure 1, show significant deviations from a uniform distribution of interatomic distances out to approximately 20 Å. The consequence of this evidence is that appreciably greater ordering exists than has been previously reported for these vitreous systems (5,6). Furthermore, serious doubt is raised that such systems can be accurately described by a continuous network of individual tetrahedra connected together randomly and restricted only by the steric hindrance of the local environment with prescribed bond angle limitations (5).

Glasses of the composition $NaAlSi_3O_8$ and $KAlSi_3O_8$ have been investigated. The radial distribution functions for these materials indicate that the basic structure of silica glass is preserved in these glasses. The Al atoms replace some of the Si atoms at the centers of the silicate tetrahedra and the Na and K atoms fill in the interstices in the network. Studies of the macroscopic properties of solid solutions of these glasses have revealed that they are closely related structurally. In order to estimate the extent to which the $NaAlSi_3O_8$ and $KAlSi_3O_8$ glasses are isostructural, neutron diffraction experiments were performed. Since the neutron scattering factors for Na and K are nearly identical ($0.35 \times 10^{12} cm^2$ and $0.351 \times 10^{-12} cm^2$, respectively) it is expected that similar radial distribution functions

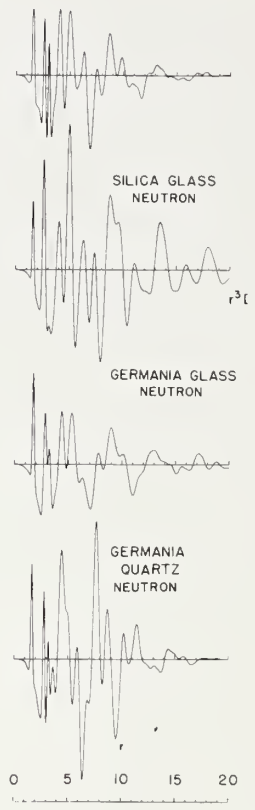

Figure 1. Radial distribution functions for silica and germania.

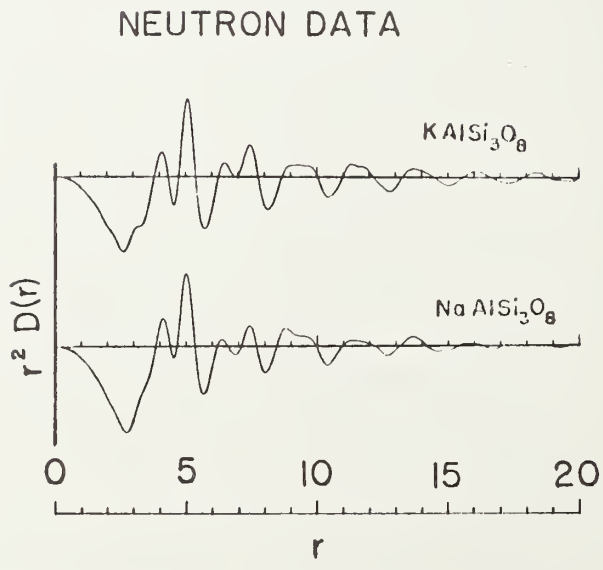

Figure 2. Radial distribution functions from neutron scattering for $KAlSi_3O_8$ and $NaAlSi_3O_8$.

would be obtained. The distribution functions obtained are given in figure 2. It is seen that the results for both glasses are comparable in the region $0<r<12$ Å. Beyond this point the maxima and minima are seen to occur at approximately the same r-values although those for $NaAlSi_3O_8$ damp rapidly. This result implies that the structure of the $NaAlSi_3O_8$ and $KAlSi_3O_8$ glasses are similar, but the $KAlSi_3O_8$ is somewhat more ordered, perhaps as a consequence of the presence of the larger K ion.

APPLICATION OF ROBUST/RESISTANT TECHNIQUES TO CRYSTAL STRUCTURE REFINEMENT

E. Prince

and

W. L. Nicholson
(Battelle Pacific Northwest Laboratories, Richland, WA)

A technique for fitting a theoretical model to a set of experimental data points, and estimating the best values of adjustable parameters in the model, is said to be "robust" if it is applicable for a broad class of distributions for the errors in experimental data, and "resistant" if the estimates are not highly dependent on any small subset of the experimental data. The method of least squares, the method most commonly used for refining crystal structures, possesses neither of these properties. Least squares is an excellent fitting technique for normally distributed errors. With broad tailed error distributions and/or the presence of a few bad data points in a large data set least squares can give anomalous results. In recent years statisticians have been developing methods of fitting and parameter estimation which work nearly as well as least squares for ideal data sets but which are robust and resistant.

The method of least-squares is based on finding the minimum value of the quantity $\sum_i w_i(y_{io}-y_{ic})^2$, where y_{io} is the value of an observed data point, y_{ic} is a calculated value of that point based on some theoretical

function containing adjustable parameters, and w_i is a weight. For the method to work well the weight, w_i, must be proportional to $1/\sigma_i^2$, where σ_i^2 is the variance of the observation y_{io}. This variance is, however, usually not known *a priori*, but is approximated by a formula containing a term arising from an assumed Poisson distribution of random counts and one or more other terms which estimate additional experimental error associated with the observed value, y_{io}. "Robust" implies an insensitivity to small errors in this approximation spread over the entire data set, whereas "resistant" implies an insensitivity to the presence of a small subset in which the variance is grossly underestimated.

The response of a refinement technique may be modified by adjusting the weights according to the formula like $w'=wW(x)$, where $x=(y_{io}-y_{ic})/K\hat{\sigma}_i$, $\hat{\sigma}_i$ is the standard deviation approximated as described above, and K is a constant. The function W(x) will be called a W-function. Tukey[1] has described certain characteristics a W-function should have in order to make the refinement procedure robust/resistant. For small values of x the procedure should closely resemble least-squares. For large values of x, that data point should be ignored, which means W(x)=0 for large x. In between the function should fill in smoothly. We can express these conditions mathematically by the following stipulations:

1. $W(x)=W(-x)$. (The function is even in x.)
2. $W(0)=1$.
3. $W'(0)=0$.
4. $W(X)\equiv 0$, $|x|\geq 1$.
5. $W'(1)=0$ (Many W functions don't have this property).
6. $W'(x)\leq 0$, $0\leq x\leq 1$.

The crystallographic least-squares program RFINE[2] has been modified to include, as an option, a W-function of the form $W(x)=1-3x^4+2x^6(|x|\leq 1)$, which, in addition to the conditions above, satisfies an additional condition $W''(0)=0$. This function has been used in several refinements in which there was initial difficulty in getting the structure to converge.

In particular, the data set for lead deuterium orthophosphate[3] was studied in some detail in order to determine an appropriate value for the constant, K, which appears tin the W function. Good results were obtained by setting $K=3.5R_q$, where R_q is the "Interquartile range," the range of values of $\Delta F_i/\hat{\sigma}_i$ which includes the middle half of the data. It should be noted that for an "ideal" data set, with normally distributed errors, $R_q/1.348$ is an unbiased estimate of $\hat{\sigma}$, the estimated standard deviation of an observation of unit weight. Therefore with such a data set the W-function will alter the weights for more than 97% of the data by less than 9%.

The robust/resistant methods will be used to repeat the refinements of the structure of D(+)-tartaric acid originally carried out by Hamilton and Abrahams[4] as part of the single-crystal intensity project of the International Union of Crystallography. We hope to determine whether the differences in refined parameters found in that project, some of which were rather large, can be reduced by application of robust/resistant methods.

---

1. J. W. Tukey in Critical Evaluation of Chemical and Physical Structural Information, National Academy of Sciences, Washington, DC, 1974.
2. L. W. Finger and E. Prince, NBS Tech. Note 854 (1975).
3. C. S. Brickenkamp and E. Prince, NBS Tech. Note 860, p. 55 (1975).
4. W. C. Hamilton and S. C. Abrahams, *Acta. Cryst.*, A26, 18, (1970).

BT-4 THREE AXIS NEUTRON SPECTROMETER

A. Cinquepalma, W. Rymes, A. Tudgay, J. M. Rowe, J. J. Rush

and

H. Prask and S. Trevino
(Picatinny Arsenal, Dover, NJ)

This three axis neutron spectrometer is now in operation. Preliminary calibration experiments show that the flux at the sample is $\sim 10^7$ neutrons per cm^2 per second at an energy of 14 meV with an energy resolution

of ∿12%, and $3x10^6$ neutrons per cm^2 per second at an energy of 14 meV with an energy resolution of ∿4%.

Initially, the spectrometer will employ one complete analyzer system, rather than the two systems which were designed and manufactured for it.

It was decided that the benefits to be derived from the improvement of the BT-6 three axis spectrometer by the installation of this new analyzer far outweighed its use as an anti-parallel analyzer on the BT-4 machine at this time. The anti-parallel arm, with its motor and drive system, is installed and ready to accept another analyzer in the future.

The final shielding configuration which includes a traveling beam stop, allows unrestricted changes of 2θ from 20° to 79°, or from 35° to 94°. Either of these ranges may be selected by the insertion or removal of one readily accessible shield and the relocation of two limit switches and stops.

The safey systems which have been incorporated into this spectrometer include; mechanical latches which prevent the dropping, through electrical or pneumatic malfunction, of any of eight traveling shutter segments that are capable of rotating out from behind the saddle shield; a latch "scram" circuit which senses any traveling shutter segment which is not latched "up;" and dual gamma sensing meters, with set point interlocks, located at the edge of the saddle shield in order to sense the approach of a "down" shutter segment. The latch "scram" interlock and the redundant gamma interlocks form an AND gate. Loss of any of these contact closures, or loss of line power, causes immediate closure of the inlet beam shutter, which is raised pneumatically only when a spring return air solenoid valve is powered "on."

A HIGH PRESSURE SYSTEM FOR NEUTRON DIFFRACTION

M. K. Farr, S. F. Trevino, and H. J. Prask
(Picatinny Arsenal, Dover, N. J.)

and

W. B. Daniels
(U. of Delaware, Newark, Del.)

A high pressure system for use in various neutron diffraction experiments has been completed. The system is capable of generating hydrostatis pressures up to 7 kbars at room temperature in the present aluminum sample cell. The cell can be mounted on a conventional neutron diffractometer or triple axis spectrometer.

The system consists of a 10 kbar handpump[1] connected to an aluminum sample cell via a stainless steel capillary tube. A fluorocarbon fluid is used as the pressure transmitting liquid. A manganin manometer is incorporated into the pump body to monitor the pressure.

The observed loss in intensity due to the cell and fluid is only 25-30%. The high pressure system could be used up to 10 kbar with a proposed steel cell but the loss in intensity would be 60-70%.

1. W. B. Daniels, Rev. Sci. Instr. 37, 1502 (1966).

ACTIVATION ANALYSIS: SUMMARY OF 1975 ACTIVITIES

Harry L. Rook
(Analytical Chemistry Division)

The Activation Analysis Section has twelve full time employees located in the NBS Reactor facility. Of these employees, eight are research scientists, three are technical support personnel and one is on sabbatical leave from Washington State University.

The Activation Analysis Section, in support of the Analytical Chemistry Division, conducts research and analyses in four basic program areas.

Basic Research in Nuclear Analytical Chemistry

This activity is primarily aimed at improving the analytical measurement system using nuclear techniques. This includes analytical method development, improvement in radiochemical separation schemes, and all relevant areas of analytical quantitation. The end result of this activity is to have a constantly expanding analytical capability which can be applied to all areas of elemental analysis.

Analytical Research Applied to Specific Programs

This activity utilizes the section's analytical capability to provide reliable analytical data in the study of systems dependent on trace element composition. Many programs in materials research, environmental studies, and clinical chemistry require a complete understanding of trace element composition in order to define their role in the system under study. The analytical data provided by the Activation Analysis Section combined with that of other analytical techniques provide this essential information.

Analytical Support for the SRM Program

Analyses performed on new Standard Reference Materials (SRM's) are an extremely important area of the section's activity. Extreme emphasis is placed on the accuracy of analytical results. Confidence in results provided by the Activation Analysis Section has been built over many years of careful work and every effort is expended to maintain and build on this confidence.

Service Analysis

Service analyses are a small but important part of the section's analytical program. As a general rule, service analyses are only undertaken when the analytical capability cannot be conveniently obtained by a commercial laboratory or when the analysis will expedite an NBS program. There are many cases where, in conjunction with other techniques of the Analytical Chemistry Division, a unique measurement has been made. This is especially true where highly accurate results are of prime importance.

Summaries of the work completed this year in the four basic program areas will be included. More detailed descriptions of specific projects can be obtained from literature references or individual program reports.

1. Basic Research in Nuclear Analytical Chemistry

   a. Instrumental Neutron Activation Analysis

      R. M. Lindstrom and H. L. Rook

For the determination of many elements in suitable matrices by neutron activation, radiochemistry is not always required. In the most favorable cases it is only necessary to irradiate samples and appropriate standards and to assay the resulting radioactivity with high-resolution

semi-conductor gamma detectors. Savings in time and effort, especially for routine analyses, are considerable once the method has been developed to be of the desired level of reliability. Considerable effort has been expended in the past year to provide this reliability.

The equipment required for this type of analysis, in addition to the NBSR, consists of Ge(Li) detectors coupled with means for automatic and accurate positioning of samples, multichannel pulse-height analyzers with live-time and time-of-day clocks, and magnetic tape data recorders.

A crucial operation in any instrumental analysis is the reduction of raw spectral data into final analytical results. The analyst, in cooperation with his surrogate, the computer, is required to make judgments on the qualitative and quantitative suitability of the data and must choose the best of several possible means of analyzing the information at hand. For our spectra, which usually contain 4096 six-digit numbers from which dozens of peak areas and positions must be extracted, a large computer program is indispensable. Spectral data are processed at the NBS Computer Science Center by the computer code QLN1, developed on contract by H. Yule (NUS Corporation) for this purpose. The program performs extensive qualitative analysis of the data for the identification of peak characteristics of the isotopes sought. The quantitative comparison of the appropriate peak areas in samples and standards to arrive at elemental concentration and error estimates are performed for specified element following qualitative analysis. This code is in a continual process of refinement, but for well-resolved peaks the reproducibility and accuracy are excellent, and clearly superior to hand calculations. Much attention must still be paid by the analyst to the quality of the input data to the program. However, this essential feature of the instrumental analytical process is common to all methods of spectral data analysis.

The instrumental analysis process has been applied extensively to date in the LESL Headlight Glass Program,, in the analysis of new biological Standard Reference Materials, and in several smaller sets of

service analyses. Standard conditions of irradiation and counting are in the process of definition in order to remove the present requirements that standards be irradiated anew for each new unknown sample in routine service analysis. To date eight elements (As, Cd, Cl, Cr, Cn, K, Mn, and Na) have defined standard sensitivities.

b. The Determination of Iodine-129 at Natural Levels

H. L. Rook, J. E. Suddueth and D. A. Becker

Iodine-129 levels have been determined and reported in biological materials that naturally accumulate iodine, such as animal thyroid and kelp. However, published procedures have insufficient sensitivity to determine I-129 in other environmental and biological matrices. This work was undertaken to demonstrate the feasibility of using a mass separator to lower the detection limit for the determination of I-129. It can be calculated that if I-130 is separated free of other radioactivity , less than 10^{-14} gram of I-129 can be detected using low level β-γ coincidence sum counting techniques. Mass separation is an extremely important tool as it can be the only means of separating I-130 from other iodine isotopes in the irradiation products. This fact, plus the virtual elimination of other radioacitve contaminants such as Br-82, accounts for the improved sensitivity.

In this project, the total analytical procedure for the quantitative analysis of I-129 was reviewed and improved wherever possible:

- a revised preseparation of total iodine was developed based on a sample combustion and quantitative isolation of iodine.
- a substantial reduction of system blank was demonstrated by preirradiation operation in a Class 100 clean room;
- design changes were made on the mass separator which resulted in substantially improved yields;

- the mass separator operation was optimized and data were obtained on yields, intermass contamination and memory;
- an improved procedure for β-γ coincidence counting was devised where the I-130 was directly implanted into β scintillator material;
- finally, real samples were run to give realistic estimates of the detection limit, blank level and its variations, and levels of I-129 in selected environmental matrices.

With all of the individual components of the analytical scheme worked out and tested with tracers, analyses were conducted for I-129 content of two natural samples. One sample was a freeze-dried hog thyroid, obtained from the U.S. Department of Agriculture, which represented samples naturally enriched in total iodine. The second was a freeze-dried, filleted albacore tuna fish sample, which is currently being developed at NBS as a trace element research material and on which numerous trace element studies have been conducted.

Initial analyses were carried out in a specially cleaned fume hood in a normal working laboratory area. One run each was carried out on the hog thyroid and tuna fish. The analyses were preceded and followed by blank runs where the entire procedure was carried out with empty, cleaned equipment (boats, combustion tubes, charcoal traps, etc.). The results are shown in table 1. As can be seen from the blanks with their associated variability, the system blank was the major limitation on the analytical system. One problem was that I-129 standard solutions which were many orders of magnitude higher than normal levels, had been prepared in an adjacent laboratory area and thus contamination of the entire laboratory area was possible.

Table 1. System Blank for Normal Laboratory Operation

Sample	Wt sample, g	Concentration, g I-129/g sample
Blank	≡ 1.0	2.2×10^{-10}
Tuna	0.973	1.7×10^{-11}
Hog Thyroid	2.131	4.2×10^{-11}
Blank	≡ 1.0	2.5×10^{-11}

In light of the severe blank problem, the entire sample preparation and preseparation apparatus was cleaned and moved in a Class 100 clean room. All sample manipulations were carried out in the clean room. Only after the preseparated samples were sealed in quartz were they removed from the clean room facility.

Analysis on the hog thyroid and tuna standard were repeated and a significant reduction in blank was observed. The results are given in table 2. As can be seen, blank levels were reduced by almost three orders of magnitude by adopting clean room operation. These blank levels were limited by variations in background counting statistics and thus could be lowered by subjecting the samples to higher neutron doses. For these samples, however, that was not necessary. The samples contained significant activity above background levels. These analyses, although limited in number, have conclusively demonstrated the ability of determining as little as 10^8 total atoms of I-129 in real biological matrices. This sensitivity is extremely important if samples of biological origin, other than iodine concentrators such as kelp and thyroid, are to be analyzed.

Table 2. I-129 Analytical Results

Sample	Wt sample, g	Concentration, g I-129/b sample
Blank	≡ 1.0	8.5×10^{-14}
Hog Thyroid	1.91	9.0×10^{-12}
Tuna	1.22	9.3×10^{-13}
Tuna	1.53	7.9×10^{-13}
Blank	≡ 1.0	4.5×10^{-14}

More detailed information on this work was published in *Analytical Chemistry*, 47, 1557 (1975).

c. Thorium Determination in Glass by the Nuclear Track Technique

B. S. Carpenter and G. M. Reimer

The Nuclear Track Technique has been applied for the determination of thorium in glasses. Two irradiations were performed. The first was with a thermalized flux to determine the uranium content via fission of U-235. The second irradiation was with a fast flux to induce the fission of thorium, in addition to uranium. By comparing track densities of both irradiations to a uranium standard, the "track excess" of the second irradiation was related to the thorium content. The accuracy was dependent on the Th/U ratio. The uncertainty for the Th/U ratio of 4 was approximately 20 percent and increased as the ratio decreased. Results obtained by this procedure on various samples and standard materials are given in table 1.

A complete account of this work was published in *Nature*, 247, 101, (1974).

Table 1. Thorium and Uranium Content by Nuclear Track Analysis

Sample	Th (ppm by weight)[a]	U (ppm by weight)	U isotopic ratio 8/5	Th (other method, ppm by weight)	density g/cm^3
La 1	87±7	0.015[b]	natural	76[c]	3.60
La 2	265±33	-[d]	"	-	3.56
La 3	466±56	0.015[b,c]	"	462[c]	3.58
La 4	712±60	-[d]	"	-	3.61
La 5	920±65	-[d]	"	-	3.55
T-1	31.5±1.0	0.046	189	31[c]	2.28
				40.6[g]	
K2a	0.42±0.04	0.345[e,f]	natural	0.352[f]	2.03
614 SRM		0.823[b,c]	387	0.746[c]	2.55

a errors are 1 standard deviation based on track counting statistics

b nuclear track determination

c isotopic dilution mass spectrometry

d since all the lanthanum glasses were made from the same base melt, it was assumed that the U content did not vary for the series of glasses

e X-ray fluorescence

f neutron activation analysis

g using α irradiation, see reference (10)

d. Selective Radiochemical Separation of Chromium

L. T. McClendon

Chromium has now been identified as a essential trace element in human nutrition. Conversely at high concentrations, or in different chemical states, it can cause deleterious or toxic effects. There is

thus a definite need for reliable methods of analysis for chromium at the trace level. A recent laboratory intercomparison of fossil fuels (coal, fly ash, fuel oil), which was conducted jointly by the Environmental Protection Agency and the National Bureau of Standards pointed up the unfortunate state of chromium determinations as performed by most of the analytical community. Three standard analytical techniques were used in the intercomparison, atomic absorption, emission spectrometry, and activation analysis. Of the twenty-two laboratories which reported results for chromium in fly ash only two were within the NBS recommended value of 131 ± 2 μg/g. The others ranged from 21 μg/g to 289 μg/g, with no discernible pattern. As a result of these round robin analyses, and other similar analytical discrepancies, it has become evident that more biological and environmental materials needed to be studied and certified for their chromium content.

When conducting NAA on samples containing less than one μg/g chromium, a radiochemical separation is almost obligatory to optimize the sensitivity and to eliminate interferences.

A destructive NAA technique, using tribenzylamine-chloroform solution to extract chromium, was developed at NBS and used to determine the chromium content in five materials--fly ash, coal, orchard leaves, urine, and bovine liver. This technique involves four basic steps: (1) irradiation; (2) dissolution with $HClO_4$-HNO_3 mixture; (3) extraction of Cr VI with a 1% tribenzylamine-chloroform solution; and (4) counting the activity of the 320 keV γ-ray of Cr-51. Tables 1-3 show the results obtained in fly ash, coal and orchard leaves using this technique.

This method is selective for Cr VI, thus for samples not requiring processing which might alter the oxidation state of the chromium this technique could allow determination of the relative amounts of Cr (III) and Cr (VI) in the sample.

A complete description of this work was published in *Trace Substances in Environmental Health*, VIII, (1974), D. D. Hemphill, Ed., University of Missouri, Columbia p. 255-257.

Table 1. Concentration of Chromium in Fly Ash

Sample #	µg/g
1	132.8
2	132.1
3	131.2
4	132.6
5	132.3
6	132.7

$\bar{X}$ = 132.3 ± 0.35*

Recommended Value 131 ± 2 µg/g

* Error expressed as $\frac{ts}{\sqrt{n}}$ at the 95% confidence level.

Table 2. Concentration of Chromium in Coal

Sample #	µg/g
1	19.28
2	20.35
3	20.44
4	20.29
5	19.57
6	21.06

$\bar{X}$ = 20.17 ± 0.76*

Recommended Value

20.2 ± 0.5 µg/g

* Error expressed as $\frac{ts}{\sqrt{n}}$ at the 95% confidence level.

Table 3. Concentration of Chromium in Orchard Leaves

Sample #	µg/g
1	2.490
2	2.472
3	2.410
4	2.447
5	2.484
6	2.433
7	2.463
8	2.481

$\bar{X} = 2.460 \pm 0.025$*

Recommended Value

2.6 ± 0.2 µg/g

* Error expressed as $\frac{ts}{\sqrt{n}}$ at the 95% confidence level.

e. A Spontaneous Deposition Radiochemical Separation for Platinum Determination in Biological Materials

D. A. Becker, P. D. LaFleur, and A. LeRoy

The spontaneous deposition technique has been used a number of times for radiochemical separations in activation analysis (1, 2). It has also been used as a preirradiation chemical separation method (3). Although this technique has been used for the analysis of one or more noble metals from inorganic materials (2) and metals (3), this technique apparently has not been applied to the determination of the noble metals in biological materials.

The use of platinum and possibly other noble metals in motor vehicle emission control systems has recently been implemented. It thus becomes

imperative that accurate and sensitive methods for the determination of these elements be available for the evaluation of environmental baseline levels and any real or imagined increases in these levels.

The method developed is capable of quantitatively determining gold, platinum and palladium in a wide variety of biological and environmental matrices. This technique is also currently being evaluated for possible use in the determination of additional noble metals simultaneously.

The analytical procedure entails wet-ashing with nitric-perchloric acids with carriers (including copper holdback carrier), redissolving the residue in aqua regia, and then plating out a silver metal powder. The removal of the noble metals can be accomplished using either the batch method, or by passing through a column of the silver particles suspended on cellulose or asbestos fibers.

Tracer studies made using this procedure showed quantitative recovery (>99.5%) for the AU-198, AU-199, and PD-109, for both the batch and the column methods.

The application of this technique to biological samples at first resulted in radioactive contamination of the silver powder with Cu-64 radioisotope. Subsequent modification of the technique to use copper holdback carrier and an ammonium hydroxide wash reduced this copper radioactivity to negligible levels.

This analytical system has been applied to the determination of gold, platinum and palladium in several biological materials.

Preliminary results on the analyses of animal tissue and botanical samples gave 1.8 and 0.2 ng/g for gold, <15 and <9 ng/g for platinum, respectively, while all palladium results were $\leq$1 ng/g. These analyses were made using a neutron flux of 5×10^{13} $n \cdot cm^{-2}$ s^{-1} for 1 hour, and counting on a 16% efficient Ge(Li) detector or LEPS system.

The results of this work are being presented at the 1975 International Nuclear and Atomic Activation Analysis Conference held in Gatlinburg, Tennessee.

f. The Simultaneous Determination of Tellurium and Uranium

E. S. Gladney and H. L. Rook

Tellurium and uranium have not been shown to play essential roles in the trace element biochemistry of higher animals. Rather, both elements are potent biotoxins. Information on the toxicology of tellurium is limited, but it is believed to resemble arsenic more than selenium in its toxic action. Tellurium binds uniformly to soluble proteins in the blood, has been implicated in nerve and brain damage in rats, and is readily transported across the placental barrier. Reduction in general activity and in longevity has been demonstrated in mice fed sub-toxic doses of tellurium in water, but no influence on carcinogenicity or on the production of other tumor types was observed. No other data appear to have been accumulated regarding the effects of long-term low-level exposures of tellurium to mammals.

The toxicology of uranium has been extensively investigated. In addition to the radiation hazard, the ingestion of uranium and its compounds has been implicated in arterial, kidney, and liver damage.

Few analytical techniques have the demonstrated sensitivity to permit the study of tellurium in biological and environmental materials at naturally occurring levels.

Atomic absorption spectrometry has been utilized to determine tellurium, generally above the μg/g concentration level , but again this technique does not have the sensitivity necessary to determine tellurium in most biological and environmental matrices without a pre-concentration step.

In this work, both tellurium and uranium were analyzed using a combustion method followed by gas phase separation of iodine-130, a decay product of tellurium-130. The procedure was adapted from a separation originally developed for the determination of mercury. Four principal advantages over currently used techniques have been attained. This procedure requires a minimum of chemical manipulations, thereby

reducing the chances of technique related errors; the separation of radioiodine is quantitative, eliminating the need for chemical yield determinations; the procedure can be utilized with a variety of matrices without modification; and the low limits of detection, especially for tellurium, permit the characterizations of these elements at their naturally occurring levels. Even though the use of iodine fission products for the determination of uranium is itself not new, the combustion technique provides a rapid, extremely sensitive method for measuring uranium simultaneously with tellurium.

Using the analytical procedure developed, the tellurium and uranium concentrations in three NBS Standard Reference Materials were determined. These materials were: SRM 1517 Orchard Leaves, SRM 1632 Trace Elements in Coal, and SRM 1633 Trace Elements in Fly Ash. The individual results are given in tables 1 and 2, along with the NBS certified values for the uranium concentrations. It was assumed that the uranium in the SRM's had the natural isotopic abundance. The results compare well with the certified values established by the other analytical techniques.

The confirmed accuracies of the uranium values obtained by this procedure (table 1) are of vital importance in confirming the reliability of the tellurium analyses. Even though tracer studies using I-125 were run to demonstrate that the separation was quantitative, the accurate uranium results indicated that the iodine separation was in fact quantitative when using real samples. By inference, one may assume that the tellurium results are also accurate, since any errors in the iodine chemistry would have been reflected in the results of the simultaneously determined uranium.

Table 1. Uranium Concentrations of Standard Reference Materials, μg/g

	SRM 1571	SRM 1632	SRM 1633
	0.0217	0.99	9.7
	0.0244	1.17	11.9
	0.0247	0.95	12.5
	0.0319	1.13	14.3
	0.0185	1.14	12.3
	0.0300	1.08	9.5
	0.0254	1.07	14.8
Mean	0.025	1.1	12.1
s[a]	0.004	0.08	2.0
NBS certified value	0.027 ± 0.003	1.4 ± 0.1	11.6 ± 0.2

[a] s is the standard deviation of a single determination.

Table 2. Tellurium Concentrations of Standard Reference Materials, μg/g

SRM 1571	SRM 1632	SRM 1633
0.012	0.56	9.5
0.017	0.66	9.9
0.007	0.61	12.1
0.010	0.60	9.9
0.011	0.62	9.0
0.008	0.54	9.1
Mean 0.011	0.60	9.9
s[a] 0.003	0.04	1.1

[a] s is the standard deviation of a single determination

This analytical procedure has also been used to measure the tellurium and uranium concentrations on atmospheric particulates collected in rural, southeastern Maryland during August 1973. The sensitivity of this technique permitted these elements to be measured on particulates from less than 40 m^3 of air. The concentrations of tellurium, uranium and aluminum for four different days sampling are reported in table 3. The aluminum concentrations were measured by non-destructive instrumental neutron activation analysis.

Table 3. Uranium and Tellurium Concentrations on Atmospheric Particulates

	Sample date	[Al] ng/g^3	[U] pg/m^3	U EF[a]	[Te] pg/m^3	x [Te EF[a]] 10^4
14	Aug. 1973	400	39.7	2.2	260	2.5
15	Aug. 1973	280	28.9	2.3	390	5.4
16	Aug. 1973	1440	110	1.7	520	1.4
23/ 24	Aug. 1973	510	49.3	2.1	290	2.2

[a]EF = Enrichment Factor relative to Wedephol's Crustal Average.

All data have been corrected for filter blank. Atmospheric enrichment factors (EF) for tellurium and uranium, relative to Wedepohl's crustal averages, have been calculated using the method of Gordon and Zoller. The low uranium EF's indicate that the airborne uranium was probably of crustal origin. The high tellurium EF's suggest a strong, non-crustal source for this trace metal in the atmosphere. Similar high EF's have also been observed for selenium in a variety of environmental measurements.

The high EF's for these chemically similar elements suggest either poorly established crustal levels, an important natural non-crustal source, or anthropomorphic pollution. The tellurium results are comparable with the only previously reported atmospheric measurement of

<0.8 ng/m^3 in College Park, Maryland.

A complete description of this work has been published in *Anal. Chem.*, 47, 1554, (1975).

g. Fission-Track Determination of Uranium in Solutions

B. S. Carpenter, G. M. Reimer, and R. Z. Zielinski

A fission-track procedure which permits the routine determination of <1.0 part-per-million uranium concentrations in solutions has been developed. As little as 1.0 ml of sample or standard is required. The solution is placed in polyethylene tubing or a snap-cap vial. A track detector is submerged; the container is heat sealed and irradiated with thermal neutrons to induce fission of uranium-235. Detectors are low-uranium plastics or fused quartz platelets, the selection depending on the nature of the sample and the irradiation conditions. After irradiation, the detectors are removed and chemically etched, and the enlarged tracks are counted with an optical microscope. The concentration of uranium is proportional to track densities and can be determined in a unknown by comparing track densities in its detector to track densities in the detector of a standard solution, providing the irradiation conditions were identical. Total uranium is determined by consideration of the uranium isotopic ratio which can be regarded as natural for most solutions.

Present sensitivity of the method allows determination of uranium concentrations of 10 μg per liter with an estimated coefficent of variation of 10 percent. Sensitivity can be improved by analyzing liquid concentrations. Initial applications of this technique are determination of the uranium in natural waters and in experimental leach solutions.

2. Analytical Research Applied to Specific NBS Programs

a. Trace Element Profile in Auto Headlamp Glass

L. T. McClendon and T. E. Gills

In cooperation with the NBS Law Enforcement Standards Laboratory (LESL), the Activation Analysis Section has completed a program to evaluate the feasibility of identifying glass from a common origin. Automobile headlamp glass was chosen as a test case because automobile headlamp glass fragments are frequently obtained as evidence specimens in various kinds of criminal investigations, particularly from automobiles involved in hit-and-run accidents. Glass fragments from the suspect's vehicle, when found at the crime scene, provide evidence to be compared for simularities. Conventional criminalistic techniques, such as the measurement of the refractive index of the glass fragments in question, are quite helpful, however, more points of comparison are often necessary for positive identification.

Previous studies of trace elements in window glass have established the potential value of multi-element analysis for the identification and characterization of various glass types. However, these studies were made without the advantages of the modern, sophisticated analytical instruments available today. With these recent advances in analytical instrumentation, greatly improved sensitivity and specificity can now be obtained for multi-element analyses.

The technique used for this work, neutron activation analysis coupled with high resolution gamma-ray spectroscopy, has been proven to have several distinct advantages, including its excellent sensitivity for many trace elements and the obtainable accuracy and precision (5-10% overall) at the trace level. This technique also has the flexibility to allow for multielement analysis of a sample and still preserve the sample for future reference. In the case of criminalistic investigations, preservation of the evidence for court examination is a desirable feature.

To assess the distribution of trace elements in auto headlamp glass, one hundred sixty-four (164) different fragments, representing thirty-six (36) headlamps have been analyzed for 10-12 trace elements using instrumental neutron activation analysis. The headlamps analyzed were representative of the two major American manufacturers, Corning and General Electric.

The data obtained on the auto headlamps analyzed indicate that: (1) consistent analytical precison can be obtained on small headlamp glass samples using the INAA technique; (2) auto headlamp glass manufactured by both Corning and General Electric is homogeneous for the major constituent (Na) and relatively homogeneous for the trace elements; (3) the trace element content of one headlamp vs any other has been shown to differ appreciably under controlled experimental conditions, demonstrating the feasibility of individualization of auto headlamps; and (4) general trace element content of Corning manufactured headlamps is not unique compared to those manufactured by General Electric, indicating the probability of class characterization through a trace element profile is relatively small.

An overall evaluation of the data obtained in this study indicated the trace element profile of automobile headlamp glass fragments using the neutron activation analysis technique could provide unambiguous identification for forensic purposes. A manuscript for publication in *Analytical Chemistry*, describing this study in detail, is in preparation.

b. Assessment of Gunshot Residue Methodology

T. E. Gills, P. D. LaFleur, and D. A. Becker

The method of gunshot residue analysis can be a powerful tool in helping to establish the innocence-or-guilt of an accused person. Ruch, et. al., demonstrated the practicality of using neutron activation to detect such residue deposits, which are indicated by barium and antimony, at very low concentrations. On numerous occasions law enforcement agencies have introduced GSR test results in court as an aid in pros-

ecution. Not only do prosecutors use it as an aid to convict or to interrogate, but defense attorneys are finding it practical to use it to exonerate a suspect.

While many methods can satisfy the sensitivity requirement for the elements determined in gunshot residues, a relatively few have combined both the sensitivity of a technique with a statistically-evaluated data base so as to set up criteria for determining a handgun discharge.

Many laboratories are using only the quantification of Ba and Sb as valuable GSR information and are ignoring information on the population distributions of handgun firings and the ratios of Ba and Sb. Because of these facts, the reliability of GSR tests has been seriously questioned.

Recently, in support of the Law Enforcement Standards Laboratory at NBS, the Activation Analysis Section has become involved in assessing current GSR methodology. The main objective was to develop and/or recommend a practical sampling and analysis procedure for gunshot residue tests which had been evaluated to give statistically reliable results. With this objective in mind, the Activation Analysis Section undertook a program to review the current analytical methodology, improve it where possible and to provide an extensive data base on both general population blank levels and post handgun firing levels of barium and antimony.

At the onset of this work, consultations with many law enforcement officials and visits to forensic laboratories were made to document their experiences with GSR and to highlight the strengths and shortcomings of the GSR methodology. Following the review of current procedures, selected areas affecting the reliability of GSR results were researched. The areas that were studied are:

- Analytical Methodology
- Handgun Firings
- Occupational Handblanks

- Persistence and Stability of Gunshot Residue
- Data Evaluation

The data from both the handblank survey and the handgun firings were used in the formulation of a firing criterion. When the GSR measurements were made, only the barium and antimony levels were logged. Copper, though commonly found in each sample, was too ambiguous to be used in any criterion formulation.

Even though there are large variations in the firing data, correlation can be made between barium and antimony by using their concentrations and their ratios. It should be restated that in any criterion, all relevant information should be included or considered. Therefore, upon this thesis we propose to separate the firing data from the handblanks by setting up a frequency distribution relating concentrations of barium and antimony, and their ratios, to average values of each element and ratio found in a known set of firing distributions. This frequency can be set up by the formula:

$$F_{(Ba,Sb)} = \frac{B_A \times Sb_A}{C + (\lambda_A - \bar{\lambda}_B)^2}$$

Constant = an empirically selected constant that maximize F.

$\bar{\lambda}_B$ = the average barium to antimony ratio of each firing distribution, i.e., 22's, 38's, and 45's.

λ_A = the barium and antimony ratio of an individual firing.

B_A, Sb_A = respective concentration of barium and antimony found in each firing.

with such calculations the ratios and concentration of barium and antimony in actual firings are mathematically related to the average ratio of barium and antimony in known firing distributions. Using these

values, a distinct demarcation can often be observed between handblanks and firings.

A manuscript containing the complete results of this study is in preparation for the *Journal of Forensic Science*.

Two Projects have been completed in the area of water analyses. These programs were funded and coordinated by the Office of Air and Water Measurement.

c. Evaluation of Lyophilization for the Preconcentration of Natural Water Samples

S. H. Harrison and P. D. LaFleur

Neutron Activation Analysis is presently used to analyze various aquatic samples, however, the applicability of the technique to the water matrix is hindered by two main factors: very low concentrations of the elements of interest, and interferences from more concentrated dissolved species.

Except for Na and Cl in sea water, most natural waters contain such low concentrations of most elements that few can be accurately determined directly on bulk water samples by completely instrumental techniques. The sensitivity of analysis can be greatly improved by concentration of the dissolved species from the water into a different medium, or removal of water to leave a residue of the dissolved material that can be irradiated in a small sample container.

The latter approach was used by Mamuro et al. who evaporated the water prior to irradiation. Since evaporation is generally a slow process carried out in the open, it is subject to possible difficulties. These difficulties include contamination by fallout particles from laboratory atmosphere, dissolution of ions from container surfaces, and loss of volatile species if performed at an elevated temperature.

Other workers have devised chemical separation methods for removal

of specific elements from water, but these could not be applied to the multielement instrumental NAA.

The work presented here deals with the preconcentration of water by freeze drying using a method which virtually eliminates sample contamination and trace element losses. Freeze drying is a method commonly used for drying biological tissues in which trace element may be bound organically. Also, it has been used for drying natural water although without associated evaluations of the technique. However, questions may be raised regarding the suitability of this method of concentration that point to the possibility of losses of volatile elements during the drying process and the ability to transfer quantitatively the dry residue from the freeze drying container to an irradiation container.

The first question arises because it is known that some trace elements can exist in chemical forms that have significant vapor pressures at room temperature, with respect to that of water. When a sample containing such compounds is placed in a vacuum system for a extended length of time, trace element losses from the sample will most likely occur. A major object of this work was to determine if there are significant losses of various elements in water when the water is subjected to freeze drying.

To evaluate this question, known quantities of radioactive tracers for 21 elements (including many known to be volatile) were added to water, the solutions freeze dried and the tracer residues counted (table 1). The results confirm that at least 95% of all but the most volatile elements studied (Hg and I) were retained in the residue. The second question, concerning sample transfer, was eliminated by designing a freeze drying container which also would serve as an irradiation and counting container. The material chosen was liner polyethylene film (Phillips Petroleum's Marlex). The preconcentration and containment system has been used successfully in our laboratory for the INAA of river and estuarine water samples.

The results of a typical analysis of dissolved species in water by INAA following the described preconcentration procedure appear in table 2. This sample was taken from the Back River, just east of Baltimore, Maryland. The ratio of trace element content in the sample to the average trace element content in a polyethylene bag is sufficiently high for most elements to result in reliable data.

A complete report of this work has been published in *Analytical Chemistry*, 47, 1685 (1975).

Table 1. Trace Element Retention Yields for Freeze-Drying Water

Element	Isotope	n	Range, %	Average, %
Na[a]	^{24}Na	3	95.8-99.4	97.4 ± 1.8
Sc	^{46}Sc	5	91.5-103.3	97.9 ± 4.3
V	^{48}V	2	100.0-100.8	100.4 ± 0.3
Cr	^{51}Cr	4	94.3-98.5	95.9 ± 2.0
Fe	^{59}Fe	1	...	101.1
Co	^{60}Co	6	94.2-100.0	97.5 ± 2.2
Zn	^{65}Zn	1	...	102.6
As	^{74}As	6	94.8-98.5	96.3 ± 1.8
Se	^{75}Se	6	93.5-100.0	96.2 ± 1.8
Br[a]	^{82}Br	3	97.4-100.8	99.3 ± 1.7
Rb	^{86}Rb	4	99.4-103.6	101.2 ± 1.8
Sr	^{85}Sr	1	...	101
Ag	^{101m}Ag	1	...	98.1
Cd	^{109}Cd	4	94.9-113	102 ± 8
Sb	^{124}Sb	6	96.7-99.7	98.6 ± 1.1
I	^{126}I	3	46.9-88.0	68 ± 21
Cs	^{137}Cs	1	...	99.3
Ba	^{133}Ba	6	91.8-100.6	97.7 ± 3.0
Au	^{195}Au	4	92.1-95.0	94.0 ± 1.3
Hg	^{203}Hg	4	50.1-71.0	61 ± 9
Tb	^{160}Tb	1	...	98.7
Ce	^{141}Ce	2	97.5-99.1	98.3 ± 1.1

[a]Tracer solution used was not acidified.

Table 2. Results of INAA of Freeze Dried Residue of Back River Sample

Element	residue, ng/g of water	ng in Poly bag
Eu	0.24	>20
Sc	0.31	118
Th	0.089	2.5
Cr	5.4	0.51
Fe	530	30
Co	1.2	10
Sr	440	>300
Ag	0.24	7.7
Zn	12.3	3.2
Ba	<35	
Sb	0.64	6.0
Se	0.33	10
Na[a]	0.53 mg/g	
Cl[a]	0.84 mg/g	
Mn[a]	0.23 µg/g	

[a]The results for Na, Cl and Mn were obtained on a liquid sample and are presented for informational purposes only.

d. A Study to Define the Long Term Stability of A Mixed Trace Element Water Standard

H. L. Rook, J. R. Moody, P. J. Paulsen, and T. C. Rains

The National Bureau of Standards is currently developing a mixed trace element in water standard. The standard will contain approximately ten trace heavy metals of ecological significance, with emphasis on elements needing improved analytical accuracy at or below the part-per-million (10^{-6} g/g) concentration level.

As a preliminary requirement to the production and certification of this standard, a study into the long-term stability of the component trace elements at the sub part-per-million level has been carried out. Initial studies were conducted with radioactive tracers to determine possible losses to container walls and interelement interactions which might result in losses. Following this initial study, a more comprehensive investigation was carried out using simultaneous analyses by three trace analytical techniques; atomic absorption, neutron activation, and isotope dilution mass spectroscopy. This second study was designed to indicate any problems of concentration elevation due to reagent blanks or leaching of trace elements of the earlier tracer study.

e. Stability Study

A solution containing ten selected heavy metals was prepared by dissolving weighed amounts of the pure elements in acid and diluting to the desired concentration. The elements included in the standard were: As, Be, Cd, Cr, Cu, Hg, Mn, Pb, Se, and Zn. They were all at or below the μg/g concentration level. The solution was stabilized with nitric acid brought to a final concentration of 0.5 M plus approximately 10 ng/g gold ion as the chloride. The gold was added to stabilize mercury as demonstrated in previous work on trace mercury standards.

Storage containers used in this study were thoroughly cleaned by prolonged leaching with dilute nitric and hydrochloric acids. All containers were emptied of the acid mixture, rinsed, and filled with ultra pure water until used.

Five radioactive tracers were added to one liter of the stock solution and stored in one of the precleaned Teflon bottles. The elemental concentration of the tracer solutions were low enough so as not to effect the total elemental concentrations of the stock solution. The time stability study was carried out by withdrawing one ml of the solution at intermittent intervals over an eight month period. The activity of the individual tracers at a given time was decay corrected

and compared to the activity at the start of the experiment. None of the metals, except possibly cadmium, gave any indication of loss during storage (table 1). This study, although indicating negligible loss on storage, yielded no information as to potential blank problems, either from reagents or from wall leaching. To study these problems areas and to determine if there would be any analytical problems during the certification phase of this work, actual analyses of the original solution was carried out.

Table 1. Tracer Study on Long-Term Stability

Relative Concentration

Isotope	Time in Days 7	14	22	35	79	94	255
^{73}As	1.00	1.04	--	0.96	1.03	1.08	.97
^{75}Se	1.01	1.04	0.99	1.01	1.00	1.00	.98
^{203}Hg	1.00	1.03	1.03	1.01	0.98	1.00	1.03
^{109}Cd	1.00	--	0.97	0.98	0.94	0.97	0.98
^{65}Zn	0.98	1.00	1.00	1.00	1.00	1.02	1.02

The initial analyses for all elements were taken within one week of preparation of the standard. With the exception of arsenic, the results were in good agreement with the calculated concentration. Arsenic was 30 percent low and may have been lost during the preparation of the sample.

The standard was again sampled and analyzed after 17 weeks of storage in the containers. The results show that no significant loss of any element occurred over this time interval. For some elements there were apparent increases in concentration when stored in Teflon but these were within analytical uncertainties.

Bibliography

1. H. L. Rook and J. R. Moody, "Stabilization and Determination of Nanogram Quantities of Mercury in Water", Proceedings Nuclear Methods in Environmental Research. University of Missouri-Columbia (July 1974) (in press).

f. A Study of the Location and Turnover of Lithium and Biogenic Amines in Brain Using the Nuclear Track Technique
B. S. Carpenter, D. Samuel, and I. Wasserman

Experiments are being conducted to further the understanding of the neurochemistry of affective disorders by mapping the distribution and turnover of biogenic amines (dopamine, norepinphrine and serotonin) using the nuclear track technique.

The method is based on the fact that Li-6 and O-17 among the few stable isotopes that emit alpha particles when irradiated with thermal neutrons. The amount and location of these isotopes in any biological material can be determined by the alpha particle tracks left in a solid state track recorder.

In preliminary work, it has been shown that the distribution of Li in the brain and the location of biogenic amines formed by inhaling O-17 can be determined.

Further work is being conducted to elucidate the action of Li which is an effective and highly specific drug for the treatment of mania and depression. The development of O-17 labelling of biogenic amines will be used to assess their regional turnover and other parameters in response to psychoactive drugs and behaviorial situations.

3. Analytical Support for the SRM Program

The Activation Analysis Section has devoted approximately one third of the entire years' effort in support of the Standard Reference Materials (SRM's) program. This effort has been divided between the improvement of analytical methodology, some of which were summarized in the first part of this report, and the actual coordination and analytical certification of new materials.

In total, the Activation Analysis Section has reported 811 elemental concentrations in 24 different Standard Reference Materials. These analyses encompassed a variety of materials including iron, copper, coal, water, fuel oil, glasses, urine, sediment, cholesterol, serum, and five different botanical materials. For a number of the above mentioned SRM's the Activation Analysis Section was responsible for a large fraction of the trace element certification data.

4. Service Analyses

In addition to the analyses conducted in support of the Standard Reference Materials; a large number of additonal analyses were made on materials from Service Programs. These include both cooperative analyses, where the analysis was made on samples of mutual interest to NBS and some other organization, and also service analyses, where the technical expertise of the Activation Analysis Section was required by NBS or another Government agency.

During the past year the Activation Analysis Section has had a total of eight different cooperative or service analytical projects, resulting in the analysis of 74 different samples for a total of 335 determinations. These projects were in conjunction with three other NBS groups, and a number of other Government agencies, including the National Institutes of Health, the National Institute of Occupational Safety and Health, the Environmental Protection Agency, the Department of Agriculture, Naval Research Laboratory, and the Department of Transportation.

1. W. D. Kinard, D. A. Becker, and P. D. LaFleur "The Determination of Indium and Copper in SRM High Purity Gold Wire by Neutron Activation Analysis", in Activation Analysis Section: Summary of Activities, edited by P. D. LaFleur and D. A. Becker, NBS Tech. Note 548 (1970)p. 66-69.
2. D. A. Becker, "Trace Analysis for Platinum in Glasses by Neutron Activation", *Anal. Chem. Acta*, 61, 1 (1972).
3. K. S. Park, R. Gijbels, and J. Hoste, "Neutron Activation Analysis of Palladium, Platinum and Rhodium in Lead Foam", *J. Radioanalytical Chem.*, 5, 31 (1970).

NEUTRON REACTION RATES AND STANDARD NEUTRON FIELDS

J. Grundl, D. Gilliam, V. Spiegel, Jr., H. Heaton
I. Schroder, R. Dallatore
(Neutron Standards Section)

The activities of the Neutron Reacton Rates Program are centered around the reactor thermal column facility. Important efforts this past year included preparation of NBS double fission chambers for experiments undertaken at NBS and at U.S. and foreign laboratories, performing fissionable deposit mass assays, and investigations of fission chamber performance for operation in hostile neutron environments. Interaction with power reactor technology in this program is via participation in the Interlaboratory LMFBR Reaction Rate Program (ILRR). This inter-laboratory program of measurement assurance for breeder reactor fuels and materials dosimetry presented a compendium of its activities and results this year in the February, 1975, issue of Nuclear Technology which devoted the entire issue to the ILLR program. Absolute fission cross section measurements with a californium 252 fission neutron source made

Table 1. Mass Assay Results for the NBS Reference Fissionable Deposits

Designation	49I-1-2	25S-2-2	28S-2-2	28N-2-2	37S-1-1
Principal Isotope	^{239}Pu (μg)	^{235}U (μg)	^{238}U (Depleted Uranium) (μg)	^{238}U (Natural Uranium) (μg)	^{237}Np (μg)
Absolute Alpha Counting					
Quantitative deposition	104.8(11)[a]	248.0(23)	252(5)	229.8(18)	---
Decay constants of constituent isotopes	105.0(10)	247.6(36)	---	227.5(23)	118.6(20)
Thermal Fission Counting					
Comparison with ^{235}U reference deposit (25S-2-2)	106.0(17)	1.00	---	231.2(30)	---
Comparison with corresponding ANL deposit	103.5(17)	249.2(31)	---	---	117.1(10)
Assigned mass value (μg)	104.8±1.2%	248.3±1.2%	252. ±2%	230.0±1.5%	117.9±1.7%

[a]The number of parentheses is the uncertainty in the least significant digit(s).

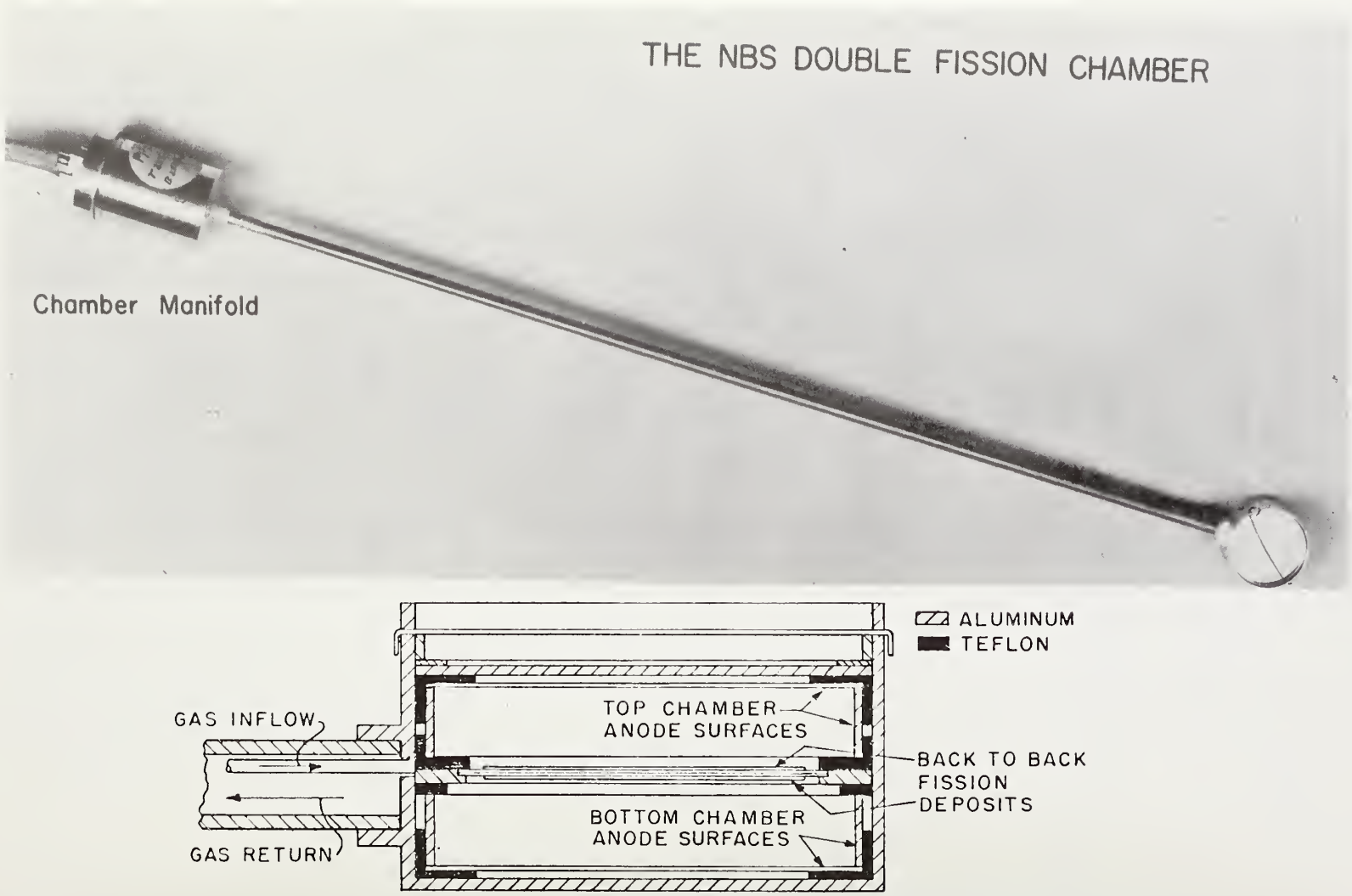

Figure 1. The drawing shows an enlarged cross-sectional view of the dual chamber head, which is seen on the right in the photograph.

use of fissionable deposit mass intercomparisons in the reactor thermal beam as did the program of international comparison of absolute fission rates measurement scales.

1. Mass Assay of NBS Fissionable Deposits

At the present time the National Bureau of Standards set of fissionable deposits includes five major isotopes, Pu-239, U-235, U-238, Np-237, and U-233. The deposits have been fabricated at four different laboratories and represent more than a dozen different batches of fissionable materials. Mass assignments for the fissionable deposits are based on interrelated measurements methods: (1) quantitative deposition from prepared solutions of known concentrations; (2) absolute alpha counting combined with isotopic assay from mass spectrometry and alpha decay constants from the literature; (3) relative fission fragment emission rates from the deposits determined with both thermal and fast neutrons. When completed each fissionable deposit will have associated with it an absolute alpha disintegration rate and a fission rate ratio which will establish the mass relative to one or more reference fissionable deposits of the same type. The reference deposits are kept aside from the normal course of programmatic fission measurements.

The components of fissionable deposit mass assay just described have been discussed in previous NBSR Annual Summaries. During this year a primary effort was undertaken to assign critically evaluated masses to the reference deposits. The final mass assignments are based on at least two independent methods of mass determination for each isotope except depleted uranium. The results are shown in table 1 where the assigned mass for each reference deposit is the weighted average of all of the independent values given. With reference deposit masses established masses for the working fissionable deposits are obtained on the basis of comparison fission counting and relative alpha counting. Standard deviations for these mass transfer determinations carried out at the NBSR thermal column are better than ±1/2 percent.

2. The NBS Double Fission Ionization Chamber

The NBS double fission chamber is a high resolution double ionization chamber of minimized volume and mass designed as a probe to measure absolute fission rates in a wide variety of neutron environments. The assembled fission chamber and enlarged cross section of the dual chamber head are shown in figure 1. The chamber contains two independent fast ionization chambers the fissionable deposits, on either platinum or quartz and positioned back to back, serve as the common grounded electrode between the chambers. In order to reduce neutron absorption and scattering effects, the electrodes and scattering elements are made of aluminum and the insulators are made of a hydrogen-free polymer. The mass of each piece has been kept to a minimum and there exists calculated geometry factors for each piece which make it possible to estimate scattering effects in both beam and isotropic neutron fields. The double chamber is designed to allow easy

Table 2. Average Fission Cross-Section Ratios for CFRMF

	Observed	Observed / Computed
$\bar{\sigma}_f(^{238}U)/\bar{\sigma}_f(^{235}U)$	0.0485±1.4%	1.138
$\bar{\sigma}_f(^{237}Np)/\bar{\sigma}_f(^{238}U)$	7.34 ±2.3%	0.975
$\bar{\sigma}_f(^{239}Pu)/\bar{\sigma}_f(^{235}U)$	1.145 ±1.5%	1.034

and repeated access for exchange of fissionable deposits. The pulse processing electronics system which has been designed for flexible use out in the field is shown in figure 2. Typical pulse height distributions for uranium deposits of different thicknesses are shown in figure 3. The pulse height distribution displays three distinct features: (1) a very broad peak with a sharp initial rise; (2) the p.h.d. valley in which the integral discriminators are set; and (3) the rising tail near

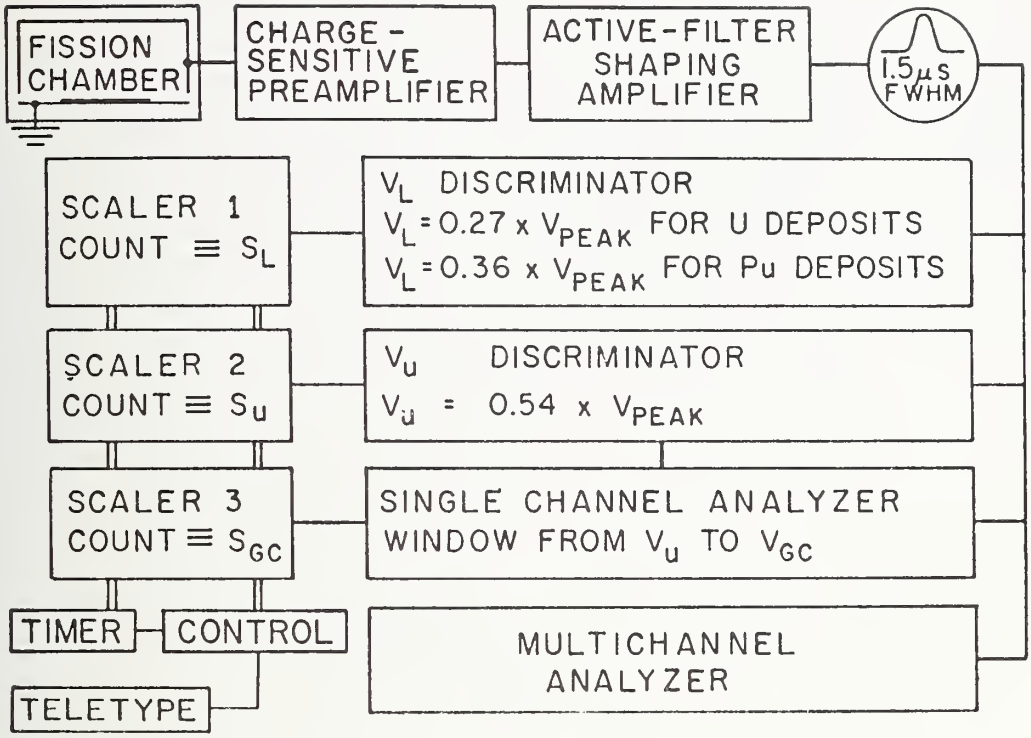

Figure 2. Each side of the dual fission chamber is monitored independently by a triple-scaler pulse-processing system as shown here. The integral discriminator counts, S_L and S_U, are the primary (redundant) counting data. The SCA count S_{GC} provides a sensitive gain check; V_{GC} = 1.37 V_{PEAK}.

zero pulse height due to alpha activity and electronic noise, etc. The correction to zero pulse height (etz) taken from the scaler data ($1-S_U/S_L$) has been found to decrease nearly linearly with decreasing deposit thickness. This dependence, established down to very thin deposits ($\sim$5 μg/cm^2) is taken presently as proper evidence that the chamber itself operates with essentially 100% detection efficiency. The reproducibility of the ($1-S_U/S_L$) data under normal conditions is such that this quantity provides a reliable indicator of the advent of any significant electronic noise above S_u. The peak-to-valley ratios of the pulse height distribution as given in figure 3 vary from 34 for a 196 μg/cm^2 deposit to 240 for a 4 μg/cm^2 deposit. Corresponding to this resolution, the counting efficiency of this chamber is highly stable even for large gain shifts. A gain shift of 10% for example leads to a change of less than 0.2% in the count rate (S_U) for deposits of up to 200 μg/cm^2 thickness.

3. Absolute Fission Rate Measurements in CFRMF

The capability to measure absolute fission rates per nucleus at a remote laboratory site (the Coupled Fast Reactivity Measurement Facility, CFRMF, at Aerojet Nuclear Corporation) has been established with the NBS double fission chamber to a precision of better than ±1 percent. This precision was sustained for a period of more than two years. During this period of time the NBS double fission chamber was used to establish absolute fission rates and to monitor a series of high level radiations designed to calibrate fission activation detectors used for breeder reactor fuels and materials dosimetry. The array of reference and

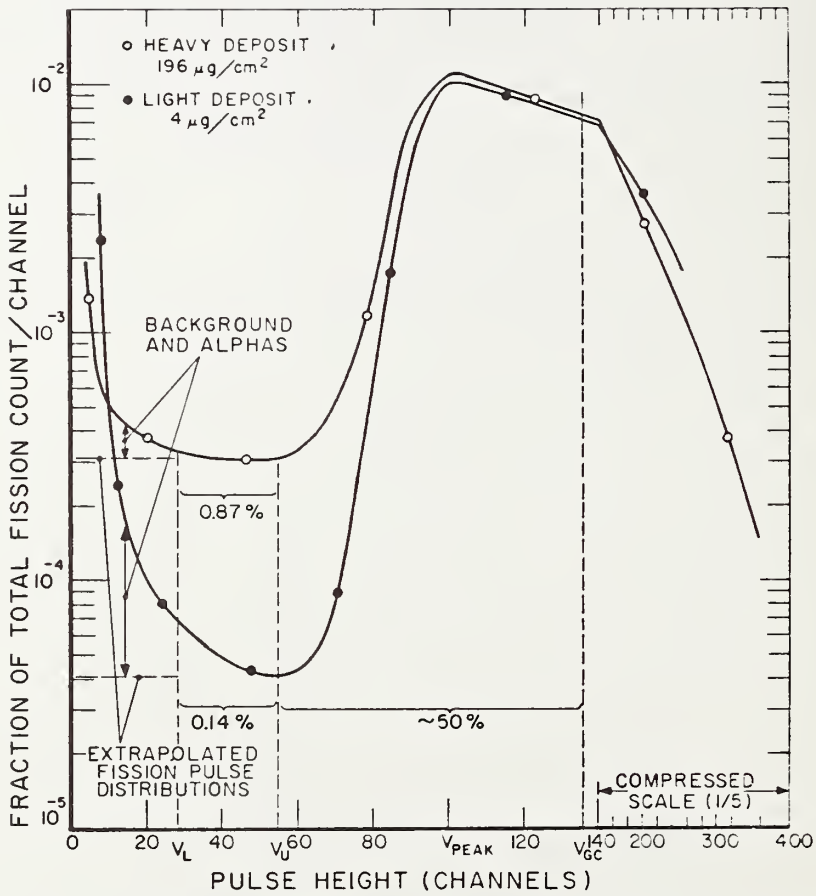

Figure 3. Typical pulse-height distributions for uranium fission counts. The pulse-height distribution of valid fission pulses is assumed to be flat in the range $0 \leq V \leq V_U$; the total count is derived from an integral discriminator count above V_L on the basis of the flat extrapolation assumption.

working fissionable deposits included four isotopes: Pu-239, U-235, U-238, and Np-237. Isotopic masses for the fissionable deposits were determined in work at the NBSR thermal column as were important performance characteristics for the fission chamber. Absolute accuracy for the fission rates per nucleus measured in CFRMF are in the range of ±1.3% to ±2.5% and are dominated by uncertainties in the fissionable deposit masses. These uncertainties were reduced by nearly a factor of two since the CFRMF measurements began. Efforts to improve the mass assignments to near ±1% and to achieve added confidence by means of inter-laboratory comparisons is an on-going project at NBS.

Fission cross section ratios provide a useful characterization of the high energy components of neutron spectra like that of CFRMF. Since the array of measured U-235 and U-238 fission rate ratios does not vary by more than ±0.3% during the CFRMF measurements, very consistent final values for these fission ratios are obtainable. Fission rate ratios obtained in CFRMF are listed in table 2 and compared there with predicted values based on neutron transport computations. The observed spectral index $\bar{\sigma}_f(^{238}U)/\bar{\sigma}_f(^{235}U)$ characterizes the spectrum as more energetic than computed. This is a commonly observed feature of fast neutron spectra although it is not always observed to this extent in a spectrum as degraded energy as CFRMF. Of equal interest is the rather good agreement between the observed and the computed Pu-239, and U-235 fission cross section ratios in table 2. If the ENDF/B-IV fission cross sections are as good as ±5% as is often presumed, this agreement indicates that the low energy component of CFRMF is closer to the results of computation than the results predicted by measured neutron spectra.

4. Thermal Fission Yields for Long Lived Fission Products

The experimental program of measuring thermal fission yields at the NBS thermal column was described briefly in the previous NBSR Annual

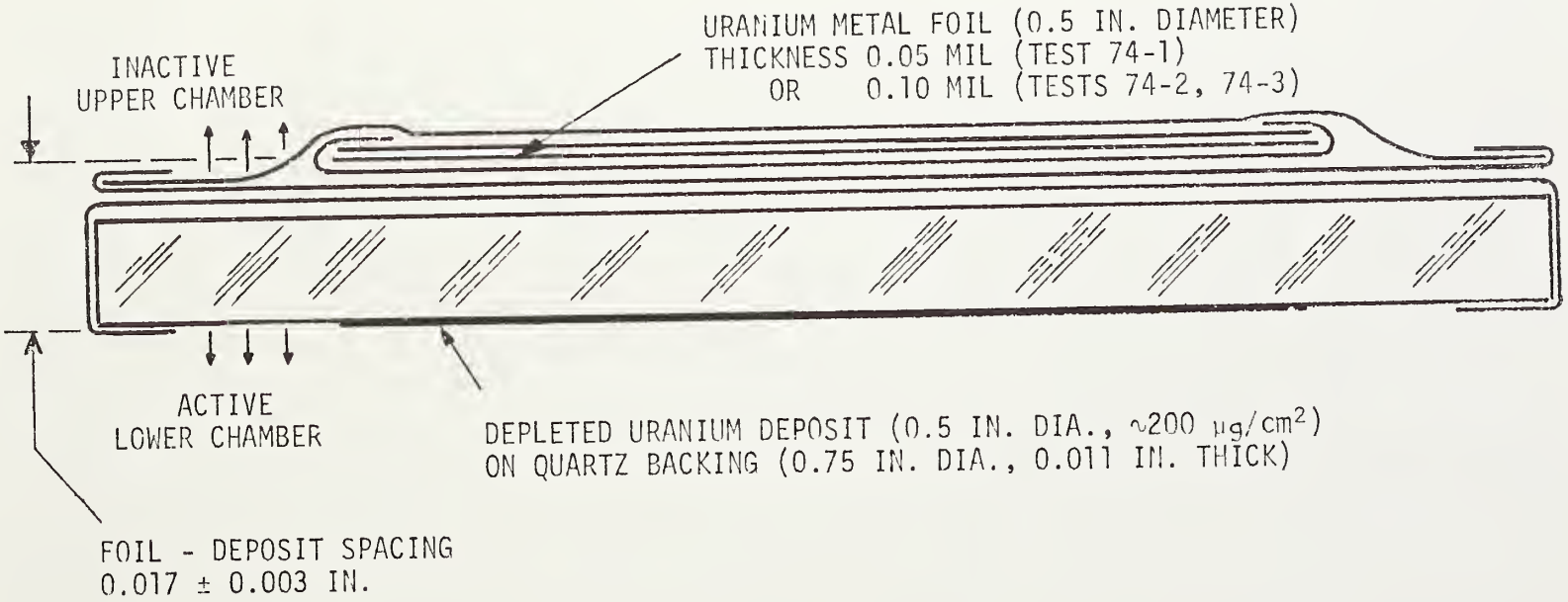

NOTES:

(1) HEAVY BLACK LINES ARE 1 MIL ALUMINUM FOIL WRAPPERS (UNLESS OTHERWISE LABELLED).

(2) VERTICAL SCALE ENLARGED BY A FACTOR OF FIVE.

Figure 4. Foil mounting for irradiation in double fission chamber.

Summary. Data reduction and reports of these measurements are now complete and a more complete summary of the measurement and its outcome are now possible.

Three U-235 fission activation foils were irradiated separately in the NBSR thermal column. During each irradiation specific fission counts (fission/mg U-235) were determined by observing fissions from a calibrated depleted uranium deposit inside of an NBS fission chamber. The fission activation foil in which the fission yield was to be measured also was positioned inside of the chamber adjacent to the calibrated deposit--see figure 4. Corrections relating the absolute fission count obtained from the deposit to the specific fission count attributed to the activation foil were computed and tested experimentally at NBS. Specific fission counts in the neighborhood of about 1×10^{13} fissions/milligram U-235 were observed with an accuracy of ±1.7% to ±2.0%. The dominating errors were the uncertainty in the mass of the reference U-235 deposit (1.2%), the uncertainty in the correction for the U-238 fission in the working deposit (0.63% to 1.25%), and the uncertainty in the calibration of the working deposit mass relative to the reference deposit mass (0.72%). The total number of fissions in the activation foils was inferred from the measured specific fission counts and the activation foil masses as reported by the supplier, The Isotope Target Laboratory at ORNL.

Four participants in the ILRR Interlaboratory Program for Fuels and Materials Dosimetry--ANC, ANL, ARHCO, HEDL--took part in the determination of the fission product activities by means of Ge(Li) gamma spectrometry. The gamma counting results furnished by these laboratories after the radiations have been combined with the fission counting data and the foil mass data to obtain absolute thermal fission yields. The thermal fission yield values obtained in these experiments both absolute, and relative to Ba-140, agree well with the ENDF/B-IV tabulation in most cases. The full table of results will not be presented here. Of equal importance and a prime motivation for these experiments is to examine

the question of fission yield energy dependence. In table 3 fission yields obtained from the CFRMF measurements described above are compared to the yield measurements obtained in the NBS thermal column. The fast/thermal yield presented in this table do not agree very well with the corresponding ENDF/B-IV ratios. Discrepancies range from 6 to 10 percent. These discrepancies are not considered final because of certain drawbacks in the thermal column fission yield experiments, but as they stand, they are of considerable significance for understanding fission rate measurements with activation dosimeters in fast reactor fuels tests in this country.

5. International Comparison of Absolute Fission Rate Measurement Scales

Interlaboratory comparisons have been made during the past two years of techniques that are currently being applied to the measurement of fission rates and U-238 capture rates in a number of zero-power fast critical assemblies related to LMFBR development programs. This effort involved the exposure of absolute fission chambers from four separate laboratories to the central neutron field in the Sigma Sigma Facility operated by the CEN/SCK laboratory at Mol Belgium. Uncertainties in measured reaction rates estimated by each laboratory relative to flux monitors at Sigma Sigma are between ±1.5% and ±3.5%. Uncertainties for the NBS fission chamber measurements at Sigma Sigma are in the range of ±1.6% for U-235, U-238 and Pu-239; Np-237 uncertainties are ±1.9%. Discounting the deposit mass error fission rate uncertainties for the Sigma Sigma measurements are between ±0.3% and ±0.6%. This last uncertainty is taken as a mark of success for remote field operation with the NBS fission chambers. Interlaboratory agreement for U-235, U-238 and Pu-239 fission rates is in the range ±0.5% to ±1.3%. Important discrepancies appear in the U-238 capture measurement and further interlaboratory efforts which will include NBS, are under consideration for solving this basic problem for fast breeder reactors.

Table 3. Fast/Thermal Fission Yield[c] Ratios

Fission Product Nuclide	CFRMF/(NBS Thermal Column) Yields[c] for ^{235}U				ENDF/B-IV Fast/ Thermal Yields[c] (August 1974)	Discrepancy HEDL-AHRCO/ ENDF/B-IV %
	AHRCO Results Foil U5 #3 (3.178 mg ^{235}U) Fast & Therm.	HEDL Results Foil U5 #3 (3.198 mg ^{235}U) Fast & Therm.	ANC Results Foil U5 #3 Fast/ Foil U5 #1 Thermal (6.288 mg ^{235}U)	Average of HEDL & AHRCO Results Foil U5 #3 Fast & Therm.		
^{95}Zr	1.059±3.1%	1.065±4.5%	0.997	1.062±3.8%	0.988±1.2%[b]	+7.5
^{103}Ru	1.177±3.0%	1.128±5.5%	1.06	1.153±5.5%	1.049±2.8%	+9.9
^{140}Ba	1.013±3.5%	1.005±3.7%	0.979	1.009±3.6%	0.952±1.5%	+6.0

[a] Error in fast/thermal fission rate measurement ratio estimated at 1.6%. Errors quoted for fast and thermal gamma activity measurements treated as independent - a very conservative assessment, since branching ratio errors (and perhaps others) cancel completely.

[b] Error estimates for ENDF/B-IV cumulative yields are from the Meek and Rider report NEDO-12154-1, 74 NED 6, Class I, January 26, 1974.

[c] Yields listed are cumulative yields for the mass chain up to the nuclide listed.

6. Fission Cross Sections for Californium-252 Fission Neutrons

Intense Cf-252 spontaneous fission sources with known source strength and of small volume and mass are attractive neutron sources for performing absolute cross section measurements in elementary geometry. An absolute determination of the U-235 cross section for Cf-252 fission neutrons has been carried out with two NBS double fission chambers in compensated beam geometry, the NBS set of reference and working double fission deposits, and the NBS manganese sulfate bath facility. In parallel measurements the ratios of fission cross sections of U-238, Pu-239 and Np-237 were determined for Cf-252 fission neutrons relative to the U-235 absolute measurements. These measurements provide normalization data for certain differential fission cross sections and for the general validation of evaluated energy dependent fission cross sections. The U-235 (n,f) absolute experiment is directly applicable for cross section normalization because fission shape uncertainties are of little significance. For any credible departure of fission shape from its normal Maxwellian description, the value of the U-235 (n,f) cross section will not vary by more than 0.4 percent. The experiments are simple and direct and hence the major effort is directed at understanding error components. A list of these error sources, corrections applied, and the percent uncertainty attached to them are listed in table 4 for the absolute U-235 cross section measurement.

The final Cf-252 fission-spectrum-averaged U-235 fission cross section obtained in these experiments is 1204±29 mb at a confidence level of 67 percent. A computed cross section value using ENDF/B-IV U-235 fission cross sections and a Californium fission spectrum evaluated by NBS is 1245 mb. The disagreement of 3.4% is a significant one and an effort will be undertaken to reduce the error in the observed value which as with other measurements of this kind at NBS is dominated by the fissionable deposit mass uncertainty. It is at the NBS reactor thermal column that much of the effort to improve fissionable deposit mass assay is centered. Results for the fission cross section ratio measurements is

Table 4. Error Components for ^{235}U Fission Cross Section Measurement

	Correction	*Percent Error
Mass of Fission Deposit Pairs (381.4 and 934.0 $\mu g/cm^2$)		1.3
Source Strength (4×10^9 n/s)		1.2
Fission in other isotopes	0.9987	0.1
Geometrical Measurements		
Fissionable Deposit Separation		0.6
Finite deposit diameter	1.0075	0.1
Source not at mid-point	1.001	0.2
Undetected Fission Fragments		
(light deposit)		
Extrapolation to zero pulse height	1.0090	0.5
Absorption in fissionable deposit	1.0132	0.3
Neutron Scattering		
Total room return	0.9955	0.2
Source capsule	0.9940	0.8
Fission chamber	0.9888	0.4
Support structures	0.9945	0.5
Platinum deposit backing	0.9870	0.8
Total Error		2.4%

*Error in $^{235}U(n,f)$ cross section due to uncertainty in the listed component.

Table 5. Fission Cross Section Ratios for ^{252}Cf Fission-Spectrum Neutrons

Nuclides	σ_f Ratio	Total Uncertainty	Mass Assay Uncertainty	σ_f Ratio ENDF/ B-IV	Discrepancy Present Work/ ENDF
	Present Work				
$^{238}U/^{235}U$	0.266	±1.7%	±1.5%	0.251	6.0%
$^{239}Pu/^{235}U$	1.500	±1.6%	±1.4%	1.440	4.2%
$^{237}Np/^{235}U$	1.105	±2.2%	±2.1%	1.080	2.3%

shown in table 5. There is a considerable discrepancy with the predictions of ENDF/B/IV; in particular, the Pu-239 to U-235 ratio, discrepancy is 4.2% well outside of the errors of the fission spectrum measurement and also outside of the presumed accuracy of the ENDF/B-IV file.

The discrepancy of the U-238/U-235 ratio in table 5 has been observed in other fission spectrum measurements but never with the clarity that has become possible with the advent of intense and isolated Californium fission sources. The 6% discrepancy is related to the discrepancy of 14% for the same cross section ratio observed in the CFRMF reactor measurements discussed above. These types of disagreements are of interest for reactor physics and for reactor fuels and materials dosimetry. Once again in order for these validation measurements to achieve maximum impact it will be necessary to reduce mass assay uncertainties to below the values listed in table 1. In this particular case where mass assay of the threshold fission isotopes (U-238 and Np-237) are involved, reference and working fissionable deposits will be exposed not only in thermal beams, but also in the cavity fission source facility which operates at the center of the thermal column. This facility provides high-quality fission neutron fluxes above one MeV at an intensity of between 10^9 to 10^{10} $n/cm^2 \cdot s$.

ANGULAR ANISOTROPY IN THE $^{6}Li(n,\alpha)^{3}H$ REACTION AT 25 keV

I. G. Schroder

and

E. D. McGarry
(Harry Diamond Laboratories, Adelphi, MD)

and

G. de Leeuw-Gierts and S. de Leeuw
(SCK-CEN Mol, Belgium)

The angular anisotropy in the $^{6}Li(n,\alpha)^{3}H$ reaction at 25 keV has been measured in two sets of experiments performed at an iron-filtered beam facility (99% of the flux at 25 keV) at the NBS reactor. First, a surface-barrier detector coated with 80 $\mu g \cdot cm^{-2}$ of ^{6}LiF (front face) was used as a 2π detector. This detector was placed in four different angular positions with respect to the neutron beam: front face at 90° and 45° to the beam; back face at 90° and 45° to the beam. The pulse-height distributions of both the H-3 and He-4 were recorded for these four positions yielding a forward-to-backward asymmetry of 1.59±0.11 in the center-of-mass system. A second detector was placed coaxially with the first (at 90° to the beam) and in such a way as to subtend a 45° cone. Coincidence measurements, that simultaneously recorded the distributions in both detectors, yielded an asymmetry in the backward-to-forward 45° cone of 1.80±0.06 in the center-of-mass system. The existence of such a large anisotropy at this low energy and the possibility of similar behavior at still lower energies (i.e., 1 - 2 keV) should result from s-p wave interference. This would give rise to a constant anisotropy that is experimentally masked by the 1/v behavior of the isotropic s-s interference terms at lower energies.

PRECISION MEASUREMENT OF THE WAVELENGTHS OF NUCLEAR GAMMA LINES AND THE COMPTON WAVELENGTH OF THE ELECTRON

R. D. Deslattes, E. G. Kessler, W. C. Sauder and A. Henins
(Optical Physics Division)

In this experiment the wavelengths of nuclear γ-lines and the Compton wavelength of the electron are measured in terms of the wavelengths of a molecularly stabilized visible laser. The γ-rays are diffracted by Ge or Si crystals which are located on a two axis Laue case transmission crystal spectrometer. The two quantities which must be accurately measured are the crystal spacing and diffraction angles.

The lattice spacing of the crystals is determined by establishing the lattice spacing of a standard silicon crystal by simultaneous optical and x-ray interferometry of a common baseline.[1] Next, a non-dispersive transfer from the standard silicon crystal to a sample of the crystals used in the experiment is performed.

The crystal diffraction angles are measured on the two axis spectrometer which is equipped with a modified Michelson angle interferometer. In this modification crystal rotation is encoded as polarization rotation with a 90° polarization charge corresponding to 70 milli arc sec. Faraday modulators and step driven Glan-Thompson analysers permit servo-control to about 0.3 milli arc sec or better. This angle measuring system was completely designed, constructed, and tested within the past nine months.

The interferometers were calibrated by summing to closure measurements of the interfacial angles of a 72-sided optical polygon. The provisional analysis of the calibration data has provided an interferometer constant accurate to 0.4 ppm.

A 40 Ci Au-198 γ-ray source was prepared by the irradiation of a Au foil in the NBS reactor. The wavelength of the 412 keV 198-Au line was measured with a result of 3.010766 pm (±2 ppm) being obtained. By applying the voltage-wavelength conversion factor to this number, the energy was found to be 411.8062 keV (±3.3 ppm).[2]

We hope to lower the uncertainty to less than 1 ppm in future γ-ray measurements by using stronger sources to obtain better statistics, by improving the Soller collimators so that the vertical divergence correction is better known, and by making the crystal spacing transfer more accurately.

---

1. R. D. Deslattes and A. Henins, *Phys. Rev. Lett.* 31, 972 (1973).

2. R. D. Deslattes, E. G. Kessler, W. C. Sauder, and A. Henins, Proceedings of the Fifth International Conference on Atomic Masses and Fundamental Constants (Plenum Press, NY) to be published.

MEASUREMENT OF THE RATIO OF THE ABSORPTION CROSS SECTIONS FOR MANGANESE AND HYDROGEN

J. R. Smith
(Aerojet Nuclear Company, Idaho Falls, Idaho)

and

S. D. Reeder
(Allied Chemical Company, Idaho Falls, Idaho)

and

B. M. Coursey
(Applied Radiation Division)

and

V. Spiegel
(Nuclear Sciences Division)

The manganese bath technique is perhaps the foremost method presently available for determining absolute yields of neutron sources. The principal of the method is quite simple. Neutrons from the source are completely absorbed in a surrounding solution of $MnSO_4$ dissolved in water. The absorbed neutrons induce in the solution an activity of Mn-56 proportional to the strength of the source.

There are a number of corrections that must be applied to the Mn-56 activity observed before the source strength is deduced. The present study is concerned primarily with just one of these: the

fact that not all of the absorbed neutrons produce Mn-56. Even in a saturated solution the fraction absorbed in manganese is less than 60%. In commonly used concentrations, the fraction ranges between 35% and 50%, with most of the remainder absorbed in hydrogen. The accuracy with which the fractional absorption in manganese can be determined, therefore, depends upon the accuracy with which the ratio of the absorption cross sections of manganese and hydrogen can be established.

Axton [1] developed the technique of varying the concentration of the manganese bath and extrapolating measurements to zero hydrogen content. From such measurements the source strength can be derived without reference to separately measured cross sections for hydrogen and manganese. However, the hydrogen-to-manganese cross section ratio can be derived from the concentration-dependent manganese bath activation data. It is determined from the ratio of the slope to the intercept of the linear curve obtained from plotting the reciprocal of the Mn-56 activity observed against the hydrogen-to-manganese atomic density of the solution.

DeVolpi [2] has also made concentration-dependent measurements, obtaining hydrogen-to-manganese cross section ratios differing from the Axton data by about 1.4%. This does not necessarily imply a corresponding error in source strength measurements, but it suggests the existence of unresolved problems in the systematics of the measurement. For example, Axton and DeVolpi disagree on the values of some of the manganese bath corrections, which must be applied to linearize the relationship between inverse Mn-56 activity and the H/Mn numerical ratio. The principal corrections in question are those for leakage, manganese resonance absorption, and high energy parasitic absorption in oxygen and sulfur. Because of the implications for Cf-252 $\bar{\nu}$ measurements by the manganese bath technique, it was thought important to make a concentration-dependence study for a neutron source for which these effects are negligible. Such a source is a

neutron beam well below the manganese resonance energies and the thresholds of the $^{16}O(n,\alpha)^{13}C$ and $^{32}S(n,\rho)^{32}P$ reactions.

At the National Bureau of Standards Reactor an experiment is in progress to determine the hydrogen-to-manganese cross section ratio in a manganese bath using a low energy neutron beam and the concentration variation technique. A Bragg beam of approximately 0.02 eV is obtained by reflection of the reactor beam from a crystal of pyrolytic graphite. Neutrons coming from higher order Bragg reflections or from potential scattering in the crystal are suppressed by filters of pyrolytic graphite and quartz crystals. The Bragg beam first passes through a manganese-aluminum monitor foil and then into the bath. The ratio of solution to monitor activity provides a measure of neutron-induced activity independent of reactor fluctuations.

The concentration of the solution is varied over a range from 30 to 530 grams of $MnSO_4$ per liter of solution. Because preliminary investigations indicated that the disagreement between Axton and DeVolpi might be traceable to concentration determinations, the concentration is being measured three ways: by evaporation of a sample of solution and weighing of the residual salt, by measuring the density and comparing with a density-vs.-concentration curve, and by titration of a sample of solution with EDTA.

The efficiency of counting Mn-56 activity in a solution varies with the concentration. Therefore, counter calibrations are carried out at each concentration. Calibrations are performed by counting in the manganese bath counting system an aliquot of Mn-56 sample whose absolute disintegration rate has been determined in the NBS ion chamber.

Measurements have thus far been made at four concentrations. At least that many additional points will be required for a reliable determination of the hydrogen-to-manganese cross section ratio.

---

1. E. J. Axton et al., J. Nucl. Energy Parts A/B 19, 409 (1965).

2. A. DeVolpi and K. G. Porges, Metrologia 5, 128 (1969).

E. Summary of Reactor Operations

Although the reactor was shut down from August 9, 1974 to January 20, 1975, for the installation of three new heat exchangers the operating productivity remained very high for the period of time available for operations (78% on-line time). A summary of the overall operating statistics for this and previous years is presented in the following table.

NBSR Operating Summary

	1972	1973	1974	1975
Reactor Operations to date, MWh	175,000	229,000	290,000	328,000
Reactor Operations for year, MWh	51,000	67,000	61,000	38,000
Hours Reactor Critical	5,200	7,000	6,600	3,900
Number of Days at 10 MW	214	279	254	157
On-line Time at 10 MW	58%	77%	70%	43%
Number of fuel elements used	26	28	24	16
Average U-235 Burnup	45%	52%	54%	53%
Number of Refueling Operations	6	7	6	4
Number of Unscheduled Shutdowns	11	14	6	0
Number of Irradiations	4,000	4,300	3,000	1,550
Number of Visitors	3,400	3,000	5,000	3,000

REPLACEMENT OF THE NBSR MAIN HEAT EXCHANGER

J. H. Nicklas

The main D_2O to process water heat exchanger made of aluminum had failures of the "U" tubes. The primary cause of failure was fretting of the "U" tubes against the baffles due to vibration.

It was decided that the replacement of the heat exchanger would include a spare because of cost advantages and the desirability of having a spare. The heat exchangers are made of stainless steel, type 304 L; low carbon chosen to eliminate carbide precipitation during welding. All tubes are welded to the solid stainless steel tubesheet in addition to being rolled into grooves of the tubesheet holes. Secondary inlet and outlet nozzles are attached to domes on the shell which reduces the impingement velocity of the fluid on the "U" tubes. Three inspection ports have been installed on each shell to observe corrosion product buildup and possible fouling from the chemical inhibitors used in the system.

The heat exchangers were installed through a floor opening in the experimental floor by professional riggers. After appropriate piping was welded and assembled to the heat exchangers, pressure and flow tests were run separately on the primary and secondary systems.

At about one-half the rated full flow in the secondary, a rattling sound was heard in the shell in the area of the "U" tubes. The last baffles in the heat exchanger next to the "U" tubes contain a window for flow and therefore contain "U" tubes of a greater unsupported length than tubes not in the window. A hole was cut in the shell in close proximity to the baffle window. The tubes in the baffle windows were "laced" with flattened tubes running between the tube rows and placed on both sides of the baffle. After closing the shell, flow testing at approximately 115% of rated flow was conducted with no rattling of the tubes being heard.

When flow tests were conducted on the primary system a scraping sound was heard in the bonnet of one heat exchanger but not in the other. Investigations through a port hole of the bonnet showed that a gasket between the tubesheet and divider plate had partially slipped out. It was determined that the divider plate had deflected sufficiently to allow the gasket to come free. Two heavy stainless steel bars were bolted to both sides of the divider plate to limit the deflection after the gasket was reinstalled in its groove. Flow tests were conducted at approximately 150% of design flow with no noise being heard in the bonnets.

Each heat exchanger has operated satisfactorily for several months. One heat exchanger is being dried out for storage as a spare unit.

F. Service Programs

Service and irradiation programs were curtailed this year because the reactor was shut down for the installation of new heat exchangers. In all, approximately 1550 irradiations were performed this year. Again, the irradiations covered a wide variety of programs. Highlights are presented in the following sections.

ACTIVATION ANALYSIS PROGRAM OF THE FOOD AND DRUG ADMINISTRATION AT THE NBSR

J. T. Tanner and M. H. Friedman
(Food and Drug Administration, Washington, D.C.)

The activation analysis unit of The Food and Drug Administration (FDA) is located at the National Bureau of Standards in the Reactor Building. Neutron activation analysis (NAA) has been used by the FDA for trace metal analysis of foods, drugs, hair, laundry aids, and cosmetics . The service of this group is available to anyone within the FDA both in the headquarters laboratory and in the field. The project described below accounts for the main effort of NAA at the FDA.

1. General

The "Total Diet" program of the Food and Drug Administration (FDA) is a continuing market basket study in which 117 food items are collected, prepared in a "table-ready" fashion, and composited into 12 commodity groups for analysis for selected metals, pesticides, and certain industrial chemicals to determine the average daily intake of these contaminants in the diet. The sampling is intended to represent the 2-week diet of a 15- to 20-year old male in each of four regions of the country in which the samples are collected: Northeastern, Southeastern, Central, and Western. The details of the selection, collection, preparation, and compositing of the samples are described elsewhere.[1] The different commodity groups are: Dairy products; meat, fish and poultry; grain and cereal products; potatoes; leafy vegetables; legume vegetables; root vegetables; garden fruits; oils and fats; beverages; and sugars.

The FDA Kansas City District Laboratory has the main responsibility for analysis of the Total Diet samples. In addition to pesticides, these composits are routinely analyzed for Hg, As, Se, Pb, Cd, Zn, Ca, Fe, P, and I. At various times the Neutron Activation Analysis (NAA) group of the FDA has aided the Kansas City Laboratory when improved limit of detection was required. Mercury was determined in Total Diet composites for one year by NAA. The results have been reported elsewhere.[2]

During the past year the FDA has been testing and evaluating NAA methodology for the surveillance of a number of trace elements in foods. Elements which are of interest to FDA include Fe, Co, Sb, Rb, Cs, Zn, Se, and Ca. Some of these elements produce long lived radionuclides on neutron irradiation and therefore offer the possibility of determination by instrumental NAA (INAA). These include Fe, Co, Rb, Cs, Zn, Se, Cr, Sc, Hg, and Ag. Others are short lived and may also be determined by INAA. These are K, Mg, Na, Dy, Mn, Ni, V, Al, In, Cl, Br, I, Ca, and As. While it may not be possible or practicable to determine all of these elements by INAA at least some of them possibly can be determined (Fe, Co, Zn, Sb, Rb, Se, K, Mg, Na, Mn, Al, and Br) and upper limits established for other elements. The purpose will be to provide additional information for elements not determined by the Kansas City Laboratory, provide an interlaboratory comparison within FDA, and provide greater sensitivity for some elements where only upper limits are now obtained by Kansas City.

Our initial survey consists of a one year Total Diet sampling. Based on the results obtained, the time required per analysis, and the total work load, the use of INAA for routine surveillance will be evaluated.

In addition to INAA, group separation methodology for multi-element analysis is being developed for FDA by researchers at the Washington State University. This will provide improved sensitivities for some elements.

2. Analysis of Elements with Long Half-Lives

The elements which are considered for analysis using a long irradiation (4-6 hours) and a long decay time (2-4 weeks) are Fe-59 (45d), Co-60 (5.3 y), Sb-124 (60d), Rb-86 (19d), Cs-134 (2.1y), Zn-65 (245d), Se-75 (120d), Cr-51 (28d), Sc-45 (84d), Hg-203 (47d), and Ag-110 (253d).

Total diet samples and standards were irradiated together for 4 to 6 hours in one of two reactor positions (flux of 10^{13} or 6 x 10^{13} n/cm^2-sec) and allowed to decay for between one to two months before analysis. For Co, Fe, Sb, Zn and Se the detection limit was considered adequate and no chemical separation was necessary; however, for mercury this was not the case and a chemical separation[2] was used. Radionuclides and energies of the gamma-rays which were used for the analyses are Co-60 (1173.1, 1332.4 keV), Fe-59 (1098.6, 1291.5), Sb-124 (1690.7), Zn-65 (1115.4), Se-75 (136.0, 264.6) and Hg-203 (279.1). The National Bureau of Standards Orchard Leaves (SRM 1571) are used as a standard for Fe and Zn and NBS Bovine Liver (SRM 1577) was used for the remaining elements as a standard. The samples and standards were counted using an automatic data acquisition system and reduced on a UNIVAC 1108 computer using the program MTELMR. The results are given in Table 1.

The remaining elements (Rb-86, Cs-134, Cr-51, Sc-46, and Ag-110) were below the detection limit. As a further extension to this part of the work, upper limits will be calculated for these elements, thus giving partial information regarding their concentration and/or occurrence in foods.

3. Analysis of Elements With Short Half-Lives

The elements which are used for analysis using a short irradiation time (15 sec) and a short decay time (60 sec) are K-42 (12.4h), Mg-27 (9.5m), Na-24 (15h), Dy-165 (2.3h), Mn-56 (2.6H), Ni-65 (2.6h), V-52 (3.8m), Al-28 (2.3m), In-116m (54m), Cl-38 (37.3m), Br-82 (36h), I-128 (25m), As-76 (26h), and Ca-49 (8.7m). The most likely elements which could occur in foods at detectable levels are K, Mg, Na, Mn, Al,

TOTAL DIET ANALYSIS**

Concentration in ppm (µg/g) wet weight

Element		Dairy 1	Meat 2	Grain 3	Potatoes 4
Calcium	Range	1143-2370	<200-1646	322-1122	79-227
	Avg.	540	<300*	606	<160*
Manganese	Range	<1-<6	<4-<6	4-12	1.3-9
	Avg.	<2*	<5*	<6*	2.9*
Magnesium	Range	99-284	213-487	240-669	166-494
	Avg.	164	<340*	360*	340
Aluminum	Range	<0.5-21	<1-5.6	5.6-92	2.6-22
	Avg.	2.9*	2.4*	32.4	10.4
Sodium	Range	852-1755	3363-5082	3479-6000	158-1000
	Avg.	1240	4150	4700	430
Potassium	Range	815-3131	1848-5619	<2000-5958	4400-10321
	Avg.	1540*	2670*	<2600*	6240
Copper	Range	<3-7	<4-19	8-12	<3-7
	Avg.	3*	<10*	<10*	4*
Chlorine	Range	1358-3154	4218-6623	4912-7845	616-2647
	Avg.	2040	5080	6160	1180
Antimony	Range	<0.002-0.02	<0.004-0.015	0.006-0.05	<0.003-0.03
	Avg.	<0.004*	0.008*	<0.01*	<0.008*
Mercury	Range	<0.001-0.003	0.004-0.03	<0.002-0.013	<0.001-0.013
	Avg.	<0.001*	0.017	<0.003*	<0.002*
Cobalt	Range	0.003-0.031	0.006-0.132	0.011-0.107	0.014-0.084
	Avg.	0.011	0.030	0.029	0.049
Iron	Range	1.5-16	18-39	21-49	9-27
	Avg.	3*	24	36	15
Zinc	Range	3.4-7.3	20-58	5.1-8.2	1.6-7.8
	Avg.	5.1	30	7.4	4
Selenium	Range	0.009-0.05	0.11-0.24	0.11-0.30	0.007-0.05
	Avg.	0.02*	0.17	0.17	<0.02*

*Median

**Based on the analysis of 20-25 samples in each group

TOTAL DIET ANALYSIS** (continued)

Concentration in ppm (µg/g) wet weight

Element		Leafy Veg. 5	Legume Veg. 6	Root Veg. 7	Garden Fruits 8
Calcium	Range	346-1019	248-961	241-578	114-282
	Avg.	600	450	400	<200*
Manganese	Range	1-8.1	2-6	1.1-4.5	<2-<5
	Avg.	2.3*	<4*	2.4*	<3*
Magnesium	Range	103-402	128-477	98-269	96-272
	Avg.	200*	300	170	<200*
Aluminum	Range	3.8-13.5	0.7-13.7	0.5-4.6	1.8-35
	Avg.	8.6	3.4	1.5	9.9
Sodium	Range	174-1626	1826-7396	404-1552	1878-4022
	Avg.	780	3200	760	3000
Potassium	Range	1225-3400	<1100-4308	1239-3487	960-2830
	Avg.	2191	1623*	2452	1626*
Copper	Range	<2-5	2.7-8	<2-<4	2.4-<8
	Avg.	<3*	<6*	<3*	<5*
Chlorine	Range	424-2550	2421-10191	410-2152	2209-5844
	Avg.	1160	4300	960	4100
Antimony	Range	0.001-0.027	<0.002-0.014	<0.002-<0.03	0.002-0.011
	Avg.	<0.006*	0.008*	<0.004*	<0.006*
Mercury	Range	<0.001-0.009	<0.001-0.002	<0.001-0.002	<0.001-0.004
	Avg.	<0.001*	<0.001*	<0.001*	<0.001*
Cobalt	Range	0.008-0.041	0.013-0.056	0.005-0.033	0.009-0.040
	Avg.	0.019	0.027	0.014	0.018
Iron	Range	5.6-21	10.3-43	5.1-9	5.8-14
	Avg.	12	21	7	<9
Zinc	Range	1.9-7.5	4.7-16.8	1.6-4.2	1.9-7.5
	Avg.	3	8.1	2.6	3.4
Selenium	Range	0.005-<0.06	0.005-<0.06	0.004-0.039	0.006-0.008
	Avg.	<0.01*	0.016*	<0.02*	0.016*

*Median

**Based on the analysis of 20-25 samples in each group

Cl, Ca, and Br. Upper limits could be calculated for the other elements as described in the preceding section. NBS Standards are used as element standards.

Radionuclides and energies of the gamma-rays which were used for the analyses are K-42 (1524.7), Mg-27 (1014), Na-24 (1368, 2754), Mn-56 (1811), Al-28 (1778), Cl-38 (1642.7, 2167.6), Ca-49 (3084.4), and Cu-66 (1039.2). The data are summarized in Table 1.

Duggan, R. E., and F. J. McFairland, Pesticides Monitoring Journal, Vol. 1, pp 1-5 (1967).

2. Tanner, J. T., and W. S. Forbes, Anal. Chim. Acta 74, 17-21 (1975).

ATF'S FORENSIC ACTIVATION ANALYSIS PROGRAM

C. M. Hoffman
(U.S. Treasury Department, Washington, DC)

Neutron activation analysis continues to be valuable as a primary or supplementary analytical tool in our Forensic Laboratory. The ability to analyze minute amounts of evidentiary material non-destructively is a distinct asset where the material must be preserved for courtroom presentation.

During FY75, 257 case related samples were analyzed by NAA. These samples consisted of gunshot residue, hair, bullet leads, paints, glass and soil.

Paint samples collected from 26 major U.S. manufacturers have been collected and will be analyzed for their trace element profiles. These data will be used to establish the probabilities necessary for comparing forensic specimens.

NAA has been used to examine writing inks for the presence of tab elements put in by the manufacturer who wishes to identify his product and its production date. This work will be continued in FY76.

THE USE OF ACTIVATION ANALYSIS IN SCIENTIFIC CRIME DETECTION BY THE FEDERAL BUREAU OF INVESTIGATION

J. F. Gallagher
(Federal Bureau of Investigation, Washington, DC)

The Neutron Activation Analysis (NAA) Group in the FBI Laboratory has continued to use NAA as one method of elemental analysis in materials as diverse as lead, copper, steel, biologicals, aluminum, gunshot residues and synthetic fibers.

For many of the elements of interest in aiding in the characterization of materials involved in criminal matters, there is no method of analysis with better precision and accuracy.

Additionally, the common problems of contamination and limited sample size can be overcome.

During FY 1975, three Special Agents assigned to the NAA Group testified on numerous occasions in local, state and federal courts.

LUNAR SAMPLE ANALYSIS FOR 17 TRACE ELEMENTS

E. Anders
(University of Chicago, Chicago, IL)

During the last year we have analyzed 12 samples for 17 trace elements (Ag, Au, Bi, Br, Cd, Cs, Ge, Ir, Ni, Rb, Re, Sb, Se, Te, Tl, U and Zn) by radiochemical neutron activation using the NBS reactor.

Abundances of siderophile elements (Au, Ge, Ir, Ni, Re, Sb) in Apollo 17 boulders and breccias show that rocks of the 2.3 km high massifs contain a uniform type of meteoritic materials. This appears to be derived from the planetesimal whose impact excavated the Serenitatis basin about 4 billion years ago (Higuchi and Morgan, 1975; James *et al.*, 1975). A light grey boulder from near the crest of the massif is the one major exception. It contains an unusual meteorite type and appears to pre-date the Serenitatis impact (Morgan *et al.*, 1975a).

A unique eucritic meteorite, Ibitira, resembles lunar basalts in

several respects; vesicularity, mineral assemblage and texture; bulk composition. Volatile trace elements are much higher in Ibitira, however, and reflect differences in composition between the Moon and the eucrite parent body (Morgan *et al.*, in preparation, 1975a).

1. H. Higuchi and J. W. Morgan, Ancient meteoritic components in Apollo 17 boulders, *Proc. Lunar Sci. Conf. 6th,* (1975) in press.

2. O. B. James, A. Brecher, D. P. Blanchard, J. W. Jacobs, J. C. Brannon, R. L. Korotev, L. A. Haskin, H. Higuchi, J. W. Morgan, E. Anders, L. T. Silver, K. Marti, D. Braddy, I. D. Hutcheon, T. Kirsten, J. F. Kerridge, I. R. Kaplan, C. T. Pillinger, and L. R. Gardiner, *Proc. Lunar Sci. Conf. 6th,* (1975) in press.

3. J. W. Morgan, H. Higuchi, and E. Anders, Meteoritic material in a boulder from the Apollo 17 site, *The Moon,* (1975a) in press.

4. J. W. Morgan, H. Higuchi, and E. Anders, Unbrecciated eucrites, in preparation (1975b).

TRACE ELEMENTS IN THE ENVIRONMENT AND RADIOACTIVE DECAY STUDIES

W. H. Zoller, G. E. Gordon and W. B. Walters
(University of Maryland, College Park, Maryland)

Our group has made extensive use of the NBSR for the irradiation of numerous samples for trace-element analysis using instrumental neutron activation analysis (INAA). We have had our computer-based Northern Scientific analyzer system and two Ge(Li) γ-ray detectors at the Reactor for periods of several weeks during the last year to count short-lived radioactive products. Most of the other samples are returned to the University of Maryland for counting when longer half-lived isotopes are involved.

During the last year numerous samples from our studies of coal- and oil-fired power plants have been analyzed for trace-element species. The projects involving the coal-fueled power plant emissions have shown that a fair amount of elemental fractionation does occur during the combustion process. The volatile elements Se, As, Pb, Sb,

and several others are redistributed onto the smaller sized particles. The enrichments relative to background values are not sufficient to account for observed atmospheric concentrations. Work on municipal incinerators has indicated that this is a very important source of many toxic trace metals in urban air. The particle size distribution also shows that the particles produced are in the resperable size range.

Samples from the South Pole and Iceland have been analyzed, and papers published on these results. More work is envisioned on the Antarctic samples throughout the next year to further substantiate our findings to date. Our results from activation analysis are described in more detail in progress reports to the NSF RANN Project (G. E. Gordon et al., Study of the Emissions from Major Air Pollution Sources, June, 1974, available from National Technical Information Service, No. PB242581/AS, $10/copy, $2.25 for microfiche; the 1975 report now in preparation will also be available through NTIS).

The radioactive decay of two nuclides have been studied using sources produced at the NBSR during the past year. The angular correlations of the Rh-105 γ-rays produced in the decay of 4.4-hr Ru-105 have been studied and low-lying $1/2^+$ and $3/2^+$ states identified. The decay of a new isomer 42-min Eu-154m has also been studied and coincidences among its γ-rays determined. Analysis of the coincidence spectra of the decay of 70-sec Se-83m has continued.

TRACE ELEMENTS IN OCEANIC FLOOR ROCKS

F. A. Frey
(Massachusetts Institute of Technology, Cambridge, MA)

Our use of the NBS reactor is for neutron activation analysis of geological samples. The analytical techniques have been documented by Gordon *et al.* (1968) and Hertogen and Gijbels (1971).

During the last year, our research has been concentrated on determination of trace element abundances in basaltic rocks drilled in the

ocean floor during the Deep Sea Drilling Project. These elements are typically abundant in the parts per million range in such rocks, and neutron activation is one of the few techniques enabling accurate analysis. The ocean floor is composed of basalts whose trace element composition is unlike similar appearing rocks on continents and oceanic islands. Because many trace element abundances, e.g., rare-earth elements are very sensitive indicators of the processes involved during magma formation, we can utilize a knowledge of trace element abundances in ocean floor basalts to learn about the nature of their source region in the upper mantle, and the mechanisms controlling the generation of magma within the earth.

---

1. G. E. Gordon, K. Randle, G. G. Goles, J. B. Corliss, M. H. Beeson and S. S. Oxley, *Geochim. Cosmochim. Acta*, 32, 369 (1968).

2. J. Hertogen and R. Gijbels, *Anal. Chim. Acta*, 56, 61-82 (1971).

CHEMICAL CHARACTERIZATION OF MARINE AEROSOLS

P. E. Wilkniss
(Naval Research Laboratory, Washington, DC)

Although the ocean is the largest natural source of aerosols (mainly in the form of sea salts), in certain regions the marine atmosphere may contain orders of magnitude greater concentrations of particulate material supplied by wind erosion of continents. Quantification and chemical characterization of this material is necessary to determine the atmospheric flux of various elements and the relative influence of anthropogenic processes on these elemental budgets. Since the transport of these continental particles (eolian dust) can vary greatly in space and time, the presence or absence of dust in the marine sedimentological record can also elucidate past wind patterns and climatic conditions of the dust source regions.

In this research, nearly one hundred eolian dust samples collected in the atmosphere over widely scattered regions of the Atlantic and Pacific oceans are being analyzed for several trace constituents. The method involves the use of neutron activation followed by gamma ray spectroscopy. Following a one hour irradiation in the NBS reactor (RT-4), samples are counted at NRL after 3 days and 40 days decay. The elements readily identified by this procedure include barium, cerium, cesium, chromium, cobalt, europium, hafnium, iridium, iron, lathanum, lutetium, potassium, rubidium, samarium, scandium, silver, sodium, tantalum, terbium and zinc. Concentrations of these elements are being compared among dust samples from various regions as well as with sediment samples from prospective source areas on land.

TRACE ELEMENT STUDIES OF SELECTED BIOLOGICAL SPECIMEN

G. A. Ferguson
(Howard University, Washington, DC)

Abnormal concentrations of trace elements have been suspected in the genesis of a number of cancers. Of special interest are the preliminary data on the high concentration of zinc in cancer of the prostate and pancreas. Neutron activation analysis (NAA) is being used as one method to study the role of trace elements in carcinogenesis. This study is being undertaken at Howard University because of its unique historical involvement with health problems of the U.S. black population which shows a rapidly increasing mortality rate attributable to cancer.

Multielement assay, using the NAA technique, of the large number of specimen required for a meaningful study of the role of trace elements has begun with preliminary data now being analyzed. Initial investigations will determine the distribution of zinc in the prostate of normal and abnormal subjects.

ACTIVATION ANALYSIS PROGRAM OF THE U.S. GEOLOGICAL SURVEY

J. J. Rowe
(U.S. Geological Survey, Reston, VA)

The U.S. Geological Survey is applying Neutron Activation Analysis to the determination of trace concentrations of elements in geological materials. The improved sensitivity of Activation Analysis, for some elements, supplements other analytical techniques in the analysis of rocks, minerals and waters for geochemical studies related to ore formation, magmatic differentiation, alternation, hydrothermal transport, energy reserves (coal, petroleum, geothermal and nuclear) and environmental problems.

The Radioactivation and Radiochemical Analysis project is developing a comprehensive instrument method, using sample changers and computer data reduction to provide data on trace concentrations of Ba, Ce, Co, Cr, Eu, Fe, Gd, Hf, Nd, Rb, Sb, Se, Ta, Th, Yb, Zn and Zr in igneous and metamorphic rocks. Sulfide minerals have been analyzed for Mn, As, Sb, Se, Ag, Hg and Au using instrumentation and radiochemical methods. Lunar samples have been analyzed for Al, V, Mn, Hf, and Ta. Thermal waters have been analyzed for gold for the Heavy Metals Program and a comprehensive analytical program is planned for the study of Geothermal Energy.

ORGANIZATION CHART

REACTOR RADIATION DIVISION

314.00

Division Office

R. S. Carter, Chief
T. M. Raby, Deputy Chief

E. Maxwell, Admin. Officer*
E. Simms, Receptionist
L. Sprecher, Sec'y*

Technical Support

H. Berger
R. Casella
M. Dorsey*
M. Ganoczy
B. Mozer
V. Myers
F. Shorten

314.01

Reactor Operations
T. M. Raby, Chief
J. F. Torrence, Deputy

D. Ahalt, Sec'y

R. Beasley
M. Bell
N. Bickford
H. Brake
D. Cea
A. Chapman
H. Dilks
D. Nelson
J. Ring
R. Scheide
R. Stiber
D. Wilkison
B. Young

314.02

Engineering Services
J. H. Nicklas, Chief

D. Davitt, Sec'y*

P. Beachley
R. Conway
J. Darr
O. Frizzell
E. Guglielmo
R. Hayes
J. Sturrock

314.03

Neutron S-S Physics
J. J. Rush, Chief

B. Crowther, Sec'y

A. Cinquepalma
D. Fravel
J. Norvell
E. Prince
J. Rowe
W. Rymes
A. Santoro
A. Tudgay
N. Vagelatos

*Temporary or part-time
**NRC post doctoral appointee

NON-RRD NBS STAFF LOCATED AT REACTOR

Division 240.01

P. R. Cassidy
H. E. DeSpain
E. J. Embree
R. Henessain
J. J. Shubiak
F. Moore

Division 241.05

R. A. Dallatore
R. Flemming
D. Gilliam
H. T. Heaton
J. A. Grundl
I. G. Schroder
R. Schwartz
V. Spiegel

Division 310.08

B. J. Clipper
S. B. Carpenter
R. H. Filby
S. S. Fine
E. Garrigues
T. E. Gills
S. H. Harrison
R. M. Lindstrom
G. J. Lutz
L. T. McClendon
H. L. Rook
J. E. Suddueth

GUEST WORKERS AND COLLABORATORS

Division 213.04

D. G. Eitzen

Division 232.06

R. D. Deslattes
W. C. Sauder
E. G. Kessler

Division 242.02

F. J. Schima

Division 310.01

D. Sweger

Division 311.03

C. Han

Division 312.02

R. Reno

Division 311.05

L. W. Schroeder
R. M. Waterstrat

Division 313.03

R. S. Roth

Division 313.04

G. J. Rosasco

Division 313.06

A. B. Mighell
C. S. Brickencamp

Argonne National Laboratory

H. Flotow
N. Lapinski
C. Pellazari
D. L. Price
K. Reimann
K. Skold

Battelle, N.W.

W. Nicholson

Federal Bureau of Investigation

D. B. Davies
J. Gallagher
J. W. Kilty
G. P. Mahoney
E. Mitchell
J. P. Riley

Food and Drug Administration

M. Friedman
J. T. Tanner

Harry Diamond Laboratory

C. Heimbach
D. McGarry

National Institutes of Health

D. Davies
R. Frank
W. Hagins
W. Robinson

Naval Air Systems Command

S. Goldberg

Naval Surface Weapons Center (Dahlgren Laboratory)

G. Blessing

Naval Surface Weapons Center (White Oak Laboratory)

H. Alperin
P. Hesse
D. Polansky
J. J. Rhyne
R. H. Williams

Naval Research Laboratory

D. Forester
G. A. Ferguson
J. Karle
J. H. Konnert
P. E. Wilkniss

Oak Ridge National Laboratory

H. A. Mook
M. Mostoller
H. G. Smith

Picatinny Arsenal

C. S. Choi
H. J. Prask
M. K. Farr
S. Trevino

U.S. Geological Survey

P. Baedecker
J. J. Rowe

U.S. Postal Service

M. Beckman
G. R. Stangohr
J. Upton

U.S. Treasury Department

R. L. Brunelle
P. C. Buscemi
C. M. Hoffman
F. A. Lundgren

American University

R. Abbundi
R. A. Segnan
R. Simon

Carnegie Institute of Washington

L. W. Finger

Colorado State University

C. E. Patton

Howard University

G. A. Ferguson

University of Maryland

W. Articola
E. Bailey
R. Cahill
C. Choquette
W. Cunningham
E. Gladney
G. Gordon
R. Greenberg
S. Jackson
W. Maenhaut
E. Mroz
J. Ondov
E. Schneider
J. Small
W. Walters
W. Zoller

Massachusetts Institute of Technology

F. A. Frey

Reed College

W. Parker

U.S. Naval Academy

C. S. Schneider

University of Chicago

E. Anders
R. Ganapathy
J. Morgan

University of Delaware

F. Williams

University of Rhode Island

S. J. Pickart

The Ford Motor Company

S. A. Werner

Gamma Industries

D. Garrett

Idaho National Engineering Laboratories

H. D. Reeder
J. R. Smith

Old Delft Corporation

D. Bracher

Thiokol Chemical Company

E. Magnusson

Union Carbide Corporation

T. Taylor

H. Publications

COLLABORATIVE PROGRAMS

BERGER, H., "Detection Systems for Neutron Radiography," *Proc. Symposium on Practical Applications of Neutron Radiography and Gauging*, National Bureau of Standards, Feb. 10-11, 1975, to be published.

BERGER, H., "An Evaluation of Radiography Paper for Thermal Neutron Radiography," *Transactions of the American Nuclear Society*, 21, pp. 148-149 (1975).

H. BERGER, "A Summary of the Conference on Emerging Techniques for Nondestructive Field Testing - Opportunities for NDT in Transportation," *Materials Evaluation*, 33, No. 7, pp. 189-191 (July 1975).

H. BERGER, "Radiographic Nondestructive Testing," *Standardization News*, 3, No. 3, pp. 21-29 (March 1975).

H. BERGER, "Summary of the American Nuclear Society Topical Meeting, Nondestructive Testing in the Nuclear Power Industry," *Nuclear News*, 18, No. 1, pp. 68-74 (Jan. 1975).

BICKFORD, N. A. and RABY, T. M., "Description of Pneumatic Facilities at the NBSR," *Transactions of the American Nuclear Society*, Aug. 12-14, 1974, p. 88-89 (1974).

CARTER, R. S., "Standards at the NBS Reactor," *Transactions of the American Nuclear Society*, August 12-14, 1974, p. 39-40 (1974).

CASELLA, R. C., ROWE, J. M., and TREVINO, S. F., "On Determining the Number of Independent Real Parameters in the Phonon Dynamical Matrix," submitted to *Phys. Rev.*

CASELLA, R. C., ROWE, J. M., and TREVINO, S. F., "On Determining the Number of Independent Real Parameters in the Phonon Dynamical Matrix," *Phys. Rev.*, in press.

CASELLA, R. C., "Algorithm for Computing the Number of Independent Parameters in the Phonon Dynamical Matrix," *Phys. Rev.*, 11B, 4795 (1975).

CHOI, C. S., SANTORO, A., and MARINKAS, P., "1,3,5-triaceta-2,4,6-trihydra-s-triazine (TRAT)," *Acta Cryst.*, in press.

CHOI, C. S., SANTORO, A., AND ABEL, J. E., "The Crystal Structure of 3,7-diacetyl-1,3,5,7-tetraazabicyclo[3,3,1]nonane (DAPT)", *Acta Cryst.*, B31, in press.

CHOI, C. S., PRASK, H. J., and PRINCE, E., "Crystal Structure of NH_4ClO_4 at 298, 78 and 10°K by Neutron Diffraction," *J. Chem. Phys.*, 61, 3523 (1974).

FINGER, L. W. and PRINCE, E., "A Fortran 10 Program for Structure Factor Calculation and Least Squares Refinement of Crystal Structures," *NBS Tech. Note* 854 (1975).

FRIZZELL, O. E., DARR, J. H., and RABY, T. M., "Non-Contact Irradiated Fuel-Plate Temperature Measurements at the NBSR," *Transactions of the American Nuclear Society*, Aug. 12-14, 1974, pp. 79-80 (1974).

GRAHAM, C. D., JR., and RHYNE, J. J., Editors, "Magnetism and Magnetic Materials", *American Inst. of Phys. Conf. Proc. Series* 24, (1975).

MIGHELL, A. D., SANTORO, A., PRINCE, E., and REIMANN, C. W., "Neutron Diffraction Structure Determination of Dichlorotetrapyrazolecopper (II), $Cu(C_3H_4N_2)_4Cl_2$," *Acta Cryst.* B31, in press.

MIGHELL, A. D. and SANTORO, A., "Geometrical Ambiguities in the Indexing of Powder Patterns," *J. Appl. Cryst.* 8, 372 (1975).

PICKART, S. J., RHYNE, J. J. and ALPERIN, H. A., "Critical Neutron Scattering in Amorphous $HoFe_2$," *AIP Conf. Proc.* 24 (1975).

PICKART, S. J., RHYNE, J. J., and ALPERIN, H. A., "Anomalous Small-Angle Magnetic Scattering from Amorphous $TbFe_2$ and YFe_2," *Phys. Rev. Letters* 33, 424 (1974).

RHYNE, J. J., PICKART, S. J. and ALPERIN, H. A., "Atomic Structure and Magnetism in Amorphous Terbium-Iron," *Proc. 11th Rare Earth Research Conf.*, p. 1020, (1974).

PRASK, H. J., RUSH, J. J. and TREVINO, S. F., "Quasielastic Neutron Scattering Studies of Ammonium-Ion Reorientation in Ammonium Perchlorate," *J. Chem. Phys.* 62, 4156 (1975).

PRINCE, E., "Dimethyl Sulfone Diimine, A Neutron Study," *Acta Cryst.*, in press.

PRINCE, E., TREVINO, S. F. and FARR, M. K., "A Refinement of the Structure of Deuterium Peroxide," *J. Chem. Phys.*, in press.

RHYNE, J. J., "Local Anistropy and Exchange Effects in Amorphous $TbFe_2$," *Proc. Conf. on Crystalline Electric Fields, Univ. of Montreal Bulletin*, (1975).

RHYNE, J. J., PRICE, D. L. and MOOK, H. A., "Inelastic Magnetic Scattering from Amorphous $TbFe_2$" *AIP Conf. Proc.* 24, (1975).

RHYNE, J. J., "A Part of the Birth and Evolution of Rare Earth Magnetism," *Proc. Eleventh Rare Earth Research Conference*, p. 247 (1974).

RHYNE, J. J., SCHELLENG, J. H., and KOON, N. C., "Anomalous Magnetization of Amorphous $TbFe_2$, $GcFe_2$, $GdFe_2$ and YFe_2," *Phys. Rev.* B10, 4672 (1974).

ROSASCO, G. J. and PRASK, H. J., "Polarized Raman Study of Lattice Modes in Ammonium Perchlorate at Low Temperature," *Sol. St. Comm.* 16, 135 (1975).

ROTSCHILD, W. G., ROSASCO, G. J. and LIVINGSTON, R. C., "Dynamics of Molecular Reorientation Motion and Vibrational Relaxation in Liquid Chloroform," *J. Chem. Phys.* 62, 1253 (1975).

ROWE, J. M., RUSH, J. J., VAGELATOS, N. and PRICE, D. L., "Crystal Dynamics of KCN and NaCN in the Disordered Cubic Phase," *J. Chem. Phys.* 62, 4551 (1975).

ROWE, J. M., NICKLOW, R. M., PRICE, D. L. and ZANIO, K., "Lattice Dynamics of Cadmium Telluride," *Phys. Rev.* 10B, 671 (1974).

RUSH, J. J., ROWE, J. M. and VAGELATOS, N., "The Acoustic Modes of the Phonon Dispersion Relation of NbD_x Alloys," *Phys. Rev.*, in press.

RUSH, J. J., SMITH, H. G., MOSTOLLER, M. and FLOWTOW, H. E., "Lattice Dynamics of a Single Crystal of $PdD_{0.63}$," *Phys. Rev. Lett.* 33, 1297 (1974).

SANTORO, A., CHOI, C. S. and ABEL, J. E., "1,5-Diacetyl-3,7 dinitro-1,3,5-tetrazacycloctane (DADN)," *Acta Cryst.* B31 (1975), in press.

SCHROEDER, L. W., PRINCE, E. and DICKENS, B., "Hydrogen Bonding in $Ca(H_2PO_4)_2\ H_2O$ as Determined by Neutron Diffraction," *Acta Cryst.* B31, 9 (1975).

SHEN, T. Y., MITRA, S. S. (U. R. Is.), PRASK, H. and TREVINO, S. F., "Order-Disorder Phenomenon in Sodium Nitrate Studied by Low Frequency Raman Scattering," *Phys. Rev.*, in press.

VAGELATOS, N., ROWE, J. M. and RUSH, J. J., "Lattice Dynamics of ND_4I in the NaCl Phase (I) of ND_4I at 296°K," *Phys. Rev.*, in press.

INDEPENDENT PROGRAMS

ARAS, N. K. and WALTERS, W. B., "The Decay of 4.44-hr ^{105}Ru to Levels of ^{105}RH," *Physical Review*, C11, 927 (1975).

DESLATTES, R. D., KESSLER, E. G., SAUDER, W. C. and HENINS, A., "Visible to Gamma-Ray Wavelength Ratio," *Atomic Masses and Fundamental Constants-5* (Plenum Press, NY) to be published.

DUCE, R. A., HOFFMAN, G. L. and ZOLLER, W. H. "Atmospheric Trace Elements at Remote Northern and Southern Hemisphere Sites: Pollution or Natural?" *Science*,187, 59 (1975).

FABER, T. M., RITTER, D. L., WEINBERGER, M. A. BIERBOWER, G., TANNER, J. T., FRIEDMAN, M. H., CARTER, C. J., EARL, F. L. and VANLOON, E. J., "The Toxicity of Brominated Sesame Oil and Brominated Soybean Oil in Miniature Swine," *Toxicology*, to be published.

FORESTER, D. W., ABBUNDI, R., SEGNAN, R. and SWEGER, D., "Magnetic Hyperfine Structure in Amorphous $DyFe_2$," AIP Conference, *Proceedings* Series XXIV, 115 (1974).

GANAPATHY, R., MORGAN, J. W., HIGUCHI, H., ANDERS, E. and ANDERSON, A. T., "Meteoric and Volatile Elements in Apollo 16 rocks and in separated phases from 14306." *Proc. Lunar Sci. Conf. 5th*, 1659-83 (1974).

GORDON, G. E., ZOLLER, W. H., GLADNEY, E. S. and GREENBERG, R. R., "The Use of Instrumental Nuclear Activation Analysis Methods in the Study of Particles from Major Air Pollution Sources," *Proceedings*, Second International Conference on Nuclear Methods in Environmental Research, Univ. of Missouri, 1974 (in press).

GREENBERG, R. R., ZOLLER, W. H. and GORDON, G. E., "Municipal Incinerators: Source of Toxic Elements on Urban Aerosols, submitted to *Science*.

JACKSON, S. V., WALTERS, W. B. and MEYER, R. A., "Decay of 30-hr ^{131}Te^{m} To Levels of ^{131}I, *Phys. Rev.* C9, 2379 (1974).

KEAYS, R. R., GANAPATHY, R., LAUL, J. C., KRAHENBUHL, U. and MORGAN, J. W. "The Simultaneous Determination of 20 Trace Elements in Terrestial, Lunar and Meteoric Material by Radiochemical Neutron Activation Analysis," *Anal. Chim. Acta*, 72, 1-29 (1974).

KILTY, J. R., "Activity After Shooting and Its Effect on the Retention of Primer Residue," *Journal of Forensic Sciences*, 20, No. 2 (1075).

KINARD, W. D and LUNDY, D. R., "A Comparison of Neutron Activation Analysis and Atomic Absorption Spectroscopy on Gunshot Residue," ACS Symposium Series #13, *Forensic Science*, 97-107 (1975).

MCGARRY, E. D. and SCHROEDER, I. G., "A 25keV Neutron Beam Facility at NBS," *Proceedings,* Conf. on Nuclear Cross Sections and Technology, Washington, DC (March, 1975).

MORGAN, J. W., GANAPATHY, R. and KRAHENBUHL, U., "Meteoritic Trace Elements in Lunar Rock 14321,184," *Geochim. Cosmochim. Acta* 39, 261-264 (1975).

MORGAN, J. W., GANAPATHY, R., HIGUCHI, H., KRAHENBUHL, U. and ANDERS, E., "Lunar Basins: Tentative Characterization of Projectiles, From Meteoric Elements in Apollo 17 Boulders," *Proc. Lunar Sci. Conf. 5th.* 1703-36 (1974).

MROZ, E. T. and ZOLLER, W. H., "Composition of Atmospheric Particulates from the Eruption of Heimaey, Iceland," *Science* (in press).

ONDOV, J. M., ZOLLER, W. H., OLMEZ, I., ARAS, N. K., GORDON, G. E., RANCITELLI, L. A., ABEL, K. H., FILBY, R. H., SHAH, K. R. and RAGAINI, R. C., "Element Concentrations in the National Bureau of Standards Environmental Coal and Fly Ash Standard Reference Materials," *Anal. Chem.*, 47, 1102-09 (1975).

ONDOV, J. M., ZOLLER, W. H., OLMEZ, I., ARAS, N. K., GORDON, G. E., RANCITELLI, L. A., ABEL, K. H., FILBY, R. H., SHAH, K. R. and RAGAINI, R. C., "Four-Laboratory Comparative Instrumental Nuclear Analysis of the NBS Coal and Fly Ash Standards," *Proceedings,* the 7th Materials Research Symposium: Accuracy in Trace Analysis, National Bureau of Standards, (1974) in press.

SCHNEIDER, C. S., "Coherent Nuclear Scattering Amplitudes of Germanium, Copper and Oxygen for Thermal Neutrons," to be published.

SCHROEDER, I. G., MCGARRY, E. D., DE LEEUW-GIERTS and DE LEEUW, S., "Angular Anisotropy in the ^{6}L.(n,α)^{3}H Reaction at 25 keV," *Proceedings,* Conference on Nuclear Cross Sections and Technology, Washington, DC (March, 1975).

SCHROEDER, I. G., SCHWARTZ, R. B. and MCGARRY, E. D., "The 2-keV Filtered Beam Facility at the NBS Reactor," *Proceedings,* Conference on Nuclear Cross Sections and Technology, Washington, DC (March, 1975).

SCHWARTZ, R. B., MCGARRY, E. D. and SCHROEDER, I. G., "Filtered Neutron Beams at the National Bureau of Standards Reactor," EUROPHYSICS Conf. on Nuclear Interactions at Medium and Low Energies, AERE, Harwell, England (March 1975).

ZOLLER, W. H., GLADNEY, E. S., GORDON, G. E. and J. J. BORS, "Emissions of Trace Elements from Coal Fired Power Plants," *Trace Substances in Environmental Health* - VIII, D. D. Hemphill, ed. (Univ. of Missouri, Columbia, 1974) pp. 167-171.

NBS-114A (REV. 7-73)

U.S. DEPT. OF COMM. BIBLIOGRAPHIC DATA SHEET	1. PUBLICATION OR REPORT NO. NBS TN-896	2. Gov't Accession No.	3. Recipient's Accession No.

4. TITLE AND SUBTITLE

NBS Reactor: Summary of Activities, July 1974 to June 1975

5. Publication Date: January 1976

6. Performing Organization Code

7. AUTHOR(S): Robert S. Carter

8. Performing Organ. Report No.

9. PERFORMING ORGANIZATION NAME AND ADDRESS

NATIONAL BUREAU OF STANDARDS
DEPARTMENT OF COMMERCE
WASHINGTON, D.C. 20234

10. Project/Task/Work Unit No.

11. Contract/Grant No.

12. Sponsoring Organization Name and Complete Address (*Street, City, State, ZIP*)

13. Type of Report & Period Covered: 7-1-74 to 6-30-75

14. Sponsoring Agency Code

15. SUPPLEMENTARY NOTES

16. ABSTRACT (*A 200-word or less factual summary of most significant information. If document includes a significant bibliography or literature survey, mention it here.*)

This report summarizes all those programs which depend on the NBS reactor. It covers the period from July 1974 through June 1975. The programs range from the use of neutron beams to study of the structure and dynamics of materials through nuclear physics and neutron standards to sample irradiations for activation analysis, isotope production and radiation effects studies.

17. KEY WORDS (*six to twelve entries; alphabetical order, capitalize only the first letter of the first key word unless a proper name; separated by semicolons*)

Activation analysis; crystal structure; diffraction; isotopes; molecular dynamics; neutron; nuclear reactor; radiation

18. AVAILABILITY

[X] Unlimited

[ ] For Official Distribution. Do Not Release to NTIS

[X] Order From Sup. of Doc., U.S. Government Printing Office Washington, D.C. 20402, SD Cat. No. C13. 46:896

[ ] Order From National Technical Information Service (NTIS) Springfield, Virginia 22151

19. SECURITY CLASS (THIS REPORT)	21. NO. OF PAGES
UNCLASSIFIED	150
20. SECURITY CLASS (THIS PAGE)	22. Price
UNCLASSIFIED	$2.15

USCOMM-DC 29042-P74

NBS TECHNICAL PUBLICATIONS

PERIODICALS

JOURNAL OF RESEARCH reports National Bureau of Standards research and development in physics, mathematics, and chemistry. It is published in two sections, available separately:

- **Physics and Chemistry (Section A)**

Papers of interest primarily to scientists working in these fields. This section covers a broad range of physical and chemical research, with major emphasis on standards of physical measurement, fundamental constants, and properties of matter. Issued six times a year. Annual subscription: Domestic, $17.00; Foreign, $21.25.

- **Mathematical Sciences (Section B)**

Studies and compilations designed mainly for the mathematician and theoretical physicist. Topics in mathematical statistics, theory of experiment design, numerical analysis, theoretical physics and chemistry, logical design and programming of computers and computer systems. Short numerical tables. Issued quarterly. Annual subscription: Domestic, $9.00; Foreign, $11.25.

DIMENSIONS/NBS (formerly Technical News Bulletin)—This monthly magazine is published to inform scientists, engineers, businessmen, industry, teachers, students, and consumers of the latest advances in science and technology, with primary emphasis on the work at NBS. The magazine highlights and reviews such issues as energy research, fire protection, building technology, metric conversion, pollution abatement, health and safety, and consumer product performance. In addition, it reports the results of Bureau programs in measurement standards and techniques, properties of matter and materials, engineering standards and services, instrumentation, and automatic data processing.

Annual subscription: Domestic, $9.45; Foreign, $11.85.

NONPERIODICALS

Monographs—Major contributions to the technical literature on various subjects related to the Bureau's scientific and technical activities.

Handbooks—Recommended codes of engineering and industrial practice (including safety codes) developed in cooperation with interested industries, professional organizations, and regulatory bodies.

Special Publications—Include proceedings of conferences sponsored by NBS, NBS annual reports, and other special publications appropriate to this grouping such as wall charts, pocket cards, and bibliographies.

Applied Mathematics Series—Mathematical tables, manuals, and studies of special interest to physicists, engineers, chemists, biologists, mathematicians, computer programmers, and others engaged in scientific and technical work.

National Standard Reference Data Series—Provides quantitative data on the physical and chemical properties of materials, compiled from the world's literature and critically evaluated. Developed under a world-wide program coordinated by NBS. Program under authority of National Standard Data Act (Public Law 90-396).

NOTE: At present the principal publication outlet for these data is the Journal of Physical and Chemical Reference Data (JPCRD) published quarterly for NBS by the American Chemical Society (ACS) and the American Institute of Physics (AIP). Subscriptions, reprints, and supplements available from ACS, 1155 Sixteenth St. N. W., Wash. D. C. 20056.

Building Science Series—Disseminates technical information developed at the Bureau on building materials, components, systems, and whole structures. The series presents research results, test methods, and performance criteria related to the structural and environmental functions and the durability and safety characteristics of building elements and systems.

Technical Notes—Studies or reports which are complete in themselves but restrictive in their treatment of a subject. Analogous to monographs but not so comprehensive in scope or definitive in treatment of the subject area. Often serve as a vehicle for final reports of work performed at NBS under the sponsorship of other government agencies.

Voluntary Product Standards—Developed under procedures published by the Department of Commerce in Part 10, Title 15, of the Code of Federal Regulations. The purpose of the standards is to establish nationally recognized requirements for products, and to provide all concerned interests with a basis for common understanding of the characteristics of the products. NBS administers this program as a supplement to the activities of the private sector standardizing organizations.

Federal Information Processing Standards Publications (FIPS PUBS)—Publications in this series collectively constitute the Federal Information Processing Standards Register. Register serves as the official source of information in the Federal Government regarding standards issued by NBS pursuant to the Federal Property and Administrative Services Act of 1949 as amended, Public Law 89-306 (79 Stat. 1127), and as implemented by Executive Order 11717 (38 FR 12315, dated May 11, 1973) and Part 6 of Title 15 CFR (Code of Federal Regulations).

Consumer Information Series—Practical information, based on NBS research and experience, covering areas of interest to the consumer. Easily understandable language and illustrations provide useful background knowledge for shopping in today's technological marketplace.

NBS Interagency Reports (NBSIR)—A special series of interim or final reports on work performed by NBS for outside sponsors (both government and non-government). In general, initial distribution is handled by the sponsor; public distribution is by the National Technical Information Service (Springfield, Va. 22161) in paper copy or microfiche form.

Order NBS publications (except NBSIR's and Bibliographic Subscription Services) from: Superintendent of Documents, Government Printing Office, Washington, D.C. 20402.

BIBLIOGRAPHIC SUBSCRIPTION SERVICES

The following current-awareness and literature-survey bibliographies are issued periodically by the Bureau:

Cryogenic Data Center Current Awareness Service

A literature survey issued biweekly. Annual subscription: Domestic, $20.00; foreign, $25.00.

Liquefied Natural Gas. A literature survey issued quarterly. Annual subscription: $20.00.

Superconducting Devices and Materials. A literature survey issued quarterly. Annual subscription: $20.00. Send subscription orders and remittances for the preceding bibliographic services to National Technical Information Service, Springfield, Va. 22161.

Electromagnetic Metrology Current Awareness Service Issued monthly. Annual subscription: $24.00. Send subscription order and remittance to Electromagnetics Division, National Bureau of Standards, Boulder, Colo. 80302.

U.S. DEPARTMENT OF COMMERCE
National Bureau of Standards
Washington, D.C. 20234

OFFICIAL BUSINESS

Penalty for Private Use, $300

POSTAGE AND FEES PAID
U.S. DEPARTMENT OF COMMERCE
COM-215

SPECIAL FOURTH-CLASS RATE
BOOK